

A.4.7 Vibration

Using bolts and spring washers, the package is fixed to the transport skid by its rear base plate and pivoting trunnions to prevent any movement during transport due to vibration.

Subsection A.4.5 shows that the tie-down devices have strength to withstand acceleration occurring during transport.

The natural frequency of this package is calculated below. The calculated frequency is compared with the frequency band received in the transport skid from loading vehicles during transport. The resulting information indicates that the package does not resonate. When this package is approximated by a simple beam supported at both ends, the natural frequency is given by the expression below.¹⁾

$$fn = Cn \sqrt{\frac{EI}{\gamma A \ell^2}}$$

where

Cn : Constant

$$Cn = n^2 \times \frac{\pi}{2}$$

E : Elastic modulus of the outer shell (SUS304) at a temperature of 80°C $1.91 \times 10^5 \text{ N/mm}^2$

I : Inertia moment of the area

$$I = \frac{\pi}{64}(d_o^4 - d_i^4)$$

d_o : Outer diameter of the outer shell 800 mm

d_i : Inner diameter of the outer shell 768 mm

$$I = \frac{\pi}{64} (800^4 - 768^4) = 3.03 \times 10^9 \text{ mm}^4$$

A : Cross sectional area

$$A = \frac{\pi}{4} (d_o^2 - d_i^2) = \frac{\pi}{4} (800^2 - 768^2) = 3.94 \times 10^4 \text{ mm}^2$$

γ : Mass density

$$\gamma = \frac{W}{A \ell} \cdot \frac{1}{g}$$

W : Package weight $1.08 \times 10^5 \text{ N}$

1) Tsumura Toshimitsu: Kyodo Sekkei Data Book, p. 420 Shyokabou, 1973
(Toshimitsu Tsumura: Strength Design Data Book, page 420, Shyokabou, 1973)

l :	Total length of the package	3.26×10^3 mm
g :	Gravitational acceleration	9.8×10^3 mm/sec ²

$$\gamma = \frac{1.08 \times 10^5}{3.94 \times 10^4 \times 3.26 \times 10^3} \times \frac{1}{9.8 \times 10^3}$$

$$= 8.58 \times 10^{-8} \text{ N/mm}^4\text{sec}^2$$

By substituting this value, the natural frequency is obtained as follows:

$$fn = Cn \sqrt{\frac{1.91 \times 10^5 \times 3.03 \times 10^9}{8.58 \times 10^{-8} \times 3.94 \times 10^4 \times (326 \times 10^3)^4}}$$

$$= 38.9 Cn \text{ (Hz)}$$

Since C_1 is $\frac{\pi}{2}$ in the primary mode, the natural frequency f_1 is approximately 61 Hz.

In vehicle loading, the frequency band received in the transport skid is 0 to 10 Hz¹⁾. In vessel loading, the frequency band is less than 10 Hz²⁾. Therefore, this package does not resonate.

1) ATR's new fuel packaging development test: Power Reactor Technical Report, No. 18, 1976
 2) Fred E Ostrem, et al: Shock and Vibration Transport

A.5 Normal Test Conditions

This package is a type B(U) package. Therefore, the normal test conditions prescribed by the relevant regulations are as follows:

- (i) Water spray test
The package shall be subjected to the tests shown below one after another after test (i) has been completed.
- (ii) Free drop test
- (iii) Compression test
- (iv) Penetration test
Allow the package to stand in the condition indicated below after completing the tests given in (i) through (iv).
- (v) Left unattended for a period of one week in an ambient temperature ranging from 38 to -40°C.

Section A.5 indicates that the test method in this analysis complies with the normal test conditions prescribed by the relevant regulations. This section also describes the influence that each test exerts on this package.

A.5.1 Thermal Test

A.5.1.1 Summary of the Temperature and Pressure

The pressure and temperature of the packaging's principal part under normal test conditions indicate the maximum temperature and pressure when Contents I (maximum heating value of 260 W) and Contents II (maximum heating value of 64 W) are stored as described in the section (II)-B.4. Table (II)-A.14 shows the temperature under these conditions.

Table (II)-A.14 Summary of the Pressure and Temperature under Normal Test Conditions

Parts	Pressure (kPa(G))	Temperature (°C)
Shock absorber steel plate	-	64
Outer shell	-	72
Resin layer (Heat disperison fin)	-	73
Outer shell lid	60	73
Lead shield	-	84
Inner shell	60	85
Inner container	-	241
Fuel supporting can	210	300
Inner container ¹⁾	-	157
Receiving tube I	610	245

1) When contents II are stored

A.5.1.2 Thermal Expansion

As shown in Table (II)-A.14, the temperature in each part of the package varies. Since thermal expansion coefficient also varies depending on the part materials, deformation and thermal stress occur in the part materials of the package due to the difference in thermal expansion. This subsection investigates the outer container, the inner container, fuel supporting can I (for Contents I), and receiving tube I (for Contents II) with internal heating contents inside. The temperature change in the shock absorbers is slighter than that of these part materials. Therefore, so the shock absorber is omitted.

(1) Outer container

For the temperature distribution of the outer container's shell part, the radial distribution in the center part of the outer container is larger than the distributions in the axial direction and near the end plates of the outer container, as described in section (II)-B. Therefore, the maximum stress occurs in the radial direction of the outer container's center part as a result of thermal expansion. The distribution in the radial direction is thus calculated. Given that the end surface has upper and lower flanges, the analysis model is a cylindrical model that uniformly displaces in the axial direction, as shown in Fig. (II)-A.16, using finite element calculation code ANSYS. Table (II)-A.15 shows the constants used for the calculation.

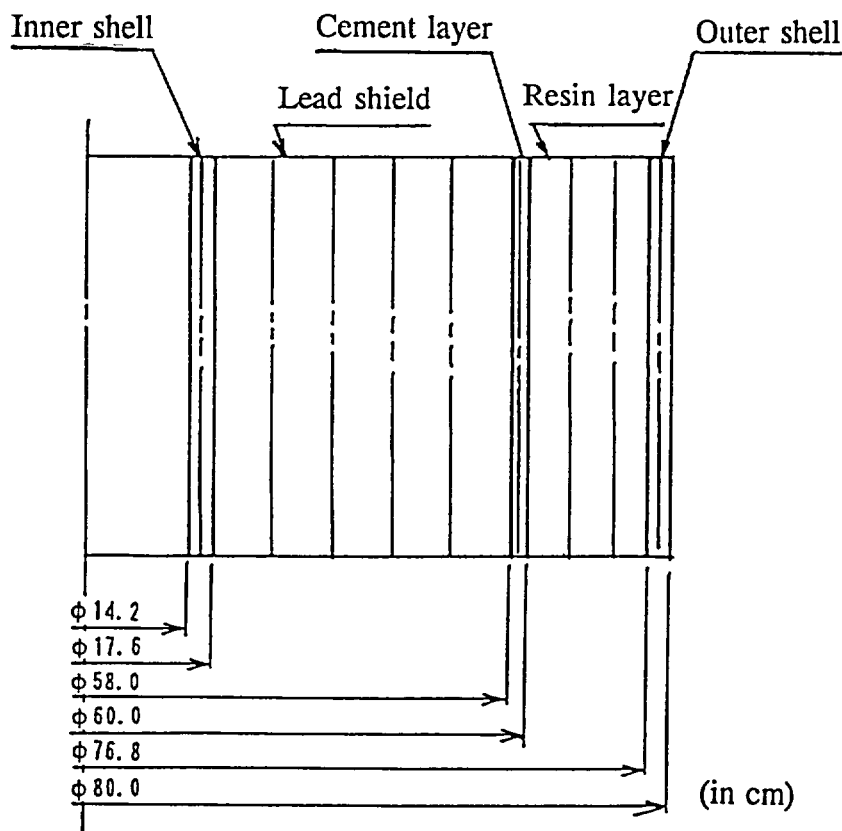


Fig. (II)-A.16 Stress Analysis Model

Table (II)-A.15 Physical Properties and Temperature of the Outer Container Materials

Part	Material	Linear thermal expansion coefficient (1/°C)	Modulus of longitudinal elasticity (N/mm ²)	Room temperature (°C)	Maximum temperature (°C)
Inner shell	SUS304	16.4×10^{-6}	1.95×10^5	20	85
Lead shield	Pb	29.3×10^{-6}	1.67×10^4	20	84
Cement layer	Cement	10.0×10^{-6}	2.94×10^4	20	79
Resin layer	Resin	60.0×10^{-6}	1.57×10^3	20	73
Outer shell	SUS304	16.4×10^{-6}	1.95×10^5	20	72

As a result of the numeric calculation using an ANSYS code, the circumferential stress (σ_i) generated in the inner shell, the stress (σ_{pb}) in the lead shield, the stress (σ_c) in the cement layer, the stress (σ_r) in the resin layer, and the stress (σ_o) in the outer shell are as shown below.

$$\begin{aligned} \sigma_i &= -83.4 \text{ N/mm}^2 \\ \sigma_{pb} &= -21.5 \text{ N/mm}^2 \\ \sigma_c &= 3.0 \text{ N/mm}^2 \\ \sigma_r &= 3.5 \text{ N/mm}^2 \\ \sigma_o &= 6.4 \text{ N/mm}^2 \quad (\text{The negative (-) sign represents the compression stress.}) \end{aligned}$$

The margin of safety for the inner and outer shells used as strength materials can thus be obtained. Using the design criterion value $\sigma_y = 174 \text{ N/mm}^2$ ($\approx 17.7 \text{ kg/mm}^2$) (temperature of 90°C) for the inner shell (material SUS304) and the design criterion value $\sigma_y = 180 \text{ N/mm}^2$ ($\approx 18.4 \text{ kg/mm}^2$) (temperature of 80°C) for the outer shell (material SUS304), the margins of safety (M.S.) for the inner and outer shells are given respectively by the expressions below.

$$\begin{aligned} M.S. &= \frac{174}{83.4} - 1 \\ &= 1.1 \\ M.S. &= \frac{180}{6.4} - 1 \\ &= 27 \end{aligned}$$

The inner and outer shells, therefore, have sufficient strength.

Lead cannot be broken by the compression load. In the cement layer, two partitions made of asbestos are provided in order to avoid circumferential thermal expansion.

The tensile stress generated in the resin layer is $\sigma_r = 3.5 \text{ N/mm}^2$. Since the tensile stress is less than the tensile strength $\sigma = 8.7 \text{ N/mm}^2$, no damage occurs.

The difference between the temperature of the various materials and the room temperature when the outside temperature is -40°C is smaller than this temperature difference during the analysis. Therefore, the stress caused by the difference in the thermal expansion of each part material is smaller than the analysis results previously given. The inner and outer shell parts thus have sufficient strength.

- (2) Inner container, fuel supporting can I (for Contents I), and receiving tube I (for Contents II)

This subsection examines the thermal expansion in the inner container, to show that the inner container is not restrained by thermal expansion. The dimensions of the inner container, outer container, fuel supporting can I, and rack are as shown in Fig. (II)-A.17.

- a) Restraint of the inner container and outer container's internal wall

The inner container is not restrained by the internal wall of the outer container when it is expanded by heat. The thermal expansion of the inner container is given by the expression below.

$$\Delta l = \alpha \Delta T l$$

α : Linear thermal expansion coefficient of the inner container (SUS304)
 $16.4 \times 10^{-6}/^\circ\text{C}$

$$\Delta T = T_1 - T_0$$

T_1 : Maximum temperature of the inner container, 241°C from Table (II)-A.14
 T_0 : Room temperature, 20°C

$$\begin{aligned} \Delta T &= 241 - 20 \\ &= 221^\circ\text{C} \end{aligned}$$

l : Length of the inner container, 1998 mm

$$\begin{aligned} \Delta l &= 16.4 \times 10^{-6} \times 221 \times 1998 \\ &= 7.2 \text{ mm} \end{aligned}$$

The clearance of the inner container and rotating plug is 8 mm at normal temperature. Therefore, the inner container and the outer container's internal wall are not restrained by the thermal expansion in the inner container even if the thermal expansion of the internal wall of the outer container is not considered.

- b) Restraint of the inner container and fuel supporting can I (for Contents I), and the inner container and rack (for Contents II)

This subsection examines, the inner container and fuel supporting can I, and the inner container and rack. As shown in Fig. (II)-A.17, the length of the fuel supporting can I and the rack is 1944.5 mm each, while the effective length inside the inner container is 1949 mm. The margin under a normal temperature is thus 4.5 mm (1949 - 1944.5). As shown in Table (II)-A.14, the difference in temperature between the inner container and

fuel supporting can I is 59°C (300 - 241), while the difference in temperature between the inner container and the rack (evaluated by receiving tube I) is 88°C (245 - 157). Since the difference in temperature between the inner container and the rack is larger, it is quite possible that the inner container and rack are restrained.

The elongation is given by

$$\begin{aligned}\Delta l &= \alpha \Delta T l \\ \Delta l &= 16.4 \times 10^{-6} \times 88 \times 1944.5 \\ &= 2.8 \text{ mm}\end{aligned}$$

This elongation does not exceed 4.5 mm. Therefore, there is no restraint between the inner container and the rack. For this same reason, there is no restraint due to thermal expansion between the inner container and fuel supporting can I.

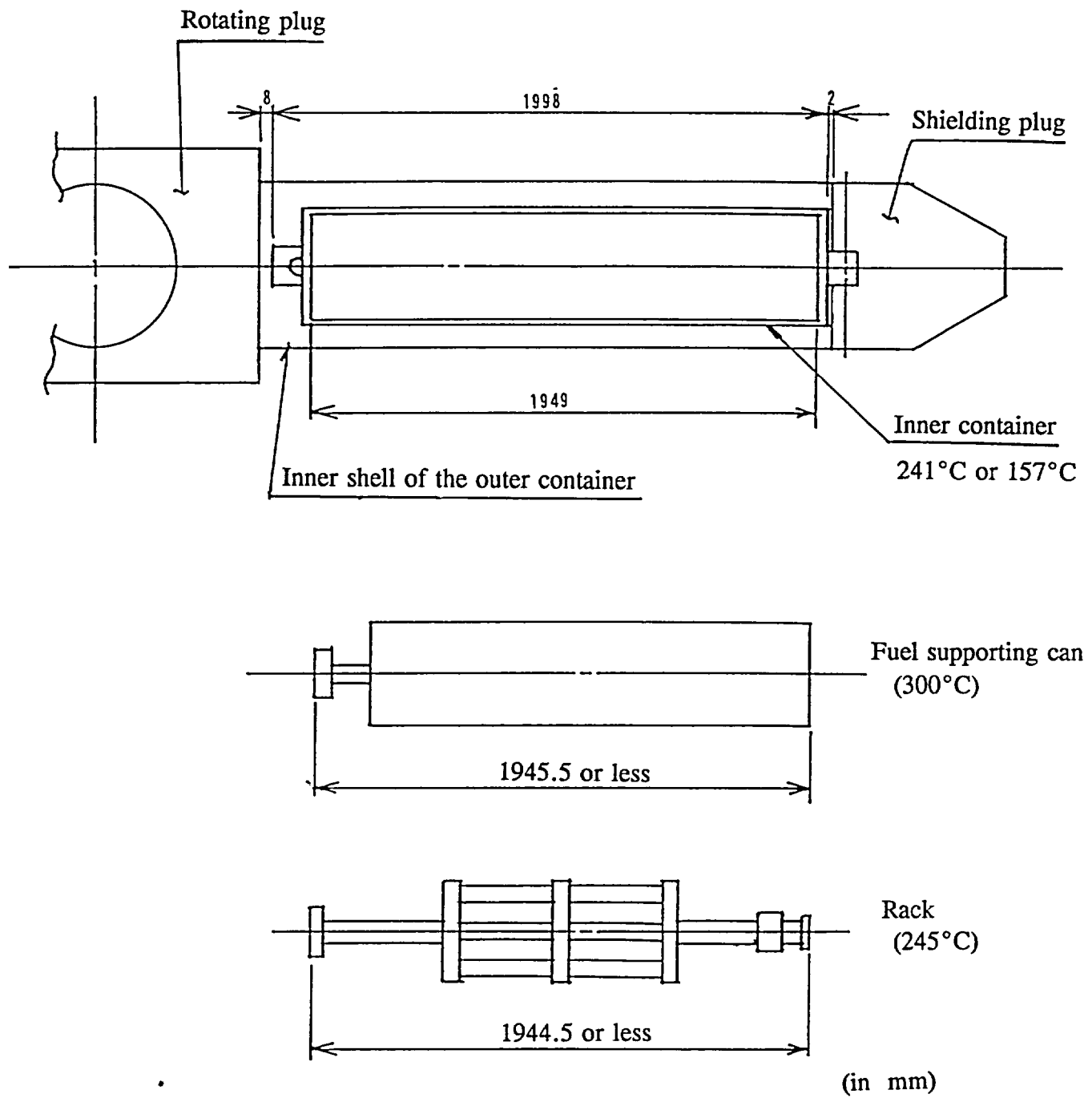


Fig. (II)-A.17 Dimensions of the Contents Under a Normal Temperature

A.5.1.3 Stress Calculation

In each part of this packaging, the stress caused by the temperature gradient is low. Moreover, the increase in heat load and pressure is also low. Repeated heat loads thus cause no fatigue deformation.

Since the load from the outside was already examined in subsections A.4.4 and A.4.5, it is omitted here. As shown in Table (II)-A.14, moreover, the pressure applied to the inner shell under normal test conditions is 60 kPa(G). Analysis under accident test conditions, shown in subsection A.6.3.2, indicates that the integrity of the containment system is maintained with the internal pressure calculated as 196 kPa(G). Therefore, the stress calculation for an internal pressure of 60 kPa(G) under normal test conditions is omitted.

A.5.1.4 Comparison with the Allowable Stress

Table (II)-A.16 compares the results calculated and analyzed in section A.4 through subsection A.5.1.3 and the design criteria shown in subsection A.1.2. As shown in this table, the evaluation results satisfy the design criteria.

Table (II)-A.16 Comparison with the Allowable Stress (1)

Condi-tions	Analysis items	Design criteria	Design criteria value	Evaluation results	Margin of safety	Remarks					
Normal transport conditions	Low-temperature strength	Can be used at the minimum service temperature. Can be used at the minimum service temperature.		Can be used at a temperature of -40°C. Can be used at a temperature of -40°C.	Meets the criteria. Meets the criteria.						
	Stainless steel (SUS304)										
	Stainless steel (SUS630 H1150)										
	Lead										
	Tungsten										
	Resin										
	Balsa wood										
	Cement										
	Fluoro rubber										
	Lifting devices						Analyzed at a load of the lifting weight multiplied by three.				
	(1) Lifting lugs for horizontal operation										
	Lug ring part							$0.6\sigma_y$	108 N/mm ²	56.8 N/mm ²	0.9
	Lug welding section							$0.6\sigma_y$	108 N/mm ²	20.3 N/mm ²	4.3
	Outer shell							σ_y	180 N/mm ²	4.43 N/mm ²	39
	(2) Lifting trunnions										
	Trunnion							$0.6\sigma_y$	108 N/mm ²	23.7 N/mm ²	3.5
	Trunnion mounting part							σ_y	180 N/mm ²	49.7 N/mm ²	2.6
	Outer shell (Trunnion mounting part)							σ_y	180 N/mm ²	60 0 N/mm ²	2.0
	Outer ring shell							$0.6\sigma_y$	108 N/mm ²	7.26 N/mm ²	14
	End plate							σ_y	180 N/mm ²	79.8 N/mm ²	1.2
								$0.6\sigma_y$	108 N/mm ²	66 2 N/mm ²	0.6
	Tie-down devices						Axial direction 10 G Horizontal direction 5 G Vertical direction 2 G Vector sum of the above				
	(1) Rear base plate welding section							$0.6\sigma_y$	108 N/mm ²	48.5 N/mm ²	1.2
(2) Pivoting trunnion	σ_y							180 N/mm ²	136 N/mm ²	0.32	

Table (II)-A.16 Comparison with the Allowable Stress (2)

Condi-tions	Analysis items	Design criteria	Design criteria value	Evaluation results	Margin of safety	Remarks	
Normal test conditions	(3) Outer shell (Trunnion mounting part)	σ_y	180 N/mm ²	142 N/mm ²	0.27	Evaluated under accident test conditions.	
	Pressure	-	-	-	-		
	Vibration Package	Resonance region	10 Hz or more	61 Hz	Meets the criteria.		
Normal transport conditions	Thermal test					Evaluated under accident test conditions.	
	Thermal expansion	σ_y	174 N/mm ²	83.4 N/mm ²	1.1		
	Inner shell	σ_y	180 N/mm ²	6.4 N/mm ²	27		
	Outer shell	-	-	-	-		
	Stress calculation	-	-	-	-		
	Water spray	No	No	No	No	Meets the criteria.	Meets the criteria.
	Water absorption						
Water swishing	Good	Good	Good	Good			
Free drop	-	-	-	-	-	Evaluated under accident test conditions.	
Stacking test							
Outer shell	σ_y	180 N/mm ²	21.5 N/mm ²	7.4			
Penetration							
Outer shell	Plate thickness	16 mm	2.7 mm	Meets the criteria.			
Free drop onto a corner or onto each of the quarters of each rim	-	-	-	-	-	Not applicable.	

A.5.2 Water Spray

This packaging body has a cylindrical structure. It is designed to prevent water from collecting and being retained on the surface. Since this packaging body also has a smooth stainless steel surface, it has a good water swishing characteristic, and no water absorbent characteristic.

A.5.3 Free Drop

In this package, shock absorbers are installed on both ends of the packaging. The shock absorbers are designed to absorb all the drop energy accumulating in the package when it is dropped.

In the drop analysis from a height of 9 m under A.6, "Accident Test Conditions" (described later), only the shock absorbers become deformed. This drop analysis indicates that the outer container, inner container, fuel supporting can, and supporting can (receiving tube) maintain their soundness.

The weight of this package is less than 11,000 kg, so the drop height under normal test conditions is 0.6 m. As in the case of a free drop from 9 m, therefore, the safety of the package is maintained.

Section D is a "Shield Analysis" conducted considering the change in the dimensions of package due to a free drop from 0.6 m. As part of this evaluation, the deformation of the shock absorbers is evaluated in this subsection.

The deformation and deceleration of the shock absorbers in three drop positions (vertical, horizontal, and corner drops) from a drop height of 0.6 m were calculated by calculation code SHOCK-2 using the drop analysis outlined under A.6, "Accident Test Conditions". Table (II)-A.17 shows the calculation results. The calculation conditions of SHOCK-2 are the same as in the case of a free drop from 9 m. Only the drop height is different. For more information, see subsection A.6.1.

Table (II)-A.17 Free Drop (0.6 m) Calculation Results

Item	Energy (N·mm)	Deceleration (G)	Deformation (mm)
Vertical drop	6.47×10^7	59	15
Horizontal drop	6.47×10^7	40	46
Corner drop	6.47×10^7	17	81

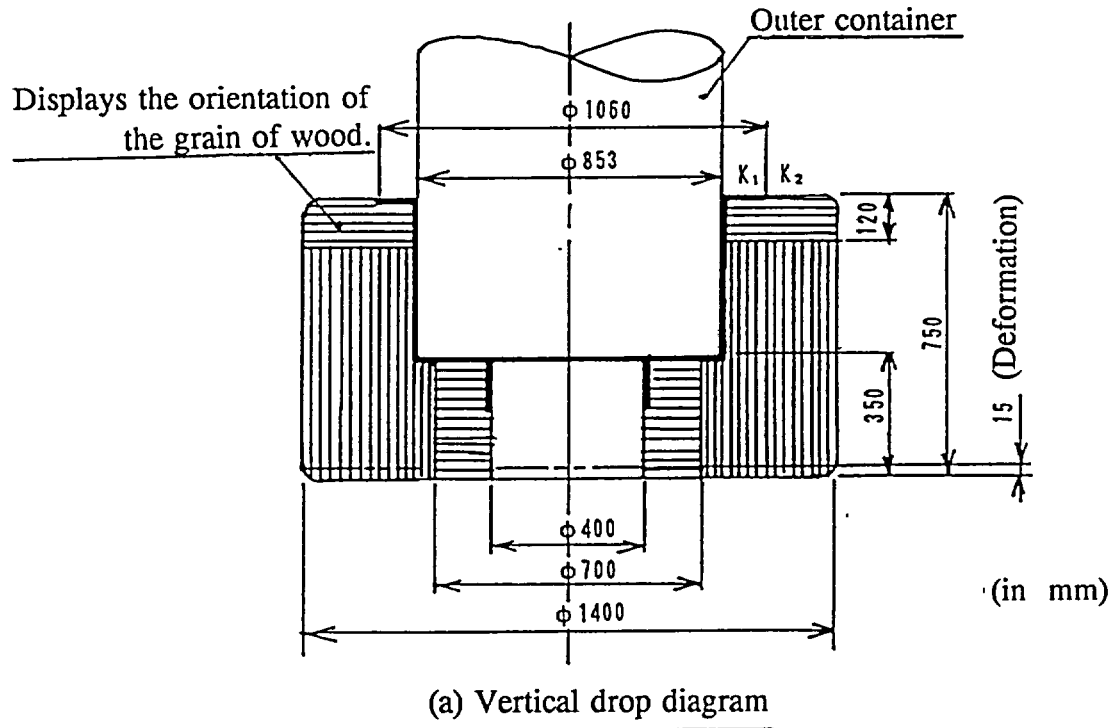


Fig. (II)-A.18 Free Drop (1/2)

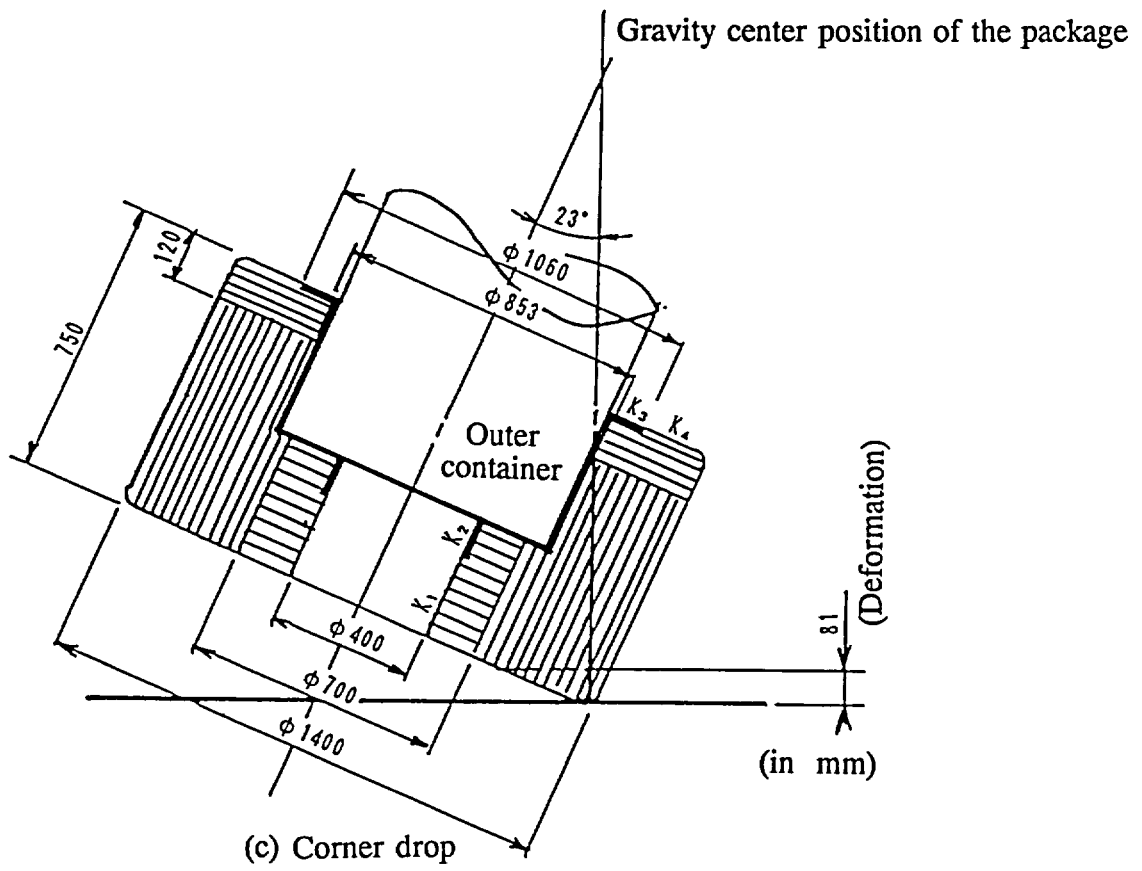
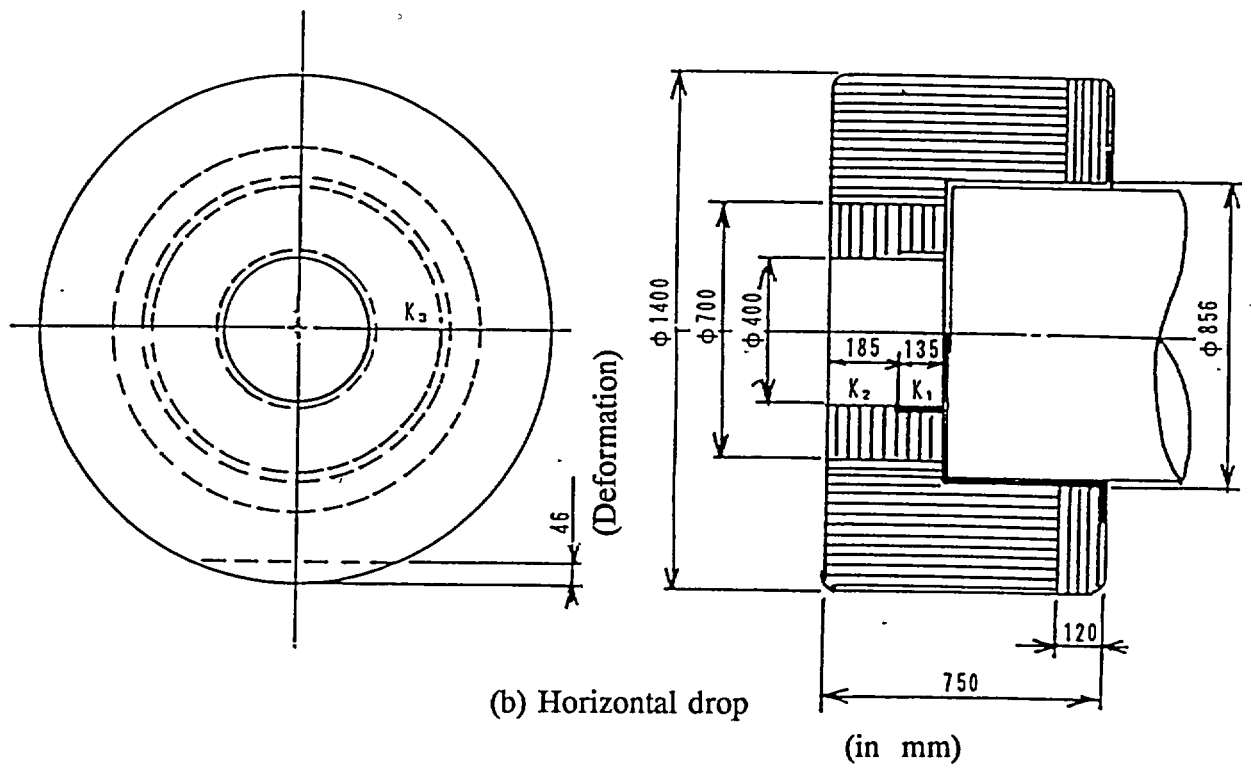


Fig. (II)-A.18 Free Drop (2/2)

A.5.4 Stacking Test

When the load (W_1) corresponding to the weight of this package multiplied by five is compared with the load (W_2) obtained when the vertical projection area is multiplied by 13 kPa ($= 1.3 \text{ N/cm}^2$), the expressions below can be obtained;

$$W_1 = 5W$$

W : Package weight 11,000 kg

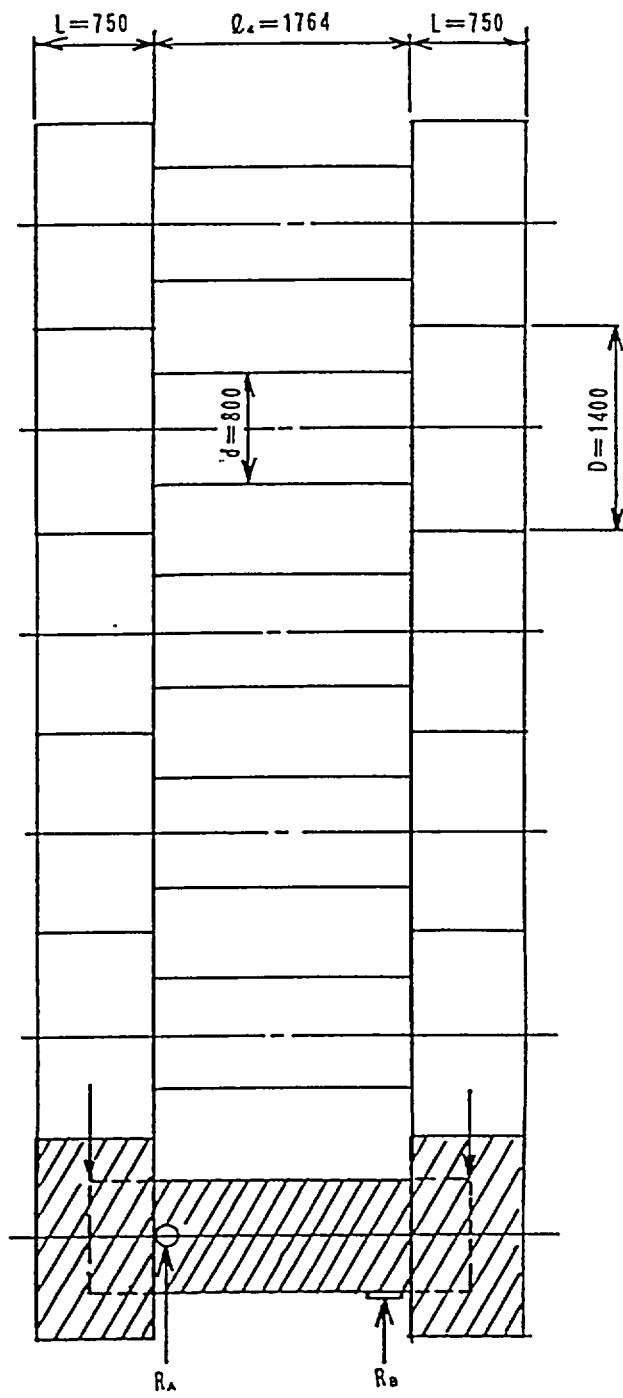
$$\begin{aligned} W_1 &= 9.807 \times 5 \times 11,000 \\ &= 5.39 \times 10^5 \text{ N} \end{aligned}$$

$$W_2 = \{2(D \cdot L) + d l_4\} \times 1.3$$

D : Outer diameter of the shock absorber 140 cm
L : Length of the shock absorber 75 cm
d : Outer diameter of the container body 80 cm
 l_4 : Length of the container body not covered by the shock absorber 176.4 cm

$$\begin{aligned} W_2 &= \{2(140 \times 75) + 80 \times 176.4\} \times 1.3 \\ &= 4.56 \times 10^4 \text{ N} \end{aligned}$$

The former is larger. Therefore, the strength of the package when the load corresponding to the package weight multiplied by five is applied is analyzed. The package at the bottom when five packages are stacked horizontally on the shock absorbers is analyzed as shown in Fig. (II)-A.19. The investigated strength indicates that the outer shell to which the load from the shock absorbers and the load multiplied by five is applied is not deformed, and that the package can withstand a compression test.



(in mm)

Fig. (II)-A.19 Stacking Test

For an analysis model, the load based on the weight of the shock absorbers and the weight of five stacked packages thereon is assumed to act on the end surfaces of the outer container. The weight of the package (not including the shock absorbers) is distributed uniformly throughout the resin layer, which acts on the outer shell. Therefore, this weight is treated as a uniform load.

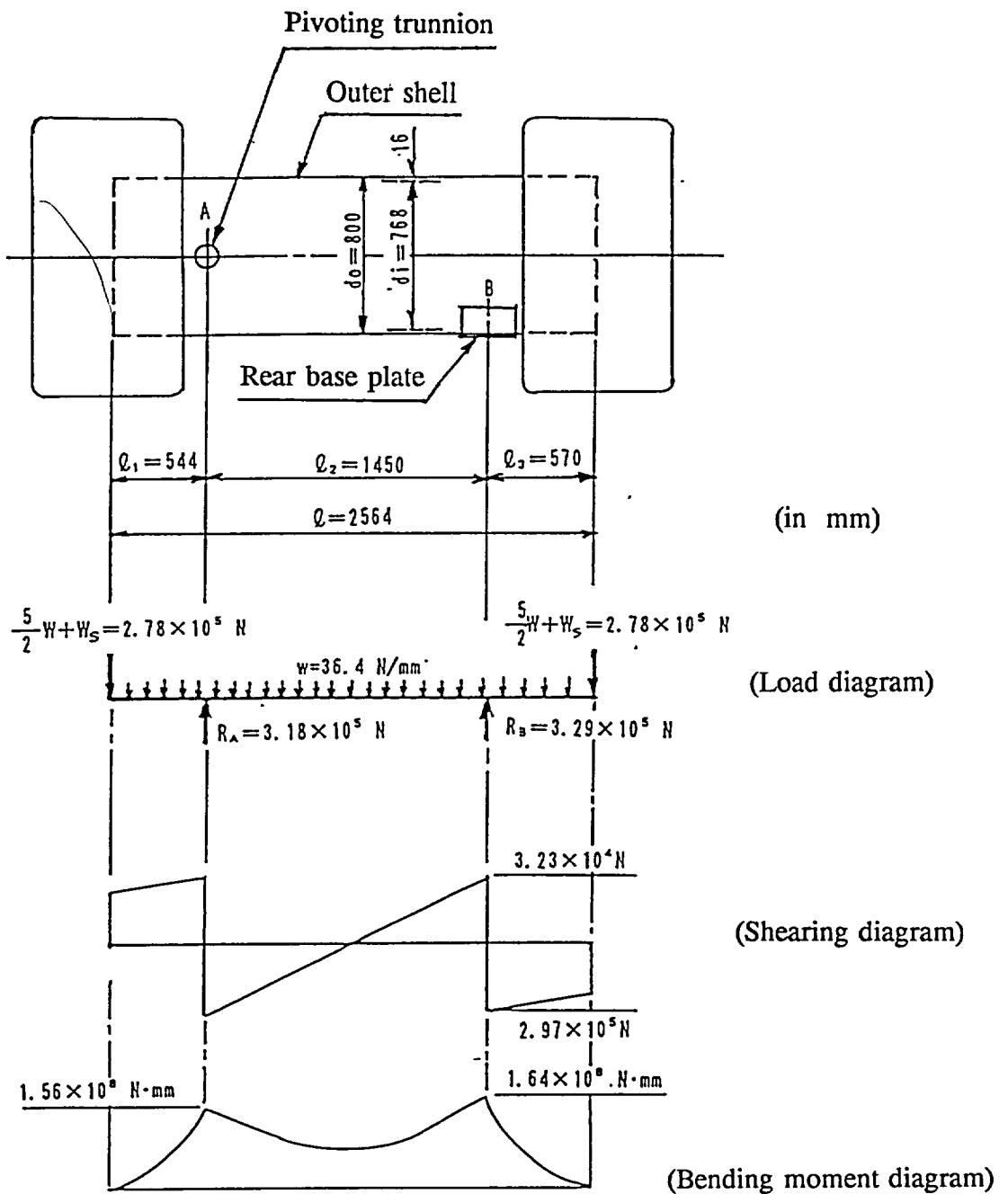


Fig. (II)-A.20 Analysis Diagram of the Stacking Test

On the basis of the balancing conditions of the force and the moment around point A, shown in Fig. (II)-A.20, the load (R_A) applied to the pivoting trunnion and the load (R_B) applied to the rear base plate are given by the expression below.

$$6W + R_A + R_B = 0$$

$$\left(\frac{5}{2} W + W_s\right)l_1 + \frac{1}{2} w l_1^2 = R_B l_2 + \left(\frac{5}{2} W + W_s\right)(l_2 + l_3) + \frac{1}{2} w(l_2 + l_3)^2$$

W	: Package load	$9.807 \times 11000 = 1.08 \times 10^5 \text{ N}$
W_s	: Shock absorber weight	$9.807 \times 750 = 7.35 \times 10^3 \text{ N}$
R_A	: Load applied to the pivoting trunnion	
R_B	: Load applied to the rear base plate	
l_1	: Moment arm (See Fig. (II)-A.20.)	544 mm
l_2	: Moment arm (See Fig. (II)-A.20.)	1450 mm
l_3	: Moment arm (See Fig. (II)-A.20.)	570 mm
l	: Length of the packaging body	2564 mm
w	: Uniform load based on the packaging body	

$$w = \frac{W - 2W_s}{l}$$

$$= \frac{10.8 \times 10^5 - 2 \times 7.35 \times 10^3}{2564}$$

$$= 36.4 \text{ N/mm}$$

From the two expressions above, R_A and R_B can be obtained;

$$R_A = -3.18 \times 10^5 \text{ N}$$

$$R_B = -3.30 \times 10^5 \text{ N}$$

Fig. (II)-A.20 shows the load distribution for the outer shell. To obtain the bending moment, first the load is integrated by a distance from the front end of the outer container in order to obtain the shearing force, and then the shearing force is integrated by the distance.

The shearing force $F(x)$ and bending moment $M(x)$ at " x " mm away from the front end of the outer container are given by the expressions below.

Position	Shearing force	Bending moment
$0 \leq x < 544$	$F(x) = \left(\frac{5}{2}W + W_s\right) + wx$ $= \left(\frac{5}{2}1.08 \times 10^5 + 7.35 \times 10^3\right) + 36.4x$ $= 2.77 \times 10^5 + 36.4x$	$M(x) = \left(\frac{5}{2}W + W_s\right)x + \frac{1}{2}wx^2$ $= 2.77 \times 10^5 x + \frac{1}{2} \times 36.4 \times x^2$ $= 2.77 \times 10^5 x + 18.2x^2$

$$\begin{array}{ll}
544 \leq x < 1994 & F(x) = \left(\frac{5}{2}W + W_s\right) + R_A + wx \\
& = 2.77 \times 10^5 - 3.18 \times 10^5 + 36.4x \\
& = -4.10 \times 10^4 + 36.4x \\
& M(x) = \left(\frac{5}{2}W + W_s\right)x + R_A(x - \ell_1) \\
& \quad + R_B(x - \ell_1 - \ell_2) + \frac{1}{2}wx^2 \\
& = 2.77 \times 10^5 x - 3.18 \times 10^5 \\
& \quad \times (x - 544) + 18.2x^2 \\
& = 1.73 \times 10^8 - 4.1 \times 10^4 x + \\
& \quad 18.2x^2 \\
1994 \leq x < 2564 & F(x) = \left(\frac{5}{2}W + W_s\right) + R_A + R_B + wx \\
& = 2.77 \times 10^5 - 3.18 \times 10^5 \\
& \quad - 3.30 \times 10^5 + 36.4x \\
& = -3.71 \times 10^5 + 36.4x \\
& M(x) = \left(\frac{5}{2}W + W_s\right)x + R_A(x - \ell_1) + \\
& \quad R_B(x - \ell_1 - \ell_2) + \frac{1}{2}wx^2 \\
& = 2.77 \times 10^5 x - 3.18 \times 10^5 \\
& \quad \times (x - 544) - 3.29 \times 10^5 (x - 544 \\
& \quad - 1450) + 18.2x^2 \\
& = 8.31 \times 10^8 - 3.71 \times 10^5 + \\
& \quad 18.2x^2
\end{array}$$

As shown in Fig. (II)-A.20, the maximum bending moment is generated at point B. The magnitude of the maximum bending moment is as follows:

$$M = 1.64 \times 10^8 \text{ N}\cdot\text{mm}$$

The plate thickness of the outer shell is 16 mm and partly 40 mm. It is assumed here that this bending moment acts on the outer shell with a plate thickness of 16 mm. In this case, the bending stress (σ) is given by

$$\sigma = \frac{M}{Z}$$

where

Z : Section modulus of the outer shell

$$Z = \frac{\pi}{32} \left(\frac{d_o^4 - d_i^4}{d_o} \right)^{1)}$$

d_o : Outer diameter of the outer shell 800 mm

1) Nihon Kokai Gakkai: Kikai Kogaku Benran, p. 4-51, 1979
(The Japan Society of Mechanical Engineers: Handbook of Mechanical Engineering, page 4-51, 1979)

d_i : Inner diameter of the outer shell

768 mm

$$Z = \frac{\pi}{32} \left(\frac{800^4 - 768^4}{800} \right)$$
$$= 7.57 \times 10^6 \text{ mm}^3$$

$$\sigma = \frac{1.64 \times 10^8}{7.57 \times 10^6}$$
$$= 21.5 \text{ N/mm}^2$$
$$\approx 2.2 \text{ kg/mm}^2$$

The design criterion value of the outer shell is $\sigma_y = 180 \text{ N/mm}^2$ ($\approx 18.4 \text{ kg/mm}^2$) (at a temperature of 80°C). The margin of safety (M.S.) is thus given by the expression below.

$$M.S. = \frac{180}{21.5} - 1$$
$$= 7.4$$

No deformation occurs in the outer shell. The soundness of the package is not damaged even if a compression load multiplied by five is applied.

A.5.5 Penetration

This subsection demonstrates the amount of deformation of the outer container when the specified mild steel bar (32 mm in diameter and weighing 6 kg) is dropped on the container from a height of 1 m. The deformation analysis assumes that the mild steel bar drops on the thin part of the outer shell (a plate thickness of 16 mm).

The effect of the resin layer is not considered in this case. The deformation is analyzed assuming that the drop energy of the mild steel bar is absorbed by only the outer shell. Fig. (II)-A.21 shows the analysis model.

The drop energy (U) of the mild steel bar is given by

$$U = WH$$

W : Weight of the mild steel bar 6 kg
H : Drop height 1000 mm

$$U = 6 \times 9.807 \times 1000 \\ = 5.88 \times 10^4 \text{ N}\cdot\text{mm}$$

Assume that the outer shell is deformed in a spherical form by δ mm when the mild steel bar strikes it. The volume (V) of the deformed part is given by the expression below.

$$V = \frac{1}{3}\pi\delta^2(3r - \delta) \quad 1)$$

δ : Deformation depth of the outer shell
r : Radius of the mild steel bar tip 16 mm

The absorption energy (E) of the outer shell is given by

$$E = \sigma_s V$$

σ_s : Deformation stress of the outer shell
(Uses a yield stress to be on the safe side.) 180 N/mm²

Deformation (δ) can be summarized as follows so that the drop energy (U) equals the absorption energy (E):

$$\delta^3 - 3r\delta^2 + \frac{3U}{\pi\sigma_s} = 0$$

The value below can then be obtained.

$$\delta = 2.7 \text{ mm}$$

Consequently, the amount of deformation is slighter than the plate thickness (16 mm) of the outer shell. As a result, no penetration occurs in this case.

1) Kikai Sekkei Benran, p. 73, Maruzen, 1973
(Handbook of Mechanical Design, page 73, Maruzen, 1973)

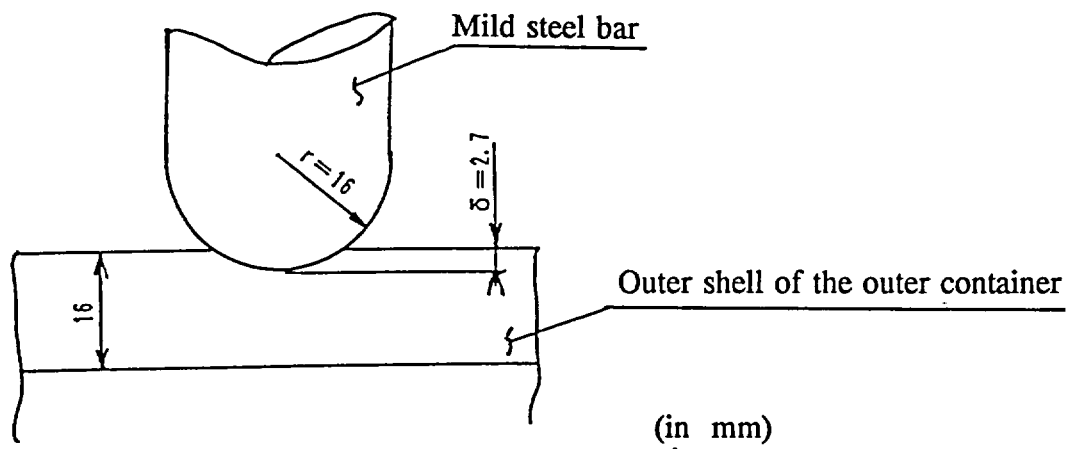


Fig. (II)-A.21 Penetration Test for the Outer Shell

A.5.6 Free Drop onto a Corner or onto Each of the Quarters of Each Rim

This packaging weighs approximately 11,000 kg. This drop condition does not apply because this packaging is heavier than 100 kg.

A.5.7 Summary and Evaluation of Results

The results of the evaluations under normal test conditions are summarized for every test item.

(1) Thermal test

The results indicate that the thermal stresses induced in the outer container, fuel supporting cans and receiving tubes, which make up the containment system, do not exceed the allowable stress.

(2) Free drop

The evaluation test demonstrates the amount of deformation of the shock absorbers for each drop attitude. The results show that the resulting deformation does not exceed the allowable degree of deformation and does not reach the outer container. The stress on the outer container, resulting from the deceleration due to the deformation of the shock absorber, was analyzed taking into account the effect of the steel plate covering the balsa wood. The results show that each part material maintains its requisite strength.

(3) Stacking test

The results indicate that the stress to which the outside containment system (including the outer container) is subjected during the stacking test does not exceed the allowable stress. Therefore, the containment system maintains its strength.

(4) Penetration

The effects of dropping a mild steel bar on the section with the minimum plate thickness of the outer shell were analyzed. The results show that no penetration occurs.

The above results demonstrate that this package maintains its requisite performance and strength.

Next, the results of the structural evaluation will be incorporated in the manner described below for the thermal analysis, containment analysis and shield analysis.

(a) Thermal analysis

In thermal analysis under normal test conditions, the shock absorber has an insulating function. As the shock absorber becomes thicker, its internal temperature increases. Therefore, an analysis is performed on the assumption that no shock absorber is deformed due to a free drop.

(b) Containment analysis

The structural evaluation indicates that the containment system (including the outer container's inner shell and lids) is sound. The secondary containment system (including the fuel supporting cans and receiving tubes) is also sound. In the containment analysis, therefore, any leak of radioactive material is evaluated on the assumption that the containment system is sound.

(c) Shielding analysis

Under normal test conditions, the shock absorber is deformed by a free drop, which reduces the dimensions of the package. An analysis is performed keeping this effect in mind.

(d) Criticality analysis

Under normal test conditions, to be on the safe side, an analysis is performed on only the package body without considering the shock absorbers. The structural evaluation results show that the outer container provides sufficient strength and that no water flows into the inner shell. However, to be on the safe side, this analysis is performed assuming that water does flow in.

A.6 Accident Test Conditions

This package is a type B(U) package. The accident test conditions are as follows:

(i) Mechanical test

Drop test-I (9-m free drop) or drop test-III (dynamic crush test)

Drop test-II (1-m penetration drop)

(ii) Thermal test

(iii) Water immersion test

This package weighs 11,000 kg. Drop test-III (dynamic collapsing test) is not applied to this package since it exceeds 500 kg.

The order of the mechanical test must be fixed so that maximum damage occurs in the thermal test performed after this test. Only the shock absorber is deformed during the mechanical test. If drop test-II is successively carried out after drop test-I, local deformation occurs cumulatively in addition to uniform deformation. If drop test-I is carried out after drop test-II, the local deformation generated by drop test-II will be included in the uniform deformation generated by drop test-I where the deformations caused by drop tests I and II are not cumulative. Therefore, in this section an evaluation shall be conducted assuming that the package is subjected to drop test II after the completion drop test I, from which a larger deformation is expected.

A.6.1 Mechanical Test - Drop Test-I (with a 9-m drop)

The deformation of the package when a package is dropped from a height of 9 m is evaluated. Table (II)-A.18 shows the possible drop attitude and a summary of the obtained results.

Table (II)-A.18 Drop Attitude of a 9-m Drop Test (1/2)

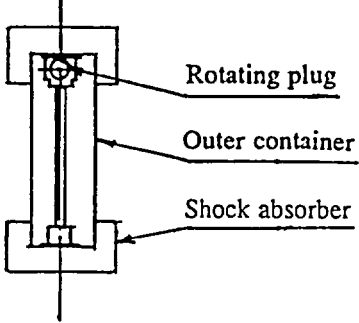
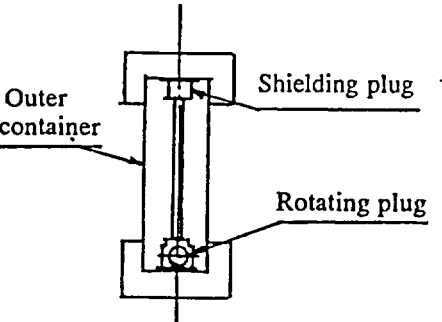
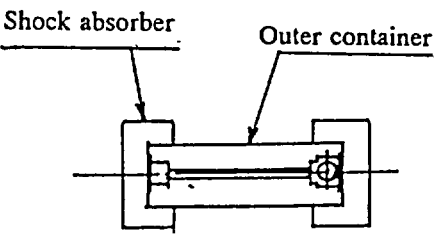
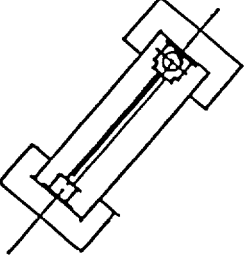
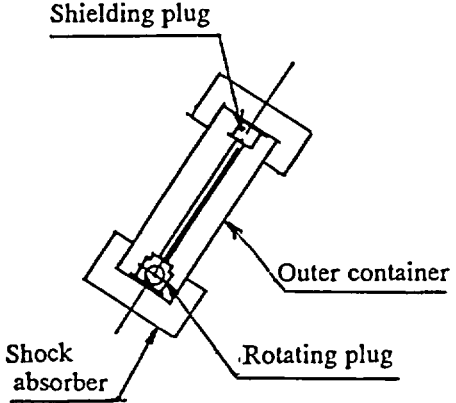
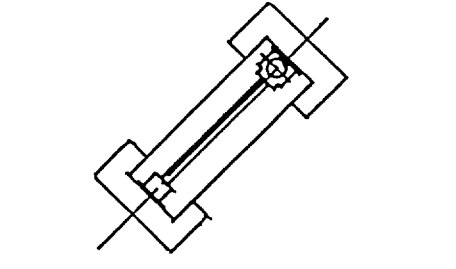
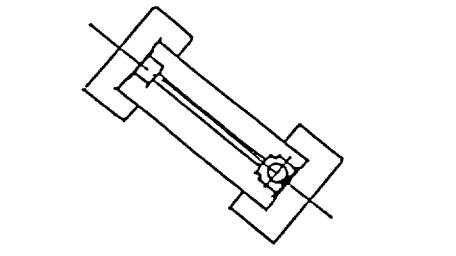
Drop attitude	Sketch	Collision status	Status evaluation after collision
Vertical drop Vertical drop from the rear end first		<ul style="list-style-type: none"> - The shock absorber collides with the target. 	<ul style="list-style-type: none"> - The shock absorber becomes deformed, but the outer container, inner container, fuel supporting can, and receiving tubes remain sound.
Vertical drop from the front end first		<ul style="list-style-type: none"> - The shock absorber collides with the target. 	<ul style="list-style-type: none"> - The shock absorber becomes deformed. - The screw, which connects the inner container with shielding plug, is damaged, but the inner container, and fuel supporting can or receiving tubes remain sound. - The outer container (except the shielding plug connecting part mentioned above) remains sound.
Horizontal drop		<ul style="list-style-type: none"> - The shock absorber collides with the target. 	<ul style="list-style-type: none"> - The shock absorber becomes deformed, but the outer container, inner container, and fuel supporting can or receiving tubes remain sound.
Corner drop Corner drop from the rear end first		<ul style="list-style-type: none"> - The shock absorber collides with the target. 	<ul style="list-style-type: none"> - The shock absorber becomes deformed, but the outer container, inner container, and fuel supporting can or receiving tubes remain sound.

Table (II)-A.18 Drop Attitude of a 9-m Drop Test (2/2)

Drop attitude	Sketch	Collision status	Status evaluation after collision
<p align="center">Corner drop</p> <p>Corner drop from the front end first</p>		<ul style="list-style-type: none"> - The shock absorber collides with the target. 	<ul style="list-style-type: none"> - The shock absorber becomes deformed. - The screw, which connects the inner container with shielding plug, is damaged, but the inner container, and fuel supporting can or receiving tubes remain sound. - The outer container (except the shielding plug connecting part mentioned above) remains sound.
<p align="center">Oblique drop</p> <p>Oblique drop from the rear end first</p>		<ul style="list-style-type: none"> - The shock absorber collides with the target. 	<ul style="list-style-type: none"> - The shock absorber becomes deformed, but the outer container, inner container, and fuel supporting can or receiving tubes remain sound.
<p align="center">Oblique drop</p> <p>Oblique drop from the front end first</p>		<ul style="list-style-type: none"> - The shock absorber collides with the target. 	<ul style="list-style-type: none"> - The shock absorber becomes deformed. - The inner screw, which connects the inner container with shielding plug, is damaged, but the inner container, and fuel supporting can or receiving tubes remain sound. - The outer container (except the shielding plug connecting part mentioned above) remains sound.

(a) Analysis

The results of each drop test shall be evaluated by applying analytical methods.

This package has shock absorbers installed on both ends of its cylindrical body. During a drop test, the drop energy is absorbed by the deformation of these shock absorbers. Reduced deceleration thus acts on the packaging body. The deceleration at that time and the deformation of the shock absorbers are calculated by the calculation code, SHOCK-2. This calculation code numerically determines the degree of balsa wood deformation and the impact deceleration under the assumption that deformation continues until the deformation energy equals the drop energy absorbed by the package.

$$E = WH$$

$$E = \int_0^{\delta} A(\epsilon)F(\epsilon)d\epsilon$$

$$G = \frac{A(\delta) \cdot F(\delta)}{W}$$

W	: Package weight
H	: Drop height
A(ϵ)	: Cross-sectional area of the part where the balsa wood is deformed
F(ϵ)	: Balsa wood deformation - Stress curve
G	: Impact deceleration
δ	: Shock absorber deformation

Assuming that the inertia force based on the impact deceleration obtained by this calculation acts on each part of the packaging, a strength analysis is performed to indicate that the package is sound.

(b) Prototype test

The results of a drop test on this package shall be evaluated by applying an analytical method. A prototype test is not performed in this case.

(c) Model test

Drop test-I and drop test-II were conducted using a 1/2-scale model package that faithfully simulates the mechanical block of this packaging's rotating plug. Deceleration, deformation, strain, and leakage rates were then measured. A comparison of these experimental results and the calculation results indicates that the evaluation results of this package are on the safe side. For more information regarding this experiment, see the attached papers 3.

A.6.1.1 Vertical Drop

(1) Vertical drop, with the rear end striking first

The deformation and impact deceleration when the packaging is dropped on the shielding plug part (rear lid unit) first (hereafter called "a rear-end-first vertical drop") are obtained by the calculation code SHOCK-2. This indicates that deformation occurs only in the shock absorber. The stress at each part is obtained assuming that the inertia force based on the obtained deceleration acts on each part of the packaging. This stress is evaluated to indicate that each material of the packaging has the necessary strength.

In the case of a rear-end-first vertical drop, the numeric value is calculated by the calculation code SHOCK-2. Fig. (II)-A.22 shows the analysis model and shape for vertical drop. For the vertical drop, the section of the shock absorber that is in contact with the outer container is made of a stainless steel plate that has a plate thickness exceeding 10 mm. The shock absorber is firmly constrained against the possible compressive deformation in balsa wood due to drops. However, the section except the parts shown by a thick line in Fig. (II)-A.22 is coated with a stainless steel plate that is 3-mm thick, and the balsa wood is not sufficiently constrained against the compressive deformation. For the section of the balsa wood that firmly is restrained, therefore, the shape coefficient should be $K_1 = 1.0$. The shape coefficient of the section that is restrained by a stainless steel plate that is 3-mm thick in its outer circumference should be $K_2 = 0.75$. (The $K_2 = 0.75$ in this case indicates that the energy absorption by the compressive deformation is 75%. This value is calculated based on the results of the experiment.)

Drop energy $E = 9.71 \times 10^8 \text{ N}\cdot\text{mm}$ is substituted and the numeric value is calculated by the calculation code SHOCK-2. The following values are therefore then obtained.

Shock absorber deformation	110 mm
Impact deceleration	130 G

The deformation of the shock absorber corresponds to approximately 70% of the axial allowable thickness (approximately 185 mm) of the shock absorber. No deformation occurs in the packaging body.

Since, in this analysis, the effects of the covering steel plate are not taken into account, the evaluation of the influence of the steel plate is shown in attached document 1. As a result, an additional deceleration of approximately 4 G because of the covering plate is found to be generated. Therefore, to be on the safe side, this deceleration is added to the result calculated by the code, SHOCK-2, and the stress generated in the parts below is obtained to indicate that they are sound on the basis of the assumption that an acceleration of 135 G acts on the container in the axial direction.

- (a) Outer shell
- (b) Inner shell
- (c) Shielding plug lid flange part
- (d) Sampling valve lid part fastening bolt
- (e) Inner container
- (f) Fuel supporting can (for Contents I)
- (g) Rack supporting rod, rack end plate, and receiving tube (for Contents II)

Shape	See Fig. (II)-A.22.
Balsa wood Strain - stress curve	See Fig. (II)-A.3.
Shape coefficient	$K_1 = 1.0$ $K_2 = 0.75$
Drop energy	$E = 9.71 \times 10^8 \text{ N}\cdot\text{mm}$

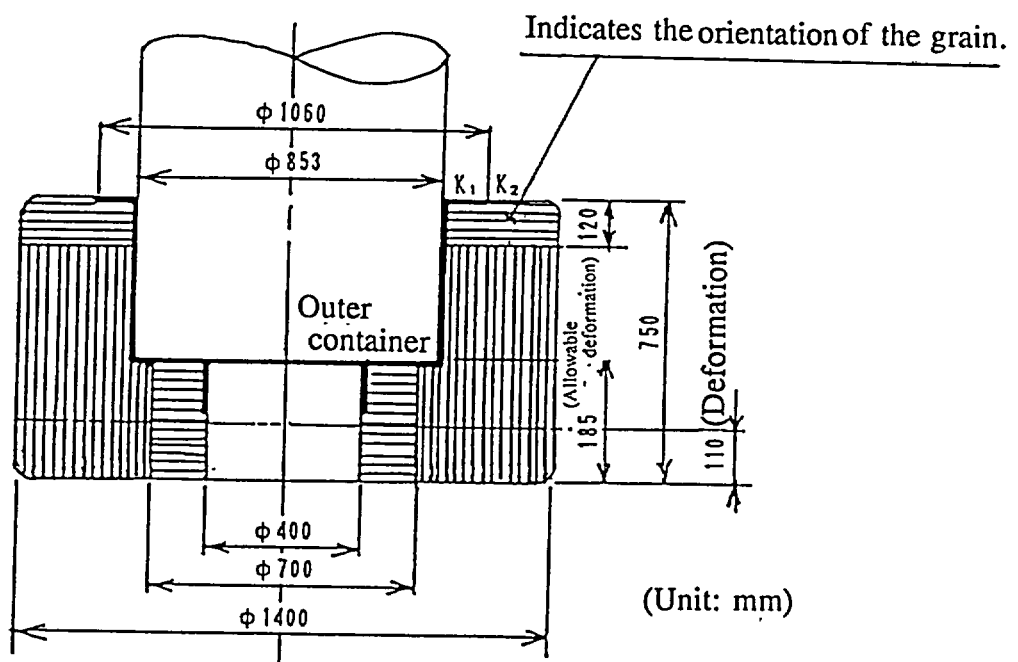


Fig. (II)-A.22 Vertical Drop

(a) Outer shell

In the case of a vertical drop, compression stress is generated in the shell of the container body by impact acceleration. Assuming that all of the inertia force by package weight acts on the outer shell to be on the safe side, the stress generated in the outer shell will be obtained to indicate that the outer shell has sufficient strength against the compression load. The inertia force (F) that acts on the outer shell is given by the expression below.

$$F = W \cdot G$$

where

W : Package weight 11,000 kg
G : Impact acceleration 135 G

and thus

$$F = 9.807 \times 11,000 \times 135 \\ = 1.46 \times 10^7 \text{ N}$$

Assuming that this inertia force acts on the outer shell, an outer shell section with a plate thickness of 16 mm is evaluated. A fusible plug (shown in Fig. (II)-A.23) that discharges gas during thermal testing is installed in the outer shell section, which also has a plate thickness of 16 mm. Taking account of the practical thickness reduction of the outer shell due to the installation of the fusible plug, the compression stress σ generated in the outer shell is given by the expression below.

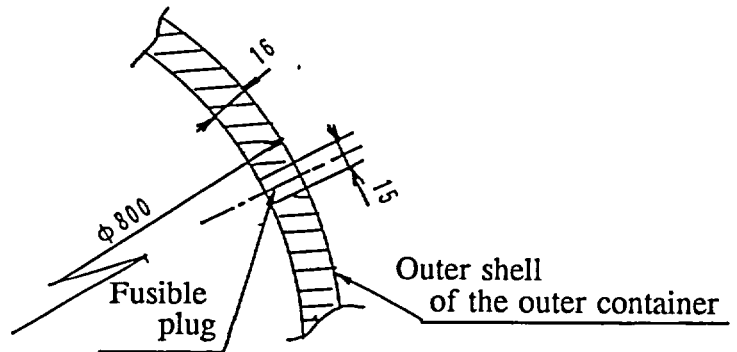


Fig. (II)-A.23 Outer Shell of the Outer Container

$$\sigma = \frac{F}{S}$$

where

S : Cross-sectional area of the outer shell

$$S = \frac{\pi}{4} (d_1^2 - d_2^2) - ntd$$

d_1 : Outer diameter of the outer shell 800 mm
 d_2 : Inner diameter of the outer shell 768 mm
n : Number of fusible plugs on the periphery of a given cross section of the outer shell 4

t	: Plate thickness of the outer shell	16 mm
d	: Mean diameter of the penetration hole for the fusible plugs	15 mm

$$S = \frac{\pi}{4}(800^2 - 768^2) - 4 \times 16 \times 15$$

$$= 3.84 \times 10^4 \text{ mm}^2$$

The expression below is given when each of the numeric values are substituted.

$$\sigma = \frac{1.46 \times 10^7}{3.84 \times 10^4}$$

$$= 380 \text{ N/mm}^2$$

$$\approx 38.8 \text{ kg/mm}^2$$

The temperature of the outer shell (SUS304) is 72°C. If the value $\sigma_{UD} = 496 \times 1.2 = 595 \text{ N/mm}^2$ ($\approx 61 \text{ kg/mm}^2$) at a temperature of 80°C is assumed to represent the dynamic tensile strength, the margin of safety (M.S.) is given by

$$M.S. = \frac{595}{380} - 1$$

$$= 0.6$$

The outer shell has sufficient strength against the compression load applied during a vertical drop. It is therefore not damaged in this case.

(b) Inner shell

Assuming that all of the inertia force generated by a rotating plug acts on the inner shell during a vertical drop on the rear end first, as shown in Fig. (II)-A.24, the compression stress generated in the inner shell is obtained to indicate that the inner shell has sufficient strength against the compression load. The inertia force (F) that acts on the inner shell is given by the expression below.

$$F = W.G$$

where

W	: Weight of the rotating plug, rotating plug lid, and rotating plug lid cover	420 kg
G	: Impact acceleration	135 G

and thus

the expression below is obtained.

$$F = 9.807 \times 420 \times 135$$

$$= 5.56 \times 10^5 \text{ N}$$

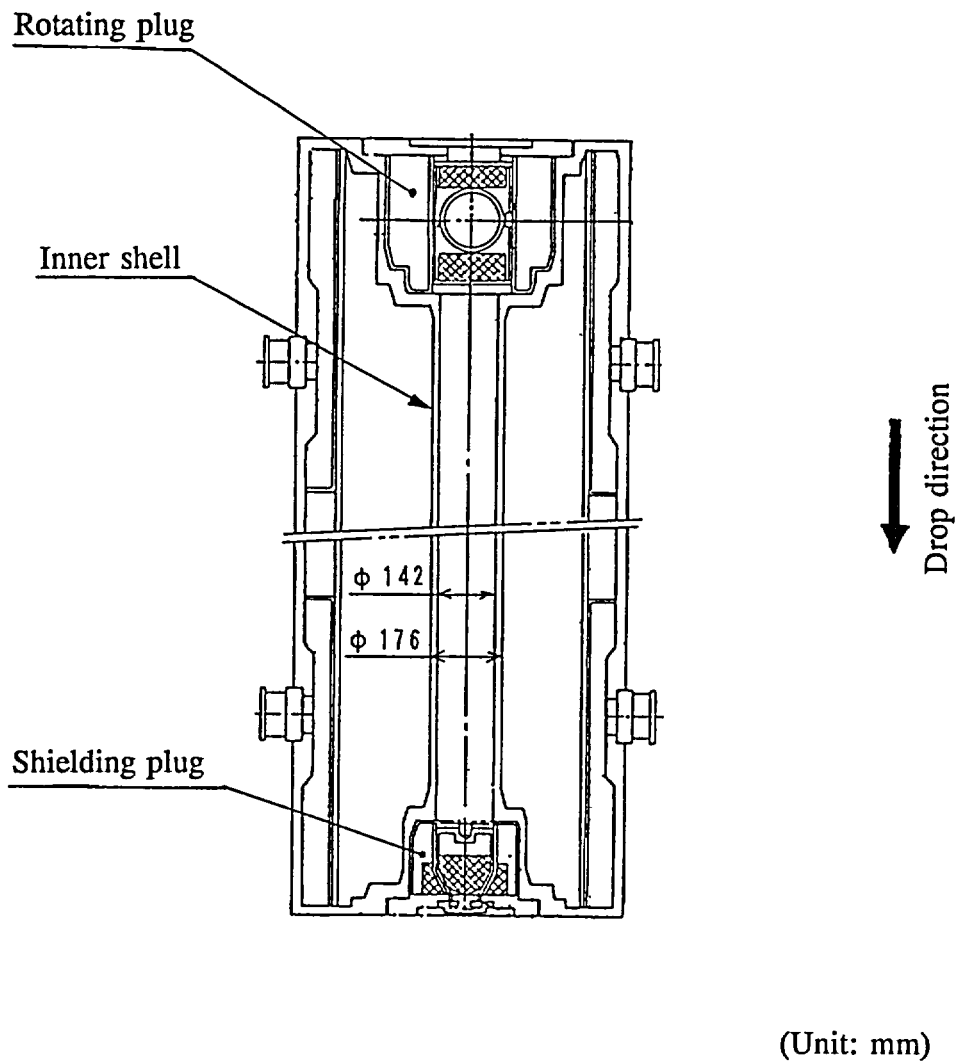


Fig. (II)-A.24 Analysis Model of the Inner Shell

Compression stress σ generated in the inner shell is given by

$$\sigma = \frac{F}{S}$$

where

S : Cross-sectional area of the inner shell

$$S = \frac{\pi}{4} (d_1^2 - d_2^2)$$

d_1 : Outer diameter of the inner shell

176 mm

d_2 : Inner diameter of the inner shell

142 mm

$$S = \frac{\pi}{4} (176^2 - 142^2)$$

$$= 8.49 \times 10^3 \text{ mm}^2$$

The results below are obtained when each of the numeric values are substituted.

$$\sigma = \frac{5.56 \times 10^5}{8.49 \times 10^3}$$

$$= 66 \text{ N/mm}^2$$

$$\approx 6.8 \text{ kg/mm}^2$$

The temperature of the inner shell (SUS304) is 85°C. If the yield stress $\sigma_y = 174 \text{ N/mm}^2$ ($\approx 17.7 \text{ kg/mm}^2$) at a temperature of 90°C is used as the criterion, the margin of safety (M.S.) is given by

$$M.S. = \frac{174}{66} - 1$$

$$= 1.6$$

The inner shell has sufficient strength to handle the compression load applied during a vertical drop. It is therefore not damaged in this case.

(c) Flange part of the shielding plug lid

The shielding plug lid is installed with the rear lid during a rear-end-first vertical drop as shown in Fig. (II)-A.25. This section also uses O-rings to form the boundary of containment. The stress and deflection generated are obtained using the finite element calculation code ANSYS. The results will be obtained to indicate that containment is maintained without damage to the rear lid unit. Fig. (II)-A.26 shows the loading model and the analysis model. The inner shell has a penetration section for the sampling valve. Since the inner diameter of the penetration section is small and is completely strengthened by a seat, it is ignored.

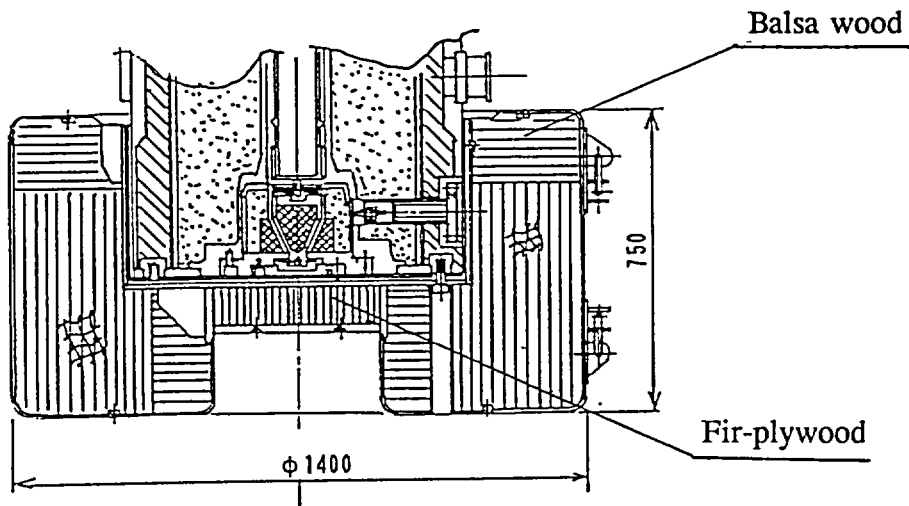
The loading conditions, supporting conditions, and the material's physical property values in this model are described below and given as the calculation conditions.

(1) Loading conditions

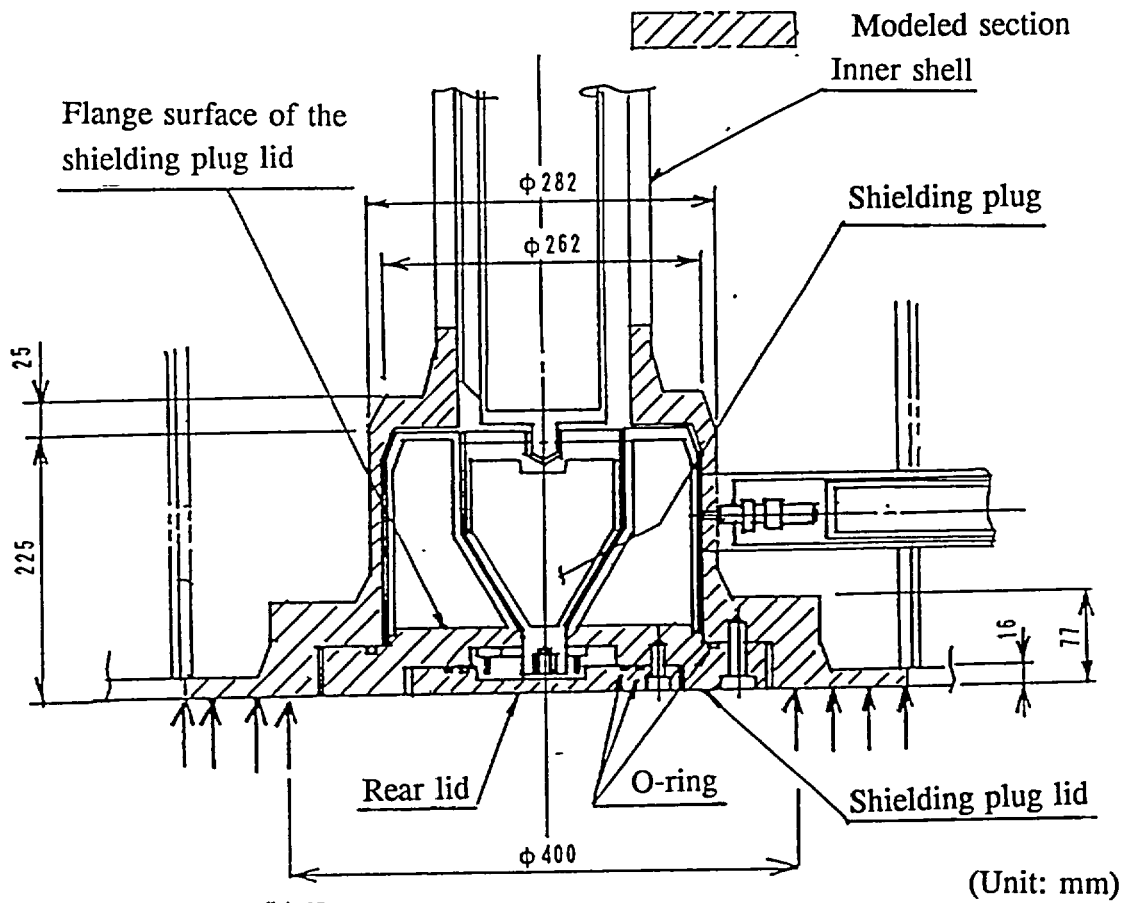
(1.1) Load (P_1) that acts on the inside of the plug lid flange

This load is generated by the contents, the shielding plug, and the shielding plug lid. This load also uniformly acts on the surface of the shielding plug lid flange through the shielding lead. It thus approximates the uniform load as described below.

$$P_1 = \frac{(W_1 + W_2) \cdot G}{\frac{\pi}{4} (d_1^2 - d_2^2)}$$



(a) Assembly of rear shock absorber and rear lid unit



(b) Expanded sketch of the rear lid

Fig. (II)-A.25 Rear Lid Unit (Rear-End-First Vertical Drop)

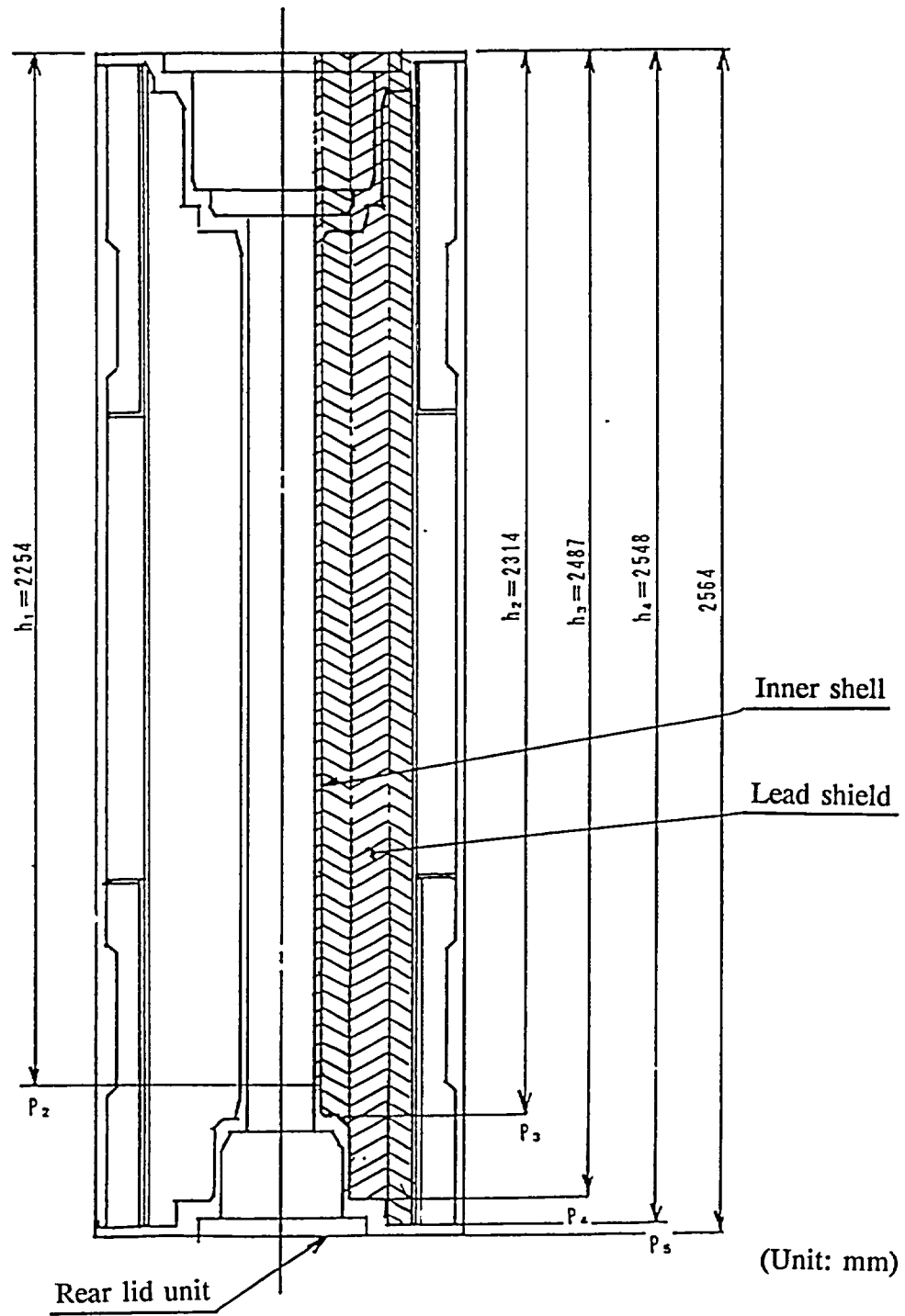


Fig. (II)-A.26 (1/2) Loading Model of the Rear Lid Unit

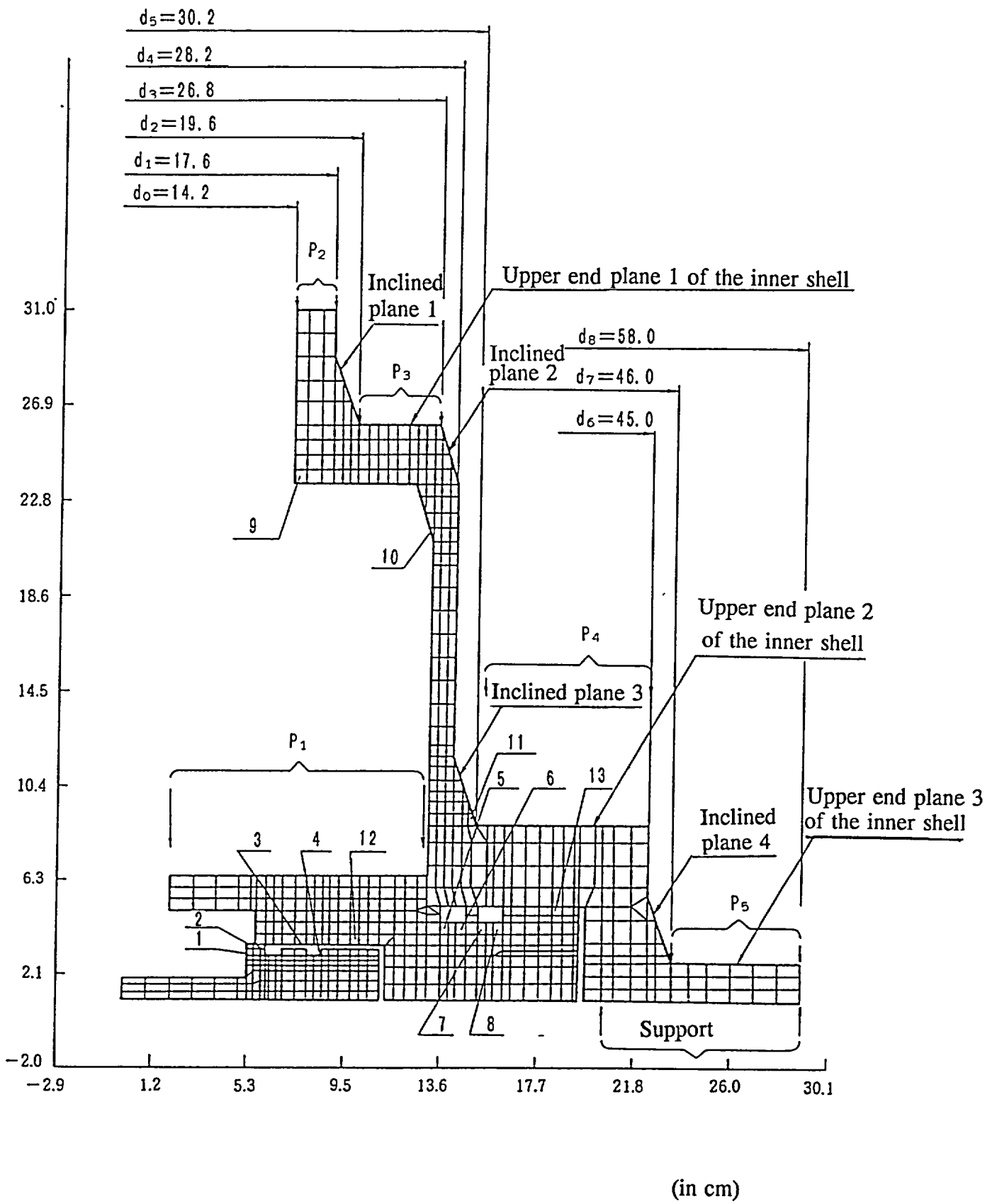


Fig. (II-A.26 (2/2) Analysis Model of the Rear Lid Unit

where

W_1	: Weight of the contents (See Table (II)-A.4.)	100 kg
		(to be on the safe side)
W_2	: Weight of the shielding plug and shielding plug lid	150 kg
G	: Impact acceleration	135 G
d_1	: Outer diameter of the shielding plug loaded plane	260 mm
d_2	: Inner diameter of the shielding plug loaded plane	40 mm

The expression below is given when each of the numeric values are substituted.

$$P_1 = \frac{9.807 \times (100 + 150) \times 135}{\frac{\pi}{4} (260^2 - 40^2)}$$

$$= 6.39 \text{ N/mm}^2$$

(1.2) Axial load of the inner shell (P_2)

The weight of the part above the modeled section is taken as the axial load.

$$P_2 = \rho_1 h_1 G$$

ρ_1	: Specific weight of the inner shell (SUS304)	
		$7.78 \times 10^{-5} \text{ N/mm}^3 \approx 7.93 \times 10^{-6} \text{ kg/mm}^3$
h_1	: Length above the modeled section	2254 mm

The expression below is given when each of the numeric values are substituted.

$$P_2 = 7.78 \times 10^{-5} \times 2254 \times 135$$

$$= 23.7 \text{ N/mm}^2$$

(1.3) Load that acts on the horizontal plane of the inner shell's upper-end part (P_3 to P_5)

The inertia force of a lead shield, for example, acts on the horizontal planes of the inner shell's upper-end part (i.e. the inner shell's end planes 1 to 3 shown in Fig. (II)-A.26). Assuming that the part above these planes is entirely made of lead, the weight of each lead is taken as the load acting on each plane. The load in the inclined section is corrected as the load that acts on the horizontal plane.

$$P_3 = \rho_2 h_2 G \frac{d_4^2 - d_1^2}{d_3^2 - d_2^2}$$

where

ρ_2	: Specific weight of the shielding lead	
		$11.1 \times 10^{-5} \text{ N/mm}^3 \approx 11.34 \times 10^{-6} \text{ kg/mm}^3$
h_2	: Length above the modeled section	2314 mm
d_1	: Outer diameter of the inner shell	176 mm

d_2	: Inner diameter of the inner shell's upper-end plane 1	196 mm
d_3	: Outer diameter of the inner shell's upper-end plane 1	268 mm
d_4	: Outer diameter of inclined plane 2	282 mm

The expression below is given when each of the numeric values are substituted.

$$P_3 = 11.1 \times 10^{-5} \times 2314 \times 135 \frac{282^2 - 176^2}{268^2 - 196^2}$$

$$= 50.4 \text{ N/mm}^2$$

P_4 and P_5 are obtained in the same manner as described above.

$$P_4 = \rho_2 h_3 G \frac{d_7^2 - d_4^2}{d_6^2 - d_5^2}$$

h_3	: Length above the modeled section	2487 mm
d_4	: Outer diameter of inclined plane 2	282 mm
d_5	: Inner diameter of the inner shell's upper-end plane 2	302 mm
d_6	: Outer diameter of the inner shell's upper-end plane 2	450 mm
d_7	: Outer diameter of the inclined plane 4	460 mm

(See page (II)-A-115.)

$$P_4 = 11.1 \times 10^{-5} \times 2487 \times 135 \frac{470^2 - 282^2}{450^2 - 302^2}$$

$$= 47.3 \text{ N/mm}^2$$

$$P_5 = \rho_2 h_4 G$$

h_4	: Length above the modeled section:	2548 mm
-------	-------------------------------------	---------

$$P_5 = 11.1 \times 10^{-5} \times 2548 \times 135$$

$$= 38.2 \text{ N/mm}^2$$

(2) Physical properties of the material

Table (II)-A.19 shows the material's physical property value. Because the analysis model is limited to two dimensions, bolts are modeled with a ring that has a width equivalent to the diameter of the bolt hole, and its Young's modulus is homogenized taking into account the materials that make up the model ring. (See attached document 2.)

Table (II)-A.19 Material Property Value of the Rear Lid Unit (80°C)

	SUS304	SUS630 (bolt material)
Modulus of longitudinal elasticity	$1.91 \times 10^5 \text{ N/mm}^2$	$2.13 \times 10^5 \text{ N/mm}^2$
Poisson's ratio	0.3	0.3
Specific weight	$7.78 \times 10^{-5} \text{ N/mm}^3$	$7.78 \times 10^{-5} \text{ N/mm}^3$

(3) Supporting conditions

The outer container end plate, shielding plug lid flange, and rear lid's external surface are supported by the end plate of the shock absorber. However, in this case, they are supported by only the external section of the shock absorber's axial concave portion (into which fir-plywood is introduced and which has a diameter of 400 mm) to be on the safe side. The arrows in Fig. (II)-A.26 show the supported sections.

Table (II)-A.20 shows the results of the principal section calculated by the finite element calculation code ANSYS under the conditions mentioned above.

Table (II)-A.20 Calculation Results of the Rear Lid Unit

Parts		Stress	Deflection *
Rear lid O-ring	1	41.2 N/mm ² (4.2 kg/mm ²)	0.31 mm
Rear lid O-ring	2	39.2 (4.0 kg/mm ²)	0.31
Rear lid O-ring	3	37.3 (3.8 kg/mm ²)	0.33
Rear lid O-ring	4	37.3 (3.8 kg/mm ²)	0.33
Shielding plug O-ring	5	109 (11.6 kg/mm ²)	0.28
Shielding plug O-ring	6	133 (13.6 kg/mm ²)	0.27
Inner shell's internal surface	7	12.7 (1.3 kg/mm ²)	0.65
Inner shell's internal surface	8	-376 (-38.3 kg/mm ²)	0.44
Inner shell's end surface	9	-422 (-43.0 kg/mm ²)	0.31
Rear lid bolt	10	83.4 (8.5 kg/mm ²)	0.34
Shielding plug lid plug	11	161 (16.4 kg/mm ²)	0.22

* Indicates the deflection in the drop direction.
The stress of the negative figure is the compression stress.

As shown in Table (II)-A.20, the maximum stress is generated near the base of the inner shell end part as compression stress. The temperature of the shielding plug flange (SUS304) is 73°C. When the dynamic tensile strength $\sigma_{UD} = 595 \text{ N/mm}^2$ ($\approx 61 \text{ kg/mm}^2$) at a temperature of 80°C is used as one of the criteria, to be on the safe side, the margin of safety (M.S.) is given by

$$M.S. = \frac{595}{422} - 1$$

$$= 0.4$$

The maximum stress generated in a fastening bolt section (modeled positions 10 and 11) is 161 N/mm². Therefore, if the yield stress of $\sigma_y = 682 \text{ N/mm}^2$ ($\approx 69.6 \text{ kg/mm}^2$) at a temperature of 80°C is adopted as one of the criteria of the fastening bolt, the margin of safety (M.S.) is given by

$$M.S. = \frac{682}{161} - 1$$

$$= 3.2$$

The shielding plug lid has sufficient strength to withstand the load applied during a vertical drop. The deflection of the O-ring groove is 0.33 mm. It is smaller than the collapsed height (0.9 mm or more) of the O-ring (5.7 mm in diameter) used.

The maximum stress is not generated in the flange junction part that tightens the O-ring, but in the part of the shell that stores the shielding plug. The flange part of the shielding plug does not exceed the yield stress ($\sigma_y = 180 \text{ N/mm}^2$) at a temperature of 80°C .

It has been confirmed that the boundary of containment was sound during the leakage test after a 1/2-scale model's drop test.

The above result indicates that the containment of the shielding plug flange part is maintained.

(d) Sampling valve lid fastening bolt

As shown in Fig. (II)-A-27, the sampling valve lid is fitted in a stainless box.

Assuming that all the inertia force of the sampling lid based on the impact acceleration during a rear-end-first vertical drop acts on the fastening bolt, the shear stress (τ) generated in the bolt is given by the expression below.

$$\tau = \frac{WG}{nA}$$

where

W	: Weight of the sampling valve lid	6 kg
G	: Impact acceleration	135 G
n	: Number of bolts	4
A	: Sectional area of the bolt	

$$A = \frac{\pi}{4}(d_B)^2$$

d_B : Diameter of the bolt thread (M12) 10.1 mm

$$A = \frac{\pi}{4}10.1^2$$

$$= 80.1 \text{ mm}^2$$

The expression below is given when these numeric values are substituted.

$$\tau = \frac{9.807 \times 6 \times 135}{4 \times 80.1}$$

$$= 24.8 \text{ N/mm}^2$$

$$\approx 2.5 \text{ kg/mm}^2$$

When the allowable stress uses value $0.6 \sigma_y = 0.6 \times 682 = 409 \text{ N/mm}^2$ ($\approx 41.8 \text{ kg/mm}^2$) at a temperature of 80°C , the margin of safety (M.S.) is given by

$$M.S. = \frac{409}{24.8} - 1$$

$$= 15$$

Therefore, no fastening bolt is sheared during a vertical drop.

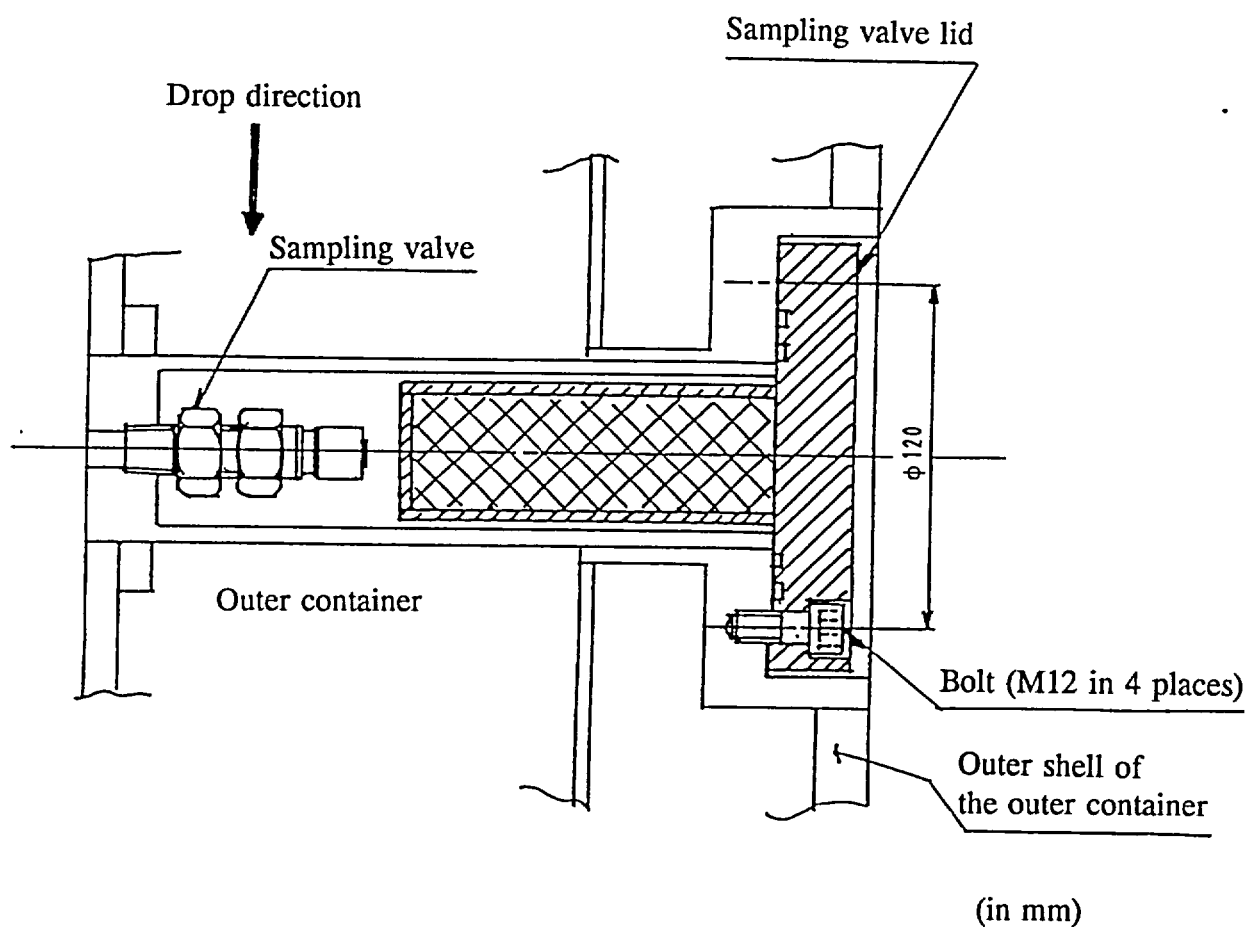


Fig. (II)-A.27 Sampling Valve Lid Fastening Bolt

(e) Inner container

For the inner container with contents, the end plate of the inner container cap is supported by the shielding plug lid through the shielding plug during a rear-end-first vertical drop as shown in Fig. (II)-A.28. Assuming that the inertia force of the inner container based on the impact acceleration during a rear-end-first vertical drop acts all on the inner container tube, the results show that the inner container does not buckle under these conditions.

Buckling in a long column of a uniform cross section within the proportional limit of the material is generated and the buckling load given by the expression below;

$$P_K = \frac{n\pi^2 EI}{\ell^2} \quad 1)$$

where

- P_K : Buckling load (Euler's equation)
 n : Constant 1
 E : Modulus of longitudinal elasticity (SUS304, 350°C)
 $1.72 \times 10^5 \text{ N/mm}^2 \approx 1.76 \times 10^4 \text{ kg/mm}^2$
 I : Principal moment of inertia of the area

$$I = \frac{\pi}{64} (d_2^4 - d_1^4)$$

- d_2 : Outer diameter of the inner container 101.6 mm
 d_1 : Inner diameter of the inner container 93.6 mm

$$\begin{aligned} I &= \frac{\pi}{64} (101.6^4 - 93.6^4) \\ &= 1.46 \times 10^6 \text{ mm}^4 \end{aligned}$$

- ℓ : Length of the inner container 1973 mm

$$\begin{aligned} P_K &= \frac{1 \times \pi^2 \times 1.72 \times 10^5 \times 1.46 \times 10^6}{1973^2} \\ &= 6.37 \times 10^5 \text{ N} \end{aligned}$$

The load (F) generated in the inner container wall during a vertical drop is given by

$$F = W \cdot G$$

1) Nihon Kikai Gakkai: Kikai Kogaku Benran, p. 4-83
(The Japan Society of Mechanical Engineers: Handbook of Mechanical Engineering, page 4-83)

W : Weight of the inner container 35 kg
G : Impact acceleration 135 G

$$F = 9.807 \times 35 \times 135 \\ = 4.63 \times 10^4 \text{ N}$$

As a result, the inner container does not buckle because of $P_k > F$. The margin of safety (M.S.) is given by

$$M.S. = \frac{6.37 \times 10^5}{4.63 \times 10^4} - 1 \\ = 13$$

Therefore, the constraining force by the deformation of the inner container does not act on the fuel supporting can, supporting can, rack or receiving tube.

Fuel supporting can I, fuel supporting can II, the supporting can (loaded with receiving tubes each of which enclose a fuel pin), the rack (loaded with receiving tubes I each of which enclose a fuel pin) or bare Contents III are loaded into the inner container.

Fuel supporting can II has the same shape as fuel supporting can I except for its inner cylinder. The supporting can also has the same shape as fuel supporting can I except for the screw part of its rear lid (plate thickness of 8 mm). Therefore, the strength of fuel supporting can II and the supporting can during a drop is represented by fuel supporting can I. The receiving tube is inserted into a separate place with a spacer between the outer and inner cylinders of the supporting can, so that it will not be deformed or damaged.

Fuel supporting can I and receiving tube I, which are not part of the containment system but rather function as a secondary containment system during fuel pin transport, are analyzed to demonstrate that they are sound and can sustain the stress generated by the impact acceleration during a vertical drop. The rack is also analyzed in the same manner as the above to show that no displacement occurs in the holding position of the contents.

(f) Fuel supporting can I

The impact acceleration during a rear-end-first vertical drop causes the inertia force that acts on fuel supporting can I and the fuel pin stored in fuel supporting can I. In this section, it is demonstrated that fuel supporting can I does not buckle, and the lid of fuel supporting can I shown in Fig. (II)-A.28, has sufficient strength.

The load under which fuel supporting can I buckles is given by the expression (used in the preceding step) below.

$$P_K = \frac{n\pi^2 EI}{\ell^2}$$

where

- n : Constant 1
E : Modulus of longitudinal elasticity (SUS304, 350°C)
1.72 × 10⁵ N/mm² = 1.76 × 10⁴ kg/mm²
I : Principal moment of inertia of the area

$$I = \frac{\pi}{64}(d_2^4 - d_1^4)$$

- d₂ : Outer diameter of fuel supporting can I 87.1 mm
d₁ : Inner diameter of fuel supporting can I 83.1 mm

$$I = \frac{\pi}{64}(87.1^4 - 83.1^4)$$
$$= 4.84 \times 10^5 \text{ mm}^4$$

- ℓ : Length of fuel supporting can I 1944.5 mm

$$P_K = \frac{1 \times \pi^2 \times 1.72 \times 10^5 \times 4.84 \times 10^5}{1944.5^2}$$
$$= 2.17 \times 10^5 \text{ N}$$

The load that is generated in the wall of fuel supporting can I during a vertical drop is given by

$$F = W \cdot G$$

- W : Weight of fuel supporting can I 25 kg
G : Impact acceleration 135 G

$$F = 9.807 \times 25 \times 135$$
$$= 3.31 \times 10^4 \text{ N}$$

As a result, fuel supporting can I does not buckle because $P_k > F$. The margin of safety (M.S.) is given by

$$M.S. = \frac{2.17 \times 10^5}{3.31 \times 10^4} - 1$$

$$= 5.6$$

The bending moment is generated in the rear lid of fuel supporting can I by the weight of fuel supporting can I and the fuel pins of Contents I. When the stress generated in this fuel supporting can I is modeled on the assumption that it is applied as uniform load between 2a and 2b as shown in Fig. (II)-A.28, the maximum stress given by the expression below occurs at spot 2b.

$$\sigma = \frac{3W}{4t^2} \left\{ \frac{4a^4(m+1)\log_e \frac{a}{b} - a^4(m+3) + b^4(m-1) + 4a^2b^2}{a^2(m+1) + b^2(m-1)} \right\}^1$$

σ : Stress generated by the bending moment that acts on the inner diameter of the rear lid

w : Modeled distributed load

$$w = \frac{(W_1 + W_2)G}{\pi(a^2 - b^2)}$$

W_1	: Weight of the contents (See Table (II)-A.4.)	10 kg
W_2	: Weight of fuel supporting can I (See Table (II)-A.4.)	25 kg
G	: Impact acceleration	135 G
a	: Outer radius of the loaded plane	43.55 mm
b	: Inner radius of the loaded plane	25 mm

$$w = \frac{9.807 \times (10 + 25) \times 135}{\pi(43.55^2 - 25^2)}$$

$$= 11.6 \text{ N/mm}^2$$

m	: Reciprocal of Poisson's ratio	3.3
t	: Plate thickness of fuel supporting can I's rear lid	6.5 mm

The expression below is given when each of the numeric values are substituted.

$$\sigma = \frac{3 \times 11.6}{4 \times 6.5^2} \left\{ \frac{4 \times 43.55^4(3.3 + 1)\log_e \frac{43.55}{25} - 43.55^4(3.3 + 3) + 25^4(3.3 - 1) + 4 \times 43.55^2 \times 25^2}{43.55^2(3.3 + 1) + 25^2(3.3 - 1)} \right\}$$

$$= 372 \text{ N/mm}^2$$

$$\approx 37.8 \text{ kg/mm}^2$$

1) R. J. Roark: Formulas for Stress and Strain, p. 223, McGraw Hill Book, 1965

When the dynamic tensile strength $\sigma_{UD} = 524 \text{ N/mm}^2$ ($\approx 53.5 \text{ kg/mm}^2$) at a temperature of 350°C is used, the margin of safety (M.S.) is given by

$$M.S. = \frac{524}{372} - 1$$

$$= 0.4$$

The rear lid of fuel supporting can I has sufficient strength against the distributed load generated by a vertical drop. Therefore, it does not break in this case.

As a result, the fuel supporting can I has sufficient strength, and its containment is maintained.

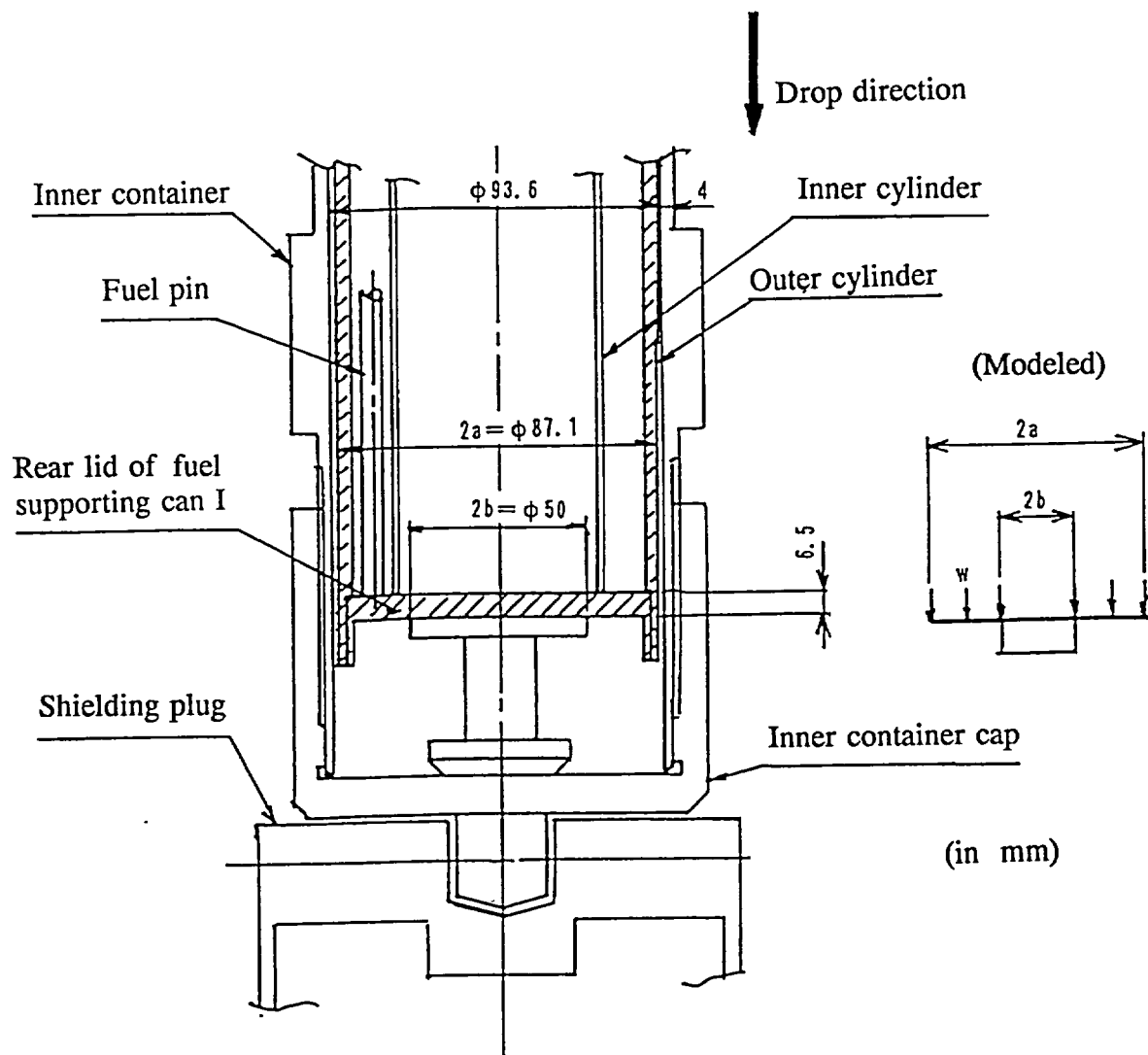


Fig. (II)-A.28 Fuel Supporting Can I (Vertical Drop)

(g) Rack supporting rod, rack end plate, and receiving tube I

The fuel pin is held in the rack after it is enclosed in receiving tube I. The following indicates that these parts remain sound during a vertical drop.

(g)-1 Rack supporting rod

As shown in Fig. (II)-A.29, inertia force acts on receiving tube I and the fuel pin because of the impact acceleration that occurs during a rear-end-first vertical drop. The resulting load acts on the supporting rod through the rack end plate. Therefore, this compression stress is obtained and indicates that the rack supporting rod has sufficient strength. The compression stress (σ) generated in a hexagonal column that has the minimum cross-sectional area of the supporting rod is given by the expression below.

$$\sigma = \frac{WG}{A}$$

where

W	: Weight of the rack and contents (See Table (II)-A.4.)	31 kg
G	: Impact acceleration	135 G
A	: Cross-sectional area of the supporting rod	

$$A = \frac{3}{4}a'b'$$

a'	: Width across the flats of the hexagonal column	17 mm
b'	: Width across the corners of the hexagonal column	19.6 mm

$$\begin{aligned} A &= \frac{3}{4} \times 17 \times 19.6 \\ &= 2.5 \times 10^2 \text{ mm}^2 \end{aligned}$$

The expression below is given when each of the numeric values are substituted.

$$\begin{aligned} \sigma &= \frac{9.807 \times 31 \times 135}{2.5 \times 10^2} \\ &= 164 \text{ N/mm}^2 \\ &\approx 16.7 \text{ kg/mm}^2 \end{aligned}$$

The temperature of the rack supporting rod (assumed to be the same as the temperature of receiving tube I) (SUS304) is 245°C. If the value $\sigma_{UD} = 437 \times 1.2 = 524 \text{ N/mm}^2$ ($\approx 53.5 \text{ kg/mm}^2$) at a temperature of 350°C is assumed to represent the tensile strength for impact load, to be on the safe side, the margin of safety (M.S.) is given by

$$M.S. = \frac{524}{164} - 1$$

$$= 2.2$$

The rack supporting rod thus has sufficient strength against the compression stress generated by a vertical drop. Therefore, it is not damaged in this case.

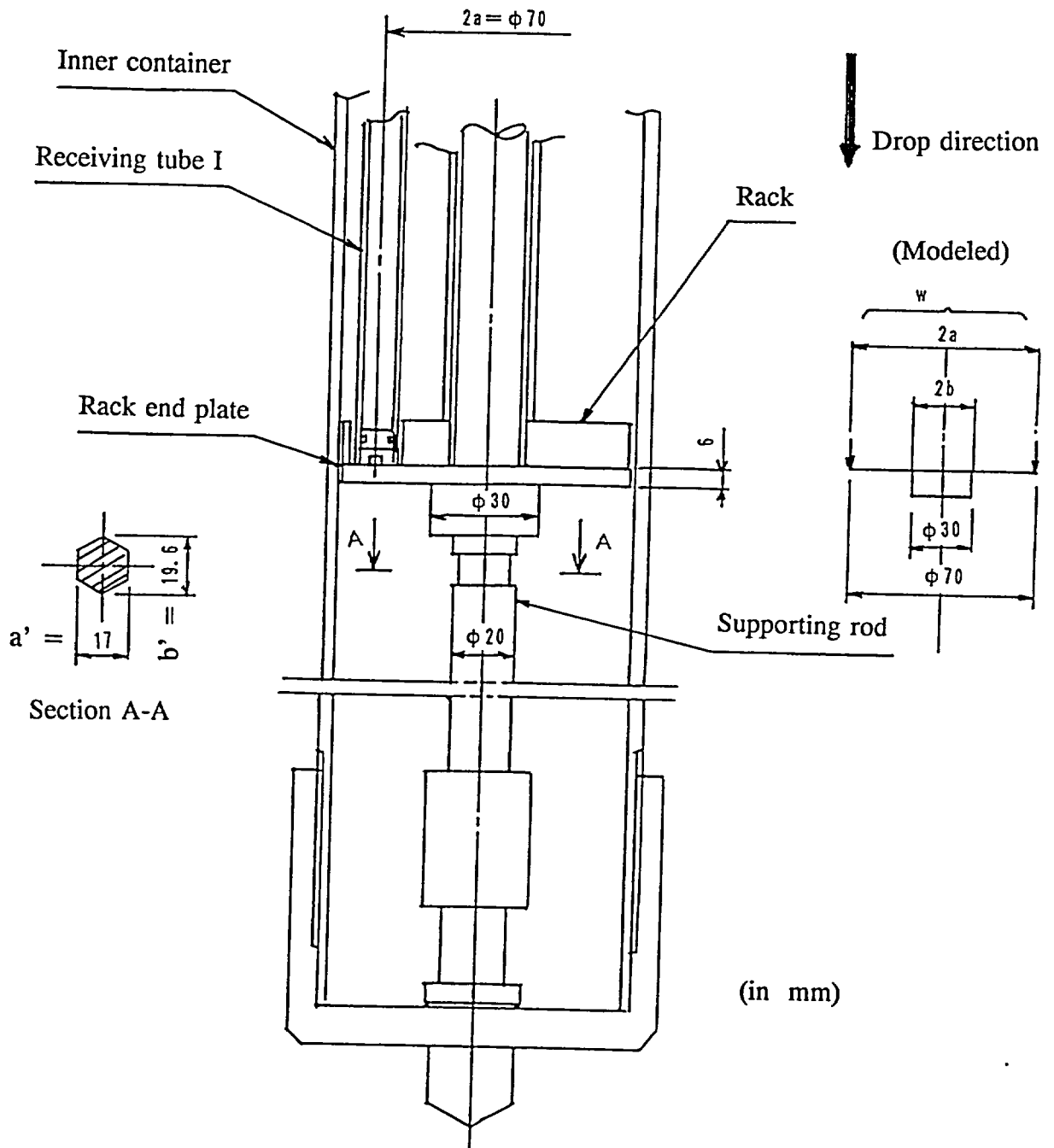


Fig. (II)-A.29 Rack

(g)-2 Rack end plate

The inertia force acts on receiving tube I and the fuel pins because of the impact acceleration that occurs during a rear-end-first vertical drop. The resulting load acts on the rack end plate as shown in Fig. (II)-A.29. The stress generated under these conditions is obtained to indicate that the rack end plate has sufficient strength. The bending stress generated in the rack end plate is given by the expression below.

$$\sigma = \frac{3W}{2\pi t^2} \left\{ \frac{2a^2(m+1)\log_e \frac{a}{b} + a^2(m-1) - b^2(m-1)}{a^2(m+1) + b^2(m-1)} \right\}^1$$

where

σ : Bending stress generated at the inner diameter edge of the end plate

W : Load generated by receiving tube I

$$W = W_1 G$$

W_1 : Weight of receiving tube I and the fuel pin 11 kg

G : Impact acceleration 135 G

$$W = 9.807 \times 11 \times 135 \\ = 1.46 \times 10^4 \text{ N}$$

a : Outer radius of the loaded plane 35 mm

b : Inner radius of the loaded plane 15 mm

m : Reciprocal of Poisson's ratio 3.3

t : Plate thickness of the end plate 6 mm

The expression below is obtained when each of the numeric values are substituted.

$$\sigma = \frac{3 \times 1.46 \times 10^4}{2\pi \times 6^2} \left\{ \frac{2 \times 35^2(3.3+1)\log_e \frac{35}{15} + 35^2(3.3-1) - 15^2(3.3-1)}{35^2(3.3+1) + 15^2(3.3-1)} \right\} \\ = 376 \text{ N/mm}^2 \\ \approx 38.2 \text{ kg/mm}^2$$

The temperature of the end plate (assumed to be the same as the temperature of receiving tube I) (SUS304) is 245°C. If the value $\sigma_{UD} = 437 \times 1.2 = 524 \text{ N/mm}^2$ ($\approx 53.5 \text{ kg/mm}^2$) at a temperature of 350°C is assumed to represent the tensile strength for impact load, to be on the safe side, the margin of safety (M.S.) is given by

$$M.S. = \frac{524}{376} - 1 \\ = 0.4$$

The end plate, therefore, does not break during a vertical drop.

1) R.J. Roark: Formulas for Stress and Strain, p. 223, McGraw-Hill, 1965

(g)-3 Receiving tube I

The inertia force by impact acceleration acts on receiving tube I and the fuel pins during a rear-end-first vertical drop. As shown in Fig. (II)-A.29, the load that acts on the fuel pin only acts on the receiving tube I plug or end plate as compression stress. The load in this case is completely supported. The force that acts on the surface of the receiving tube I when the inertia force resulting from the weight of receiving tube I is applied, is obtained and indicates that receiving tube I does not buckle.

The buckling that occurs in a long column of a uniform cross section is generated when the following value of the buckling load (P_K) occurs.

$$P_K = \frac{n\pi^2 EI}{\ell^2}$$

where

- P_K : Buckling load (Euler's equation)
 n : Constant 1
 E : Modulus of longitudinal elasticity
 $1.72 \times 10^5 \text{ N/mm}^2 = 1.76 \times 10^4 \text{ kg/mm}^2$
 I : Principal moment of inertia of the area

$$I = \frac{\pi}{64}(d_2^4 - d_1^4)$$

- d_2 : Outer diameter of receiving tube I 13.8 mm
 d_1 : Inner diameter of receiving tube I 10.5 mm

$$I = \frac{\pi}{64}(13.8^4 - 10.5^4)$$
$$= 1.18 \times 10^3 \text{ mm}^4$$

- ℓ : Length of receiving tube I 1035 mm

$$P_K = \frac{1 \times \pi^2 \times 1.72 \times 10^5 \times 1.18 \times 10^3}{1035^2}$$
$$= 1.87 \times 10^3 \text{ N}$$

The load (F) generated in the wall of receiving tube I during a vertical drop is given by the expression below.

$$F = W \cdot G$$

- W : Weight of receiving tube I 1 kg
 G : Impact acceleration 135 G

$$F = 9.807 \times 1 \times 135$$
$$= 1.32 \times 10^3 \text{ N}$$

Receiving tube I, therefore, does not buckle. The margin of safety (M.S.) is given by

$$M.S. = \frac{1.87 \times 10^3}{1.32 \times 10^3} - 1$$
$$= 0.4$$

No constraining force resulting from buckling is generated in the fuel pin that is stored in receiving tube I. The soundness of receiving tube I is therefore maintained.

The evaluation results above show that the outer container, the inner container, and fuel supporting can I or the rack, as well as receiving tube I have sufficient strength to withstand rear-end-first vertical drop, and do not change their shapes.

(2) Front-end-first vertical drop

The next subsection examines the case in which the package drops with the rotating plug side first in the vertical direction (hereafter called "a front-end-first vertical drop") as shown in Fig. (II)-A.30. Since the rotating plug side includes a shock absorber that has the same shape as one on the shielding plug side, shock absorber deformation and impact deceleration during a front-end-first vertical drop are the same as they are during a rear-end-first vertical drop. Therefore, assuming the same impact acceleration (135 G) as in the case of a rear-end-first vertical drop, the stress applied to each part below has been calculated to investigate its soundness.

- (a) Shells of the outer container
- (b) Front lid unit
- (c) Inner container screw and locking plate
- (d) Inner container
- (e) Fuel supporting can and receiving tube

(a) Shells of the outer container (outer and inner shells)

The stress conditions generated in the outer shell part are the same as those analyzed during a rear-end-first vertical drop. For the soundness, see the preceding section.

The inertia force generated by the shielding plug acts on the inner shell part. However, the weight of this shielding plug is less than that of the rotating plug during a rear-end-first vertical drop, so the stress generated in the inner shell is actually smaller. Consequently, the stress generated in the inner shell during a front-end-first vertical drop is less than yield stress, as in the case of a rear-end-first vertical drop. As a result, the inner shell remains sound.

The shells of the outer container also maintain their integrity during a front-end-first vertical drop.

(b) Front lid unit

During a front-end-first vertical drop, the inertia force of the contents acts on the internal O-ring of the lid flange, while the inertia force of the lead shield resulting from the impact acceleration acts on the end plate of the outer container. The stress and deflection generated in the front lid unit under these conditions have been calculated, and indicate that the O-rings have been satisfactorily tightened and the front lid unit does not break even if deflection occurs. The rotating plug section under these conditions is modeled as shown in Fig. (II)-A.31.

Since the penetration hole for the rotating plug and the penetration hole section for the sampling valve have small inner diameters, and are constituted by a thick pedestal, they are ignored in this model.

The load conditions, supporting conditions, and material's physical property values in this model are described below and are taken as the calculation conditions.

(1) Load conditions

(1.1) Load (P_1) that acts on the inside surface of the flange

The inner container screw or locking plate described later may be damaged during a front-end-first vertical drop. Therefore, in addition to the rotating plug, rotating plug lid, and rotating plug lid cover, the shielding plug and the weight of the contents (including the weight of the inner container) are added when evaluating the load that acts on the inside surface of the flange. The load that acts on the flange is assumed to be uniformly distributed through the shielding lead. This load becomes approximate to the uniform load as described below.

$$P_1 = \frac{(W_1 + W_2 + W_3)G}{\frac{\pi}{4}(d_{1i}^2 - d_{1o}^2)}$$

where

W_1	: Weight of the contents (See Table (II)-A.4.)	100 kg
		(To be on the safe side)
W_2	: Weight of the shielding plug	30 kg
W_3	: Weight of rotating plug, rotating plug lid, and rotating plug cover	420 kg
G	: Impact acceleration	
D_{1i}	: Outer diameter of the flange	402 mm
D_{1o}	: Inner diameter of the flange	142 mm

and thus

$$P_1 = \frac{9.807 \times (100 + 30 + 420) \times 135}{\frac{\pi}{4}(402^2 - 142^2)}$$

$$= 6.55 \text{ N/mm}^2$$

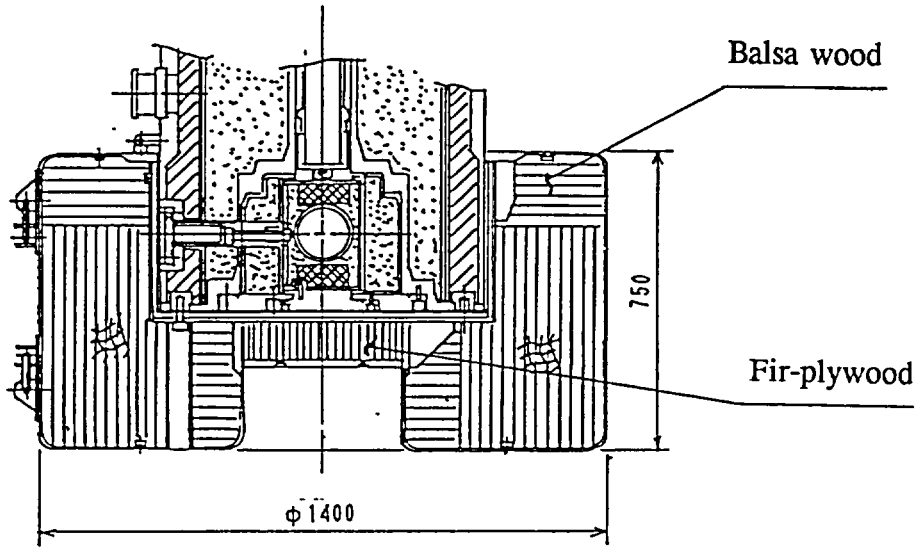
(1.2) Axial load (P_2) of the inner shell

The weight of the part above the modeled section shown in Fig. (II)-A.31 is assumed to represent the load.

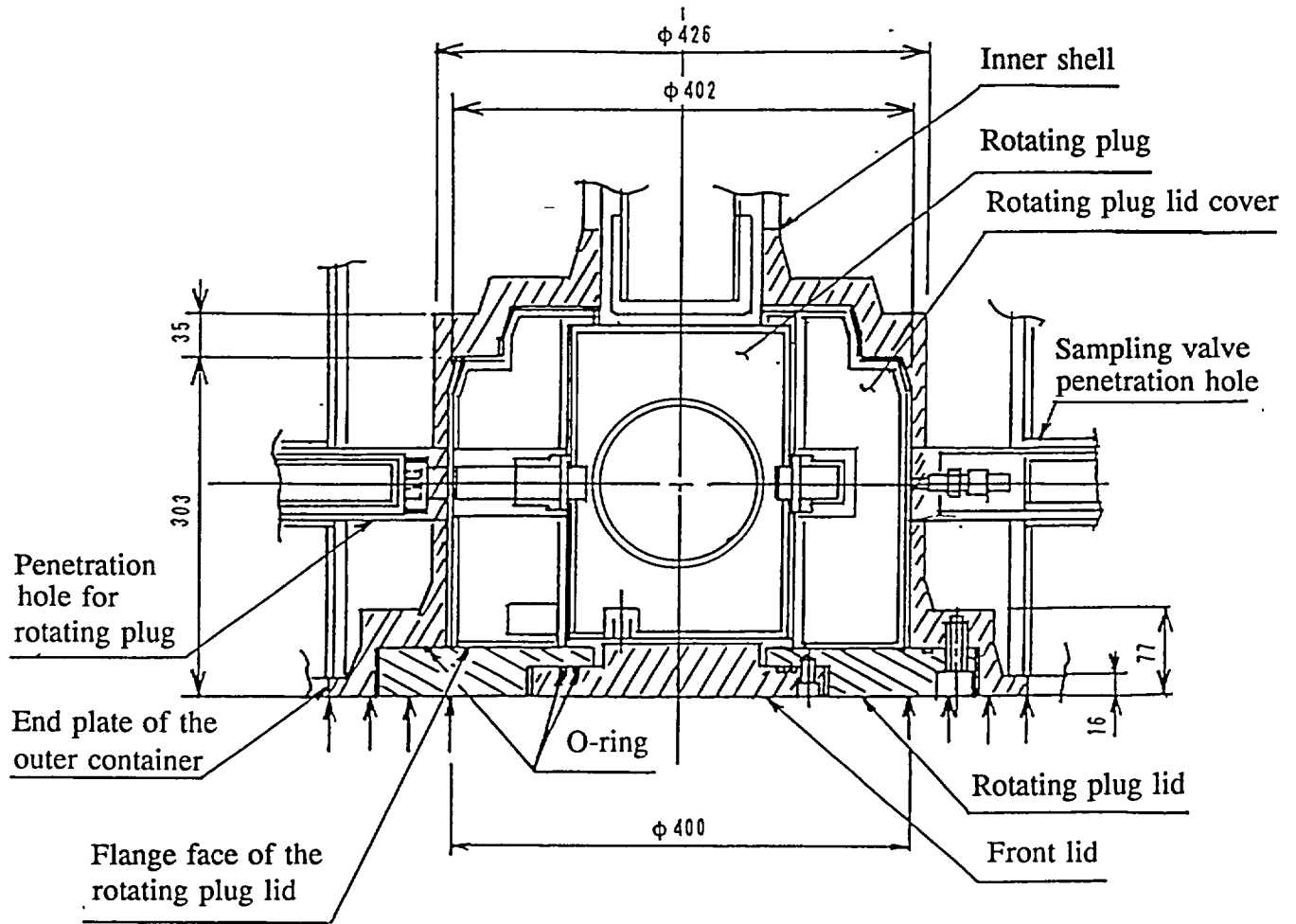
$$P_2 = \rho_1 h_1 G$$

where

ρ	: Specific gravity of the inner shell	
		$7.78 \times 10^{-5} \text{ N/mm}^2 \approx 7.93 \times 10^{-6} \text{ kg/mm}^2$
h_1	: Length above the modeled section	2129 mm



(a) Assembly of the front shock absorber and front lid unit Modeled section



(b) Expanded sketch of the front lid unit (in mm)

Fig. (II)-A.30 Front Lid Unit (Front-end-first Vertical Drop)

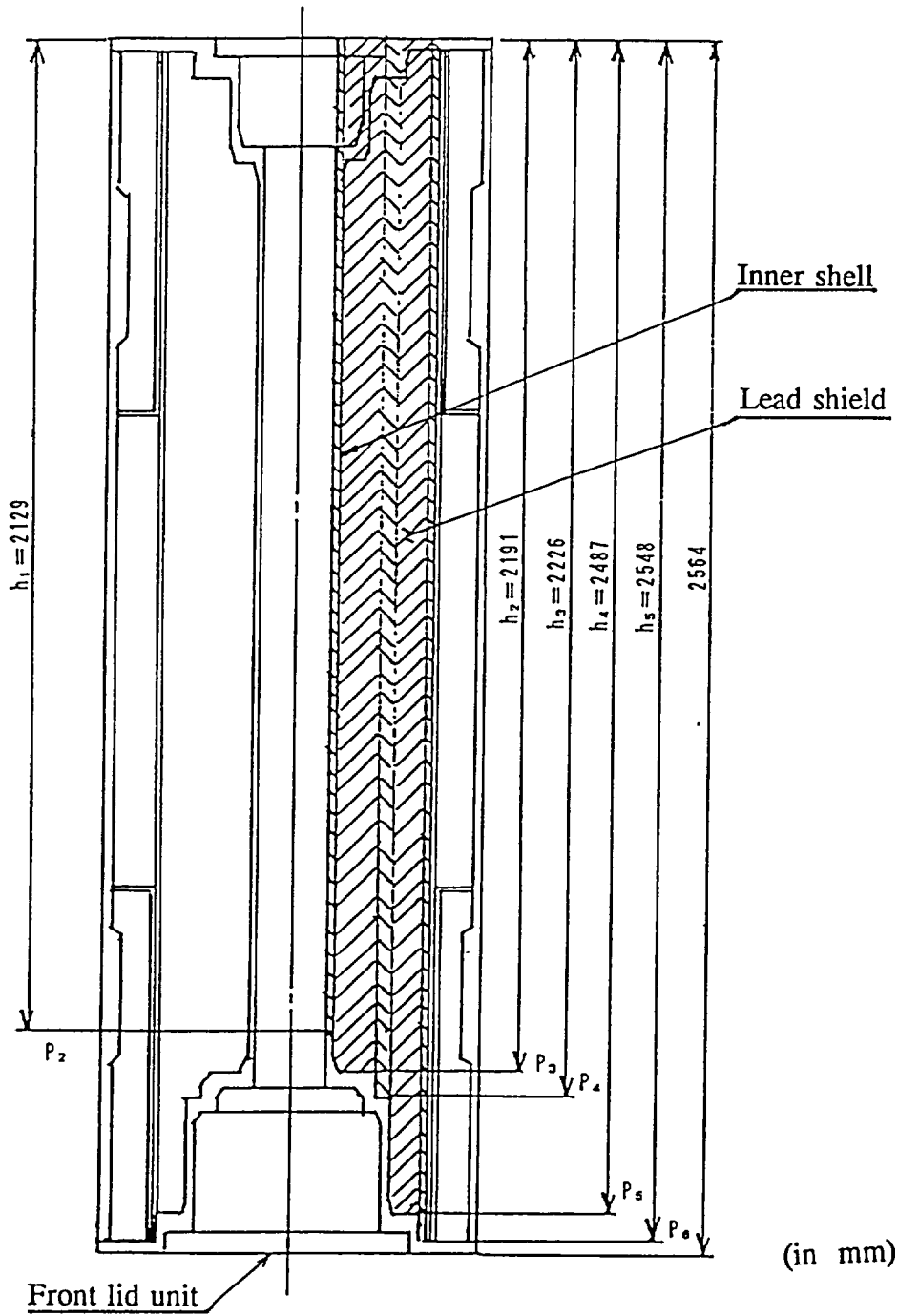


Fig. (II)-A.31 Loading Model of the Front Lid Unit

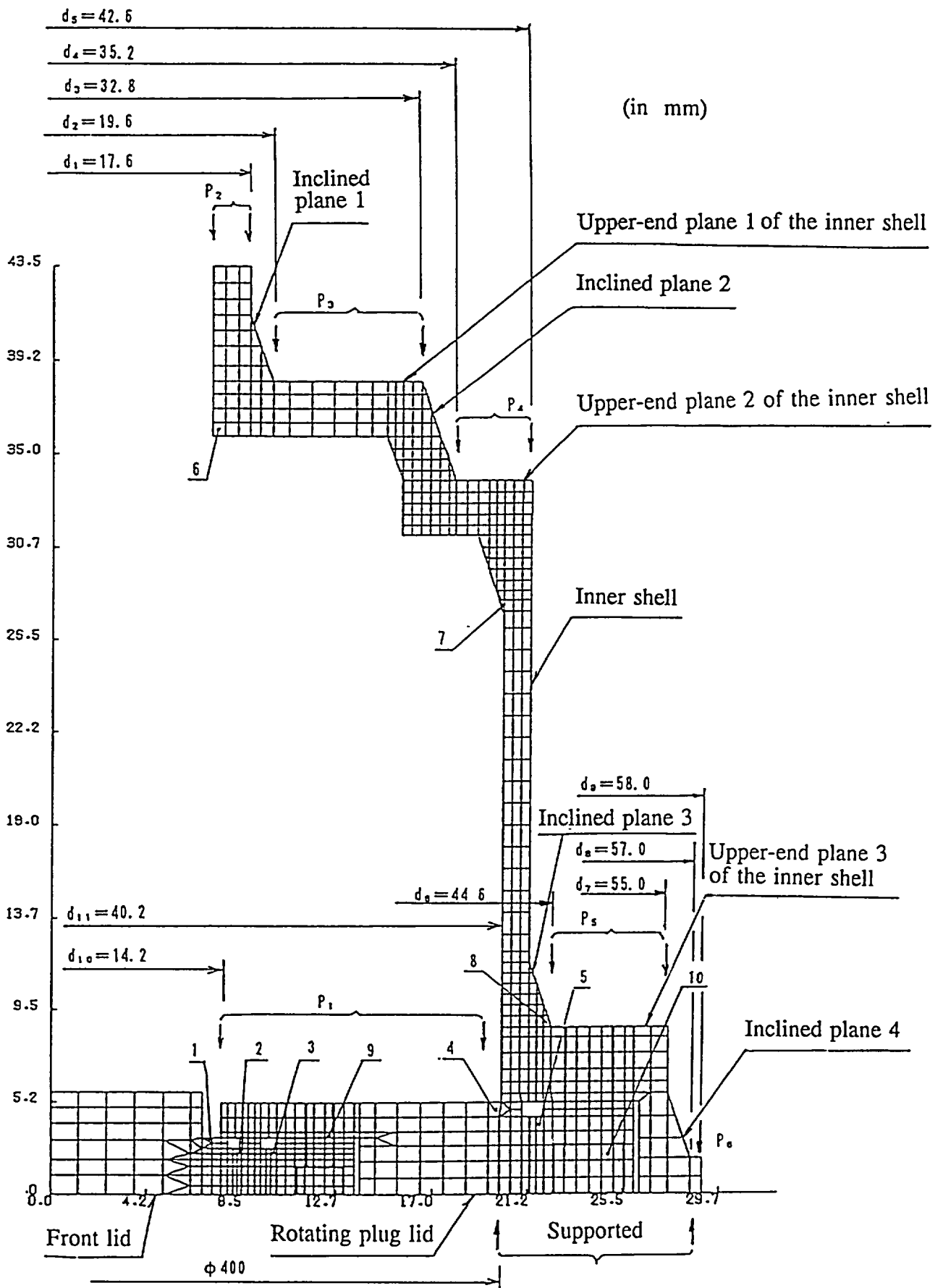


Fig. (II)-A.32 Analysis Model of the Front Lid Unit

$$P_2 = 7.78 \times 10^{-5} \times 2129 \times 135$$

$$= 22.4 \text{ N/mm}^2$$

(1.3) Load (P_3 to P_6) that acts on the outside surface of the inner shell

The inertia force of the shield lead acts on the outside plane of the inner shell. The part above the plane in question is assumed to be made entirely of lead. The load for the inclined section is corrected as the load that acts on the plane.

$$P_3 = \rho_2 h_2 G \frac{d_3^2 - d_1^2}{d_3^2 - d_2^2}$$

where

ρ_2	: Specific gravity of the shielding lead	
	$11.1 \times 10^{-5} \text{ N/mm}^3 \approx 11.34 \times 10^{-6} \text{ kg/mm}^3$	
h_2	: Length of the part above the modeled section	2191 mm
d_3	: Outer diameter of the inner shell's upper end plane 1	328 mm
d_2	: Inner diameter of the inner shell's upper end plane 1	196 mm
d_1	: Outer diameter of the inner shell	176 mm

and thus

$$P_3 = 11.1 \times 10^{-5} \times 2191 \times 135 \frac{328^2 - 176^2}{328^2 - 196^2}$$

$$= 36.4 \text{ N/mm}^2$$

Likewise

$$P_4 = \rho_2 h_3 G \frac{d_5^2 - d_3^2}{d_5^2 - d_4^2}$$

h_3	: Length of the part above the modeled section	2226 mm
d_4	: Inner diameter of the inner shell's upper end plane 2	352 mm
d_5	: Outer diameter of the inner shell's upper end plane 2	426 mm

$$P_4 = 11.1 \times 10^{-5} \times 2226 \times 135 \frac{426^2 - 328^2}{426^2 - 352^2}$$

$$= 42.8 \text{ N/mm}^2$$

$$P_5 = \rho_2 h_4 G \frac{d_7^2 - d_5^2}{d_7^2 - d_6^2}$$

h_4 : Length of the part above the modeled section 2487 mm
 d_6 : Inner diameter of the inner shell's upper end plane 3 446 mm
 d_7 : Outer diameter of the inner shell's upper end plane 3 550 mm

$$\begin{aligned}
 P_5 &= 11.1 \times 10^{-5} \times 2487 \times 135 \frac{550^2 - 426^2}{550^2 - 446^2} \\
 &= 43.5 \text{ N/mm}^2
 \end{aligned}$$

$$P_6 = \rho_2 h_5 G$$

h_5 : Length of the part above the modeled section 2548 mm

$$\begin{aligned}
 P_6 &= 11.1 \times 10^{-5} \times 2548 \times 135 \\
 &= 38.2 \text{ N/mm}^2
 \end{aligned}$$

(2) Material's physical properties

Because the analysis model is limited to two dimensions, bolts are modeled with a ring that has a width equivalent to the diameter of the bolt hole, and its Young's modulus is homogenized taking into account the materials that make up the model ring. (See attached document 2.)

Table (II)-A.21 Physical Property Value of the Front Lid Unit

	SUS304	SUS630 (Bolt material)
Modulus of longitudinal elasticity	$1.91 \times 10^5 \text{ N/mm}^2$ $\approx 1.96 \times 10^4 \text{ Kg/mm}^2$	$2.13 \times 10^5 \text{ N/mm}^2$ $\approx 2.18 \times 10^4 \text{ Kg/mm}^2$
Poisson's ratio	0.3	0.3
Specific gravity	$7.78 \times 10^{-5} \text{ N/mm}^3$ $\approx 7.93 \times 10^{-6} \text{ kg/mm}^3$	$7.78 \times 10^{-5} \text{ N/mm}^3$ $\approx 7.93 \times 10^{-6} \text{ kg/mm}^3$

(3) Supporting conditions

The front lid unit is supported by the end plate of a shock absorber. However, in this case, the front lid unit is supported by only the external section of the shock absorber's axial concave portion (into which fir-plywood is put, and which has a diameter of 400 mm) to be on the safe side.

The arrows in Figs. (II)-A.30 and (II)-A.32 indicate the supported section. Table (II)-A.22 shows the results of the principal section calculated by the finite element calculation code, ANSYS, under the above-mentioned conditions.

Table (II)-A.22 Calculation Results of the Front Lid Unit

Parts		Stress	Deflection *
Front lid O-ring part	1	16.7 N/mm ² (1.7 kg/mm ²)	0.15 mm
Front lid O-ring part	2	41.2 (4.2 kg/mm ²)	0.15
Front lid O-ring part	3	24.5 (2.5 kg/mm ²)	0.15
Rotating plug lid O-ring part	4	77.5 (7.9 kg/mm ²)	0.03
Rotating plug lid O-ring part	5	103 (10.5 kg/mm ²)	0.02
Inner shell plane	6	16.7 (1.7 kg/mm ²)	1.0
Inner shell plane	7	-549 (-56.0 kg/mm ²)	0.31
Inner shell end plane	8	-116 (-11.8 kg/mm ²)	0.05
Front lid bolt part	9	93.2 (9.5 kg/mm ²)	0.15
Rotating plug lid bolt part	10	13.7 (1.4 kg/mm ²)	0.01

Note: * Indicates the deflection in the drop direction.
The stress represented by the negative figure is the compression stress.

The maximum stress is generated as compression force in the rotating plug lid (modeled position 7) of the inner shell. The margin of safety in this section is thus as shown below.

The temperature (outer shell lid temperature) of the rotating plug lid (SUS304) is 73°C. When the tensile strength $\sigma_{UD} = 496 \times 1.2 = 595 \text{ N/mm}^2$ ($\approx 61 \text{ kg/mm}^2$) for impact load at a temperature of 80°C is used as one of the criteria, to be on the safe side, the margin of safety (M.S.) is given by

$$M.S. = \frac{595}{549} - 1$$

$$= 0.08$$

The maximum stress occurring in the fastening bolt section is 93.2 N/mm² ($\approx 9.5 \text{ kg/mm}^2$). Since the yield strength σ_y of a fastening bolt is 682 N/mm² ($\approx 69.6 \text{ kg/mm}^2$), the margin of safety (M.S.) is given by

$$M.S. = \frac{682}{93.2} - 1$$

$$= 6.3$$

The rotating plug lid unit has sufficient strength to withstand the load applied during a drop.

The deflection of the O-ring is no more than 0.15 mm, and it is also less than the collapsed height (0.9 mm) of the O-ring used.

The maximum stress is not generated in the flange junction part that tightens the O-ring, but rather in the part of the shell that stores a rotating plug. The flange part of the rotating plug does not exceed the yield stress ($\sigma_y = 180 \text{ N/mm}^2$) at a temperature of 80°C .

A leakage test after a 1/2 scale model's drop test has confirmed that the boundary of containment is sound.

The aforementioned results indicate that the containment of the rotating plug flange part is maintained.

(c) Locking plate and inner container screw

The inertia force (F) based on the impact acceleration of the shielding plug, the inner container, and the contents acts on the locking plate during a front-end-first vertical drop.

$$F = G \cdot W$$

G	: Impact acceleration	135 G
W	: Weight (Shielding plug, inner container, and contents)	
	= 30 + 35 + 35	
	= 100 kg	

$$F = 9.807 \times 135 \times 100$$

$$= 1.32 \times 10^5 \text{ N}$$

When this load (F) acts on the locking plate through the shielding plug, the shear stress (τ), generated at the junction part shown in Fig. (II)-A.33 is given by the expression below.

$$\tau = \frac{F}{nA}$$

n	: Number of sections to which shear stress is applied	2
A	: Cross-sectional area	
A	= tℓ	
t	: Plate thickness	10 mm
ℓ	: Length of the junction part	20 mm

$$A = 10 \times 20$$

$$= 200 \text{ mm}^2$$

$$\tau = \frac{1.32 \times 10^5}{2 \times 200}$$

$$= 330 \text{ N/mm}^2$$

Given the temperature (350°C) of the inner container, the design criterion value is $\tau_{UD} = 1.2 \times 0.6 \times 437 = 315 \text{ N/mm}^2$ ($\approx 32.1 \text{ kg/mm}^2$). The locking plate (material: SUS304, plate thickness: 10 mm) may thus be deformed by the shear stress. This subsection evaluates the strength of the inner container screw that fixes the inner container, as well as the locking plate, under the assumption that the locking plate is broken.

The inertia force (F) of the inner container and the contents acts on the screw of the inner container.

$$F = G \cdot W$$

where

G : Impact acceleration

135 G

W : Weight (Inner container and contents)

$$W = 35 + 35 = 70 \text{ kg}$$

$$F = 9.807 \times 135 \times 70$$

$$= 9.27 \times 10^4 \text{ N}$$

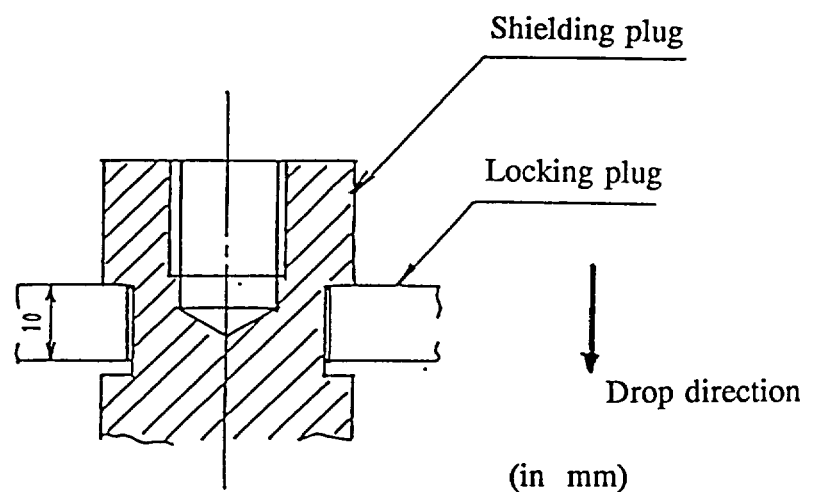
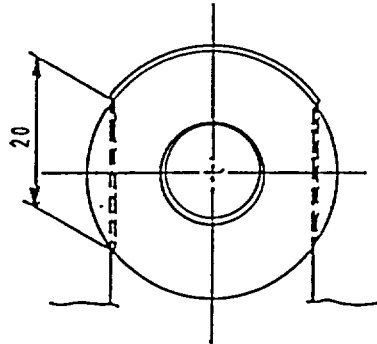


Fig. (II)-A.33 Locking Plate

The inner container screw has a diameter of 12 mm. As shown in Fig. (II)-A.34, the shear stress (τ) generated in the cross section of the screw by the shear load (F) is given by the expression below.

$$\tau = \frac{F}{A}$$

A : Cross-sectional area of the inner container screw

$$A = \frac{\pi}{4} d^2$$

d : Screw diameter

12 mm

$$A = \frac{\pi}{4} \times 12^2$$

$$\begin{aligned}
 &= 113 \text{ mm}^2 \\
 \tau &= \frac{9.27 \times 10^4}{113} \\
 &= 820 \text{ N/mm}^2 \\
 &\approx 83.6 \text{ kg/mm}^2
 \end{aligned}$$

Since this value exceeds the design criteria value $0.6 \sigma_u = 0.6 \times 863 = 517 \text{ N/mm}^2$ ($\approx 52.9 \text{ kg/mm}^2$) of the inner container screw (material: SUS630) at a temperature of 350°C , the inner container screw may be broken by the shear load. In the analysis of the front lid described previously, the locking plate is assumed to have been broken. In the same manner, a subsequent analysis will be performed based on the assumption that the inner container screw has also broken. This analysis will demonstrate that the inner container, the fuel supporting can and the receiving tube maintain their integrity, even if the entire weight of the shielding plug and inner container (including the contents) is loaded onto the rotating plug flange.

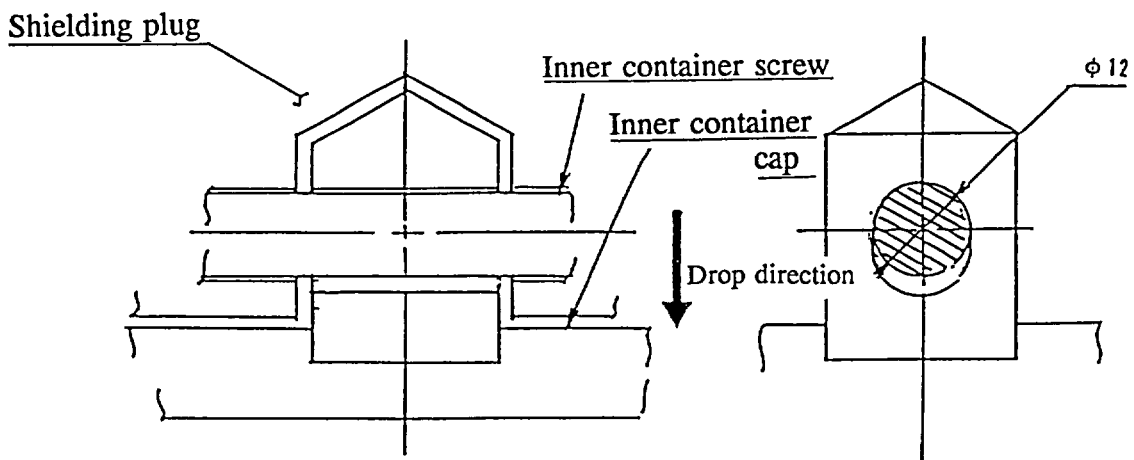


Fig. (II)-A.34 Inner Container Screw

(d) Inner container

As previously described, the locking plate or inner container screw may be broken during a vertical drop. In this case, to be on the safe side it is assumed that the locking plate has broken and that the impact load of the shielding plug acts on the inner container. The result shows that the inner container does not buckle and that no constraining force is generated on the fuel supporting can or rack stored in the inner container.

Using Euler's buckling equation, which is described in step (d) of (1) "Rear-end-first Vertical Drop", the load (P_k) under which the inner container buckles is given by the expression below because the dimensions required for the calculation are all the same.

$$P_k = 6.37 \times 10^5 \text{ N}$$

The load occurring in the wall surface of the inner container during vertical drop is generated by the weight of the shielding plug and inner container as shown in Fig. (II)-A.35.

$$F = (W_1 + W_2)G$$

W_1	: Weight of the inner container	35 kg
W_2	: Weight of the shielding plug	30 kg
G	: Impact acceleration	135 G

$$F = 9.807 \times (35 + 30) \times 135 \\ = 8.61 \times 10^4 \text{ N}$$

Therefore, the inner container does not buckle. The margin of safety (M.S.) is given by

$$M.S. = \frac{6.37 \times 10^5}{8.61 \times 10^4} - 1 \\ = 6.4$$

The fuel supporting can, the rack and the receiving tube stored in the inner container are not affected by constraining forces resulting from buckling.

(e) Fuel supporting can, receiving tube, and rack

The load generated during a front-end-first vertical drop is the same as the load that is generated during a rear-end-first vertical drop. As confirmed in the preceding section, the fuel supporting can, receiving tube, and rack also remain sound during a front-end-first vertical drop.

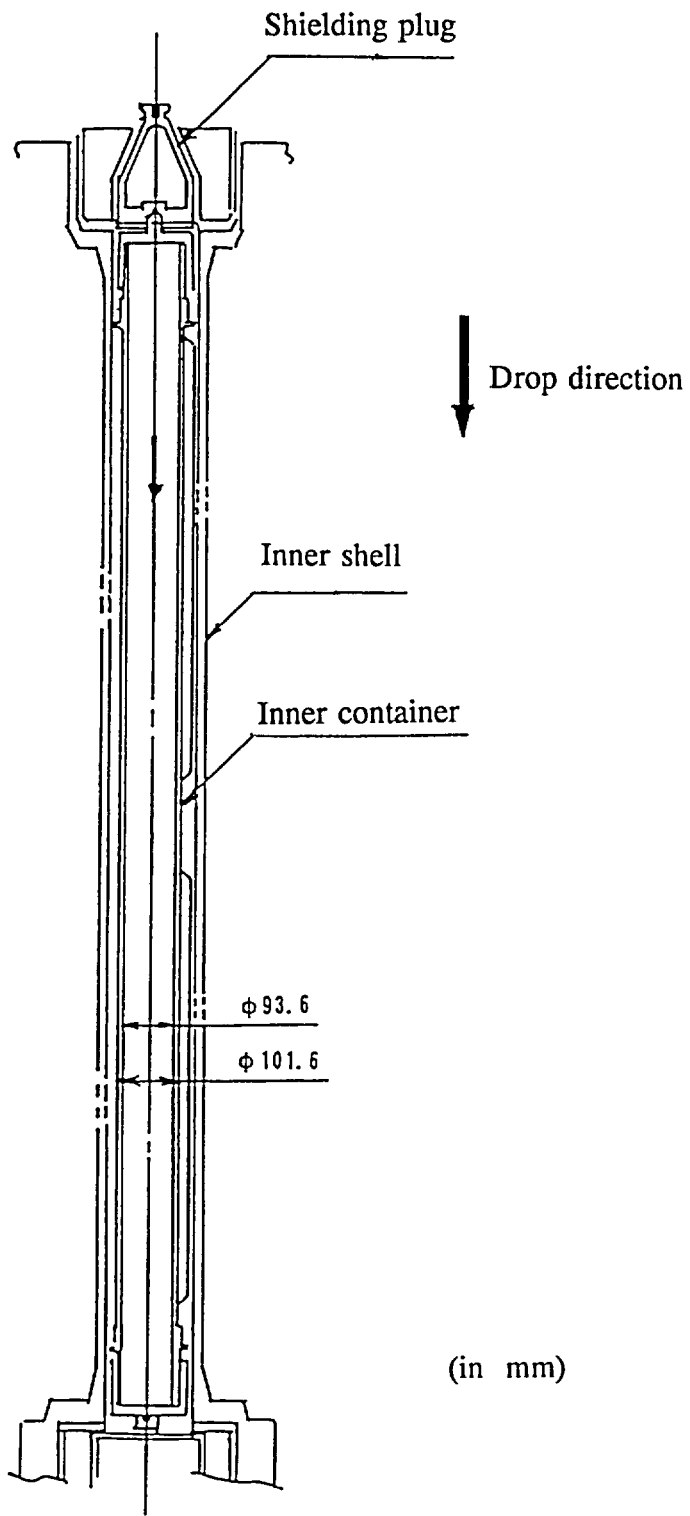


Fig. (II)-A.35 Inner Container

A.6.1.2 Horizontal Drop

The deformation and impact deceleration of the shock absorbers in the case of a 9-m horizontal drop are obtained by the calculation code SHOCK-2. This calculation indicates that deformation occurs only in the shock absorbers. The stress at each part is obtained by assuming that the inertia force based on the obtained impact deceleration acts on each part of the container. This stress is evaluated to indicate that each material used in the container has sufficient strength.

The deformation and impact deceleration of the shock absorbers are calculated numerically using the calculation code SHOCK-2. Fig. (II)-A.36 shows the analysis model and shape during a horizontal drop. The thick line portion of the figure that touches the outer container is made of a stainless steel plate that has a thickness greater than 10 mm and exhibits no compressive deformation of the balsa wood during a horizontal drop. The form factor of this constrained portion is assumed to be $K_1 = 1.0$.

Its circumferential portion is coated with a stainless steel plate that has a 3-mm thickness, and the form factor of this portion is assumed to be $K_2 = 0.75$. The horizontal plane of the balsa wood that is not constrained by the outer container is assumed to be constrained at 75%. Therefore, the boundary condition is assumed to be $K_3 = 0.75$.

The numeric value below is calculated when drop energy $E = 9.71 \times 10^8 \text{ N}\cdot\text{mm}$ is substituted.

Shock absorber deformation	160 mm
Impact deceleration	98 G

The deformation of the shock absorber corresponds to approximately 60% of the shock absorber's allowable thickness (approximately 272 mm) during a horizontal drop. No deformation occurs anywhere other than in the shock absorber. Fig. (II)-A.37 shows the results of evaluations on the front and rear base plates. As shown in this figure, the base plate parts do not touch the drop test target.

Since, in this analysis, the effect of the covering plate is not taken into account, an evaluation is provided in attached document 1. As a result, a deceleration of approximately 10 G is generated by the covering plate. Therefore, this deceleration must be added to the results calculated by the code SHOCK-2 and the stress generated in the parts below must be determined to indicate that they are sound assuming an acceleration of 120 G, to be on the safe side.

- (a) Outer and inner shells of the outer container
- (b) Front and rear lid units
- (c) Inner container
- (d) Fuel supporting can (for Contents I)
- (e) Receiving tube (for Contents II)
- (f) Sampling valve lids and penetration hole lid
- (g) Sampling valve lids and penetration hole lid fastening bolts

Shape	See Fig. (II)-A.36.
Balsa wood Strain - stress curve	See Fig. (II)-A.3.
Shape coefficient	$K_1 = 1.0$ $K_2 = 0.75$ $K_3 = 0.75$
Drop energy	$E = 9.71 \times 10^8 \text{ N}\cdot\text{mm}$

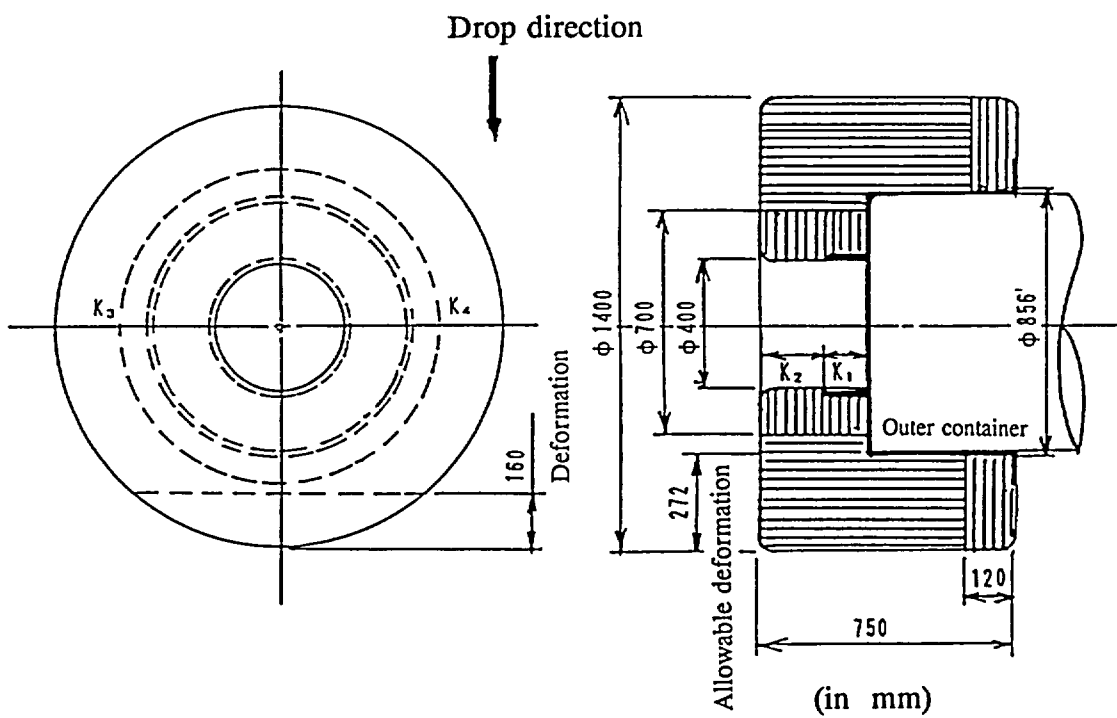


Fig. (II)-A.36 Horizontal Drop

(II)-A-145

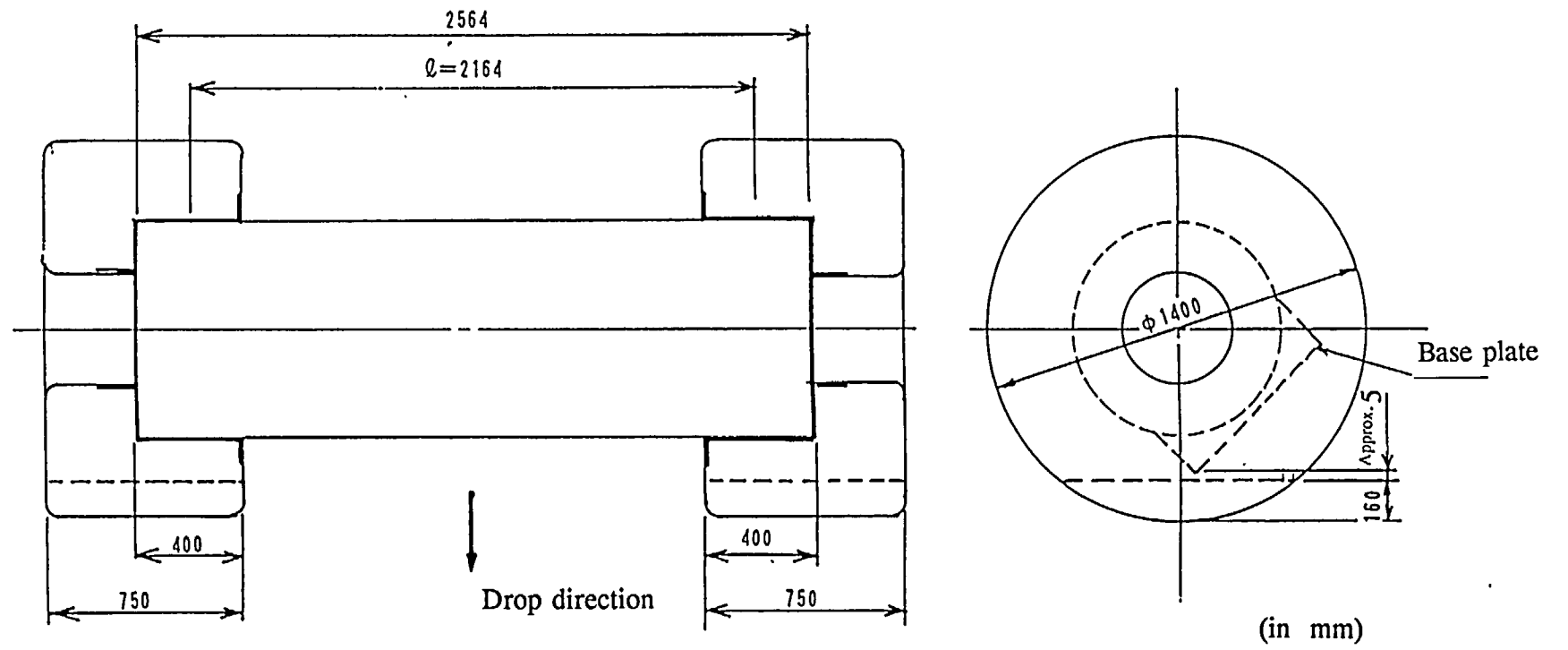


Fig. (II)-A.37 Horizontal Drop Model

(a) Outer and inner shells of the outer container

The impact force of a shock absorber generates a bending moment in the outer container during a horizontal drop. Assuming that this load is all applied to the outer and inner shells as shown in Fig. (II)-A.37, the corresponding stress that is obtained indicates that the outer and inner shells have sufficient strength.

The stress generated in the shells is given by the expression below¹⁾ when it is approximated for a beam supported on both ends.

$$\sigma = \frac{WGl}{8I} \cdot e$$

W	: Package weight	11,000 kg
G	: Impact acceleration	120 G
l	: Supporting interval	2164 mm
I	: Moment of inertia of the outer and inner shell areas	

$$I = \frac{\pi}{64} \times \left\{ (d_{o2}^4 - d_{o1}^4) + (d_{i2}^4 - d_{i1}^4) \right\} \quad 2)$$

d _{o2}	: Outer diameter of the outer shell	800 mm
d _{o1}	: Inner diameter of the outer shell	768 mm
d _{i2}	: Outer diameter of the inner shell	176 mm
d _{i1}	: Inner diameter of the inner shell	142 mm

$$I = \frac{\pi}{64} \times \left\{ (800^4 - 768^4) + (176^4 - 142^4) \right\}$$

$$= 3.05 \times 10^9 \text{ mm}^4$$

e	: Distance between the principal axis and the cross-sectional edge	
	For the outer shell	400 mm
	For the inner shell	88 mm

The stress generated in the outer shell is given by

$$\sigma = \frac{9.807 \times 11000 \times 120 \times 2164}{8 \times 3.05 \times 10^9} \times 400$$

$$= 460 \text{ N/mm}^2$$

$$\approx 46.9 \text{ kg/mm}^2$$

The temperature of the outer shell (SUS304) is 72°C. If the value $\sigma_{UD} = 496 \times 1.2 = 595 \text{ N/mm}^2$ ($\approx 61 \text{ kg/mm}^2$) at a temperature of 80°C is assumed to represent the dynamic tensile strength, the margin of safety (M.S.) is given by

-
- 1) Nihon Kikai Gakkai: Kikai Kogaku Benran, p. 4-54, 1979 (The Japan Society of Mechanical Engineers: Handbook of Mechanical Engineering, page 4-54, 1979)
 - 2) Nihon Kikai Gakkai: Kikai Kogaku Benran, p. 4-5, 1979 (The Japan Society of Mechanical Engineers: Handbook of Mechanical Engineering, page 4-5, 1979)

$$M.S. = \frac{595}{460} - 1$$

$$= 0.3$$

The outer shell has sufficient strength to withstand the load during a drop and is not damaged. The stress generated in the inner shell is given by the expression below.

$$\sigma = \frac{9.807 \times 11000 \times 120 \times 2164}{8 \times 3.05 \times 10^9} \times 88$$

$$= 101 \text{ N/mm}^2$$

$$\approx 10.3 \text{ kg/mm}^2$$

The temperature of the inner shell (SUS304) is 85°C. If a yield stress $\sigma_y = 174 \text{ N/mm}^2$ ($\approx 17.7 \text{ kg/mm}^2$) at a temperature of 90°C is adapted as one of the criteria, the margin of safety (M.S.) is given by

$$M.S. = \frac{174}{101} - 1$$

$$= 0.7$$

The inner shell has sufficient strength to withstand the load during a drop and is therefore not damaged.

(b) Front and rear lids

The shielding plug lid, rear lid, rotating plug lid, and front lid can all be set by inserting them into the inner shell part. As a result, loads acting on those items are supported by the inner shell, and no deformation occurs due to the load generated during a horizontal drop.

(c) Inner container

The inner container is supported by the inner shell during a horizontal drop. Therefore, no deformation occurs.

(d) Fuel supporting can and supporting can

When fuel supporting cans I and II, and the supporting can are dropped horizontally, these outer cylinders are not deformed because they are supported by the inner container. The load shown in Fig. (II)-A.38 is applied to the spacers of the inner cylinders that maintain the intervals between the fuel pins. The next subsection examines the supporting can spacers having a large bending moment arm with large load.

Assuming that the load on the fuel pin acts on the tip of the spacer when it is subject to impact acceleration, the stress generated is obtained, and indicates that the spacer has sufficient strength. The stress generated under these conditions is given by the expression below.

$$\sigma = \frac{WG\ell}{Z}$$

W	: Weight of one fuel pin and receiving tube II	4 kg
G	: Impact acceleration	120 G
ℓ	: Spacer arm length (for the supporting can)	23 mm
Z	: Section modulus of the spacer	

$$Z = \frac{1}{6} \times bh^2$$

b	: Spacer length	Max. 800 mm
h	: Spacer thickness	2 mm

$$\begin{aligned} Z &= \frac{1}{6} \times 800 \times 2^2 \\ &= 5.33 \times 10^2 \text{ mm}^3 \end{aligned}$$

$$\begin{aligned} \sigma &= \frac{9.807 \times 4 \times 120 \times 23}{5.33 \times 10^2} \\ &= 203 \text{ N/mm}^2 \\ &\approx 20.7 \text{ kg/mm}^2 \end{aligned}$$

Given a temperature of 300°C for the supporting can (SUS304), to be on the safe side, the value $\sigma_{UD} = 1.2 \times 437 = 524 \text{ N/mm}^2$ ($\approx 53.5 \text{ kg/mm}^2$) at a temperature of 350°C is assumed to represent the dynamic tensile strength. The margin of safety (M.S.) is given by the expression below including a welding efficiency of 0.6 because the spacers are welded.

$$\begin{aligned} M.S. &= \frac{524 \times 0.6}{203} - 1 \\ &= 0.54 \end{aligned}$$

Therefore, the spacers have sufficient strength to withstand the load applied during a horizontal drop, and the interval between the fuel pins is secured.

(II)-A-149

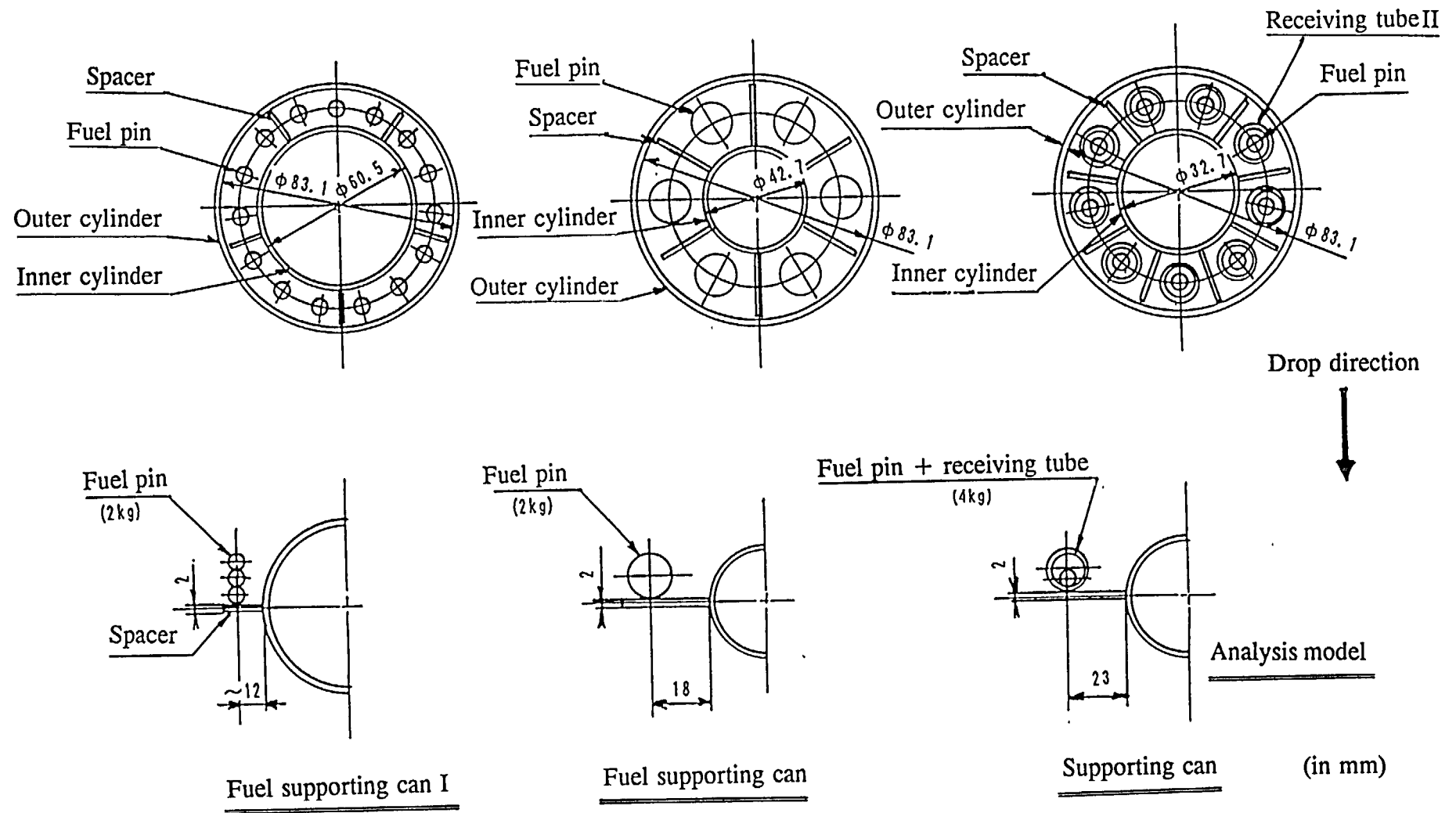


Fig. (II)-A.38 Horizontal Drop of the Supporting Can

(e) Receiving tube

The receiving tube is classified into receiving tube I and receiving tube II. Receiving tube II is not deformed because it is supported by the supporting can during a horizontal drop. Receiving tube I is accommodated in the rack and stored in the inner container. Since receiving tube I is supported at intervals of approximately 500 mm by the spacers in the rack as shown in Fig. (II)-A.39, the inertia force during a horizontal drop, and thus the bending stress acts on receiving tube I. This stress is obtained to indicate that receiving tube I has sufficient strength. The bending stress is given by the expression below, assuming a uniform load.

$$\sigma = \frac{WG\ell}{12Z} \quad 1)$$

W	: (Receiving tube I + fuel pin weight) / 2	1 kg
G	: Impact acceleration	120 G
ℓ	: Spacer interval	510 mm
Z	: Section modulus of receiving tube I	

$$Z = \frac{\pi}{32} \times \frac{d_2^4 - d_1^4}{d_2}$$

d_2	: Outer diameter of receiving tube I	13.8 mm
d_1	: Inner diameter of receiving tube I	10.5 mm

$$\begin{aligned} Z &= \frac{\pi}{32} \times \frac{13.8^4 - 10.5^4}{13.8} \\ &= 1.72 \times 10^2 \text{ mm}^3 \\ \sigma &= \frac{9.807 \times 1 \times 120 \times 510}{12 \times 1.72 \times 10^2} \\ &= 291 \text{ N/mm}^2 \\ &\approx 29.7 \text{ kg/mm}^2 \end{aligned}$$

The temperature of receiving tube I (SUS304) is 245°C. If the value σ_{UD} ($437 \times 1.2 = 524 \text{ N/mm}^2$ ($\approx 53.5 \text{ kg/mm}^2$)) at a temperature of 350°C is assumed to represent the dynamic tensile strength, the margin of safety (M.S.) is given by

$$\begin{aligned} M.S. &= \frac{524}{291} - 1 \\ &= 0.8 \end{aligned}$$

Therefore, receiving tube I has sufficient strength to withstand the load applied during a horizontal drop and is not damaged.

1) Nihon Kikai Gakkai: Kikai Kogaku Benran p. 4-55
(The Japan Society of Mechanical Engineers: Handbook of Mechanical Engineering, page 4-55)

ISI-V-(II)

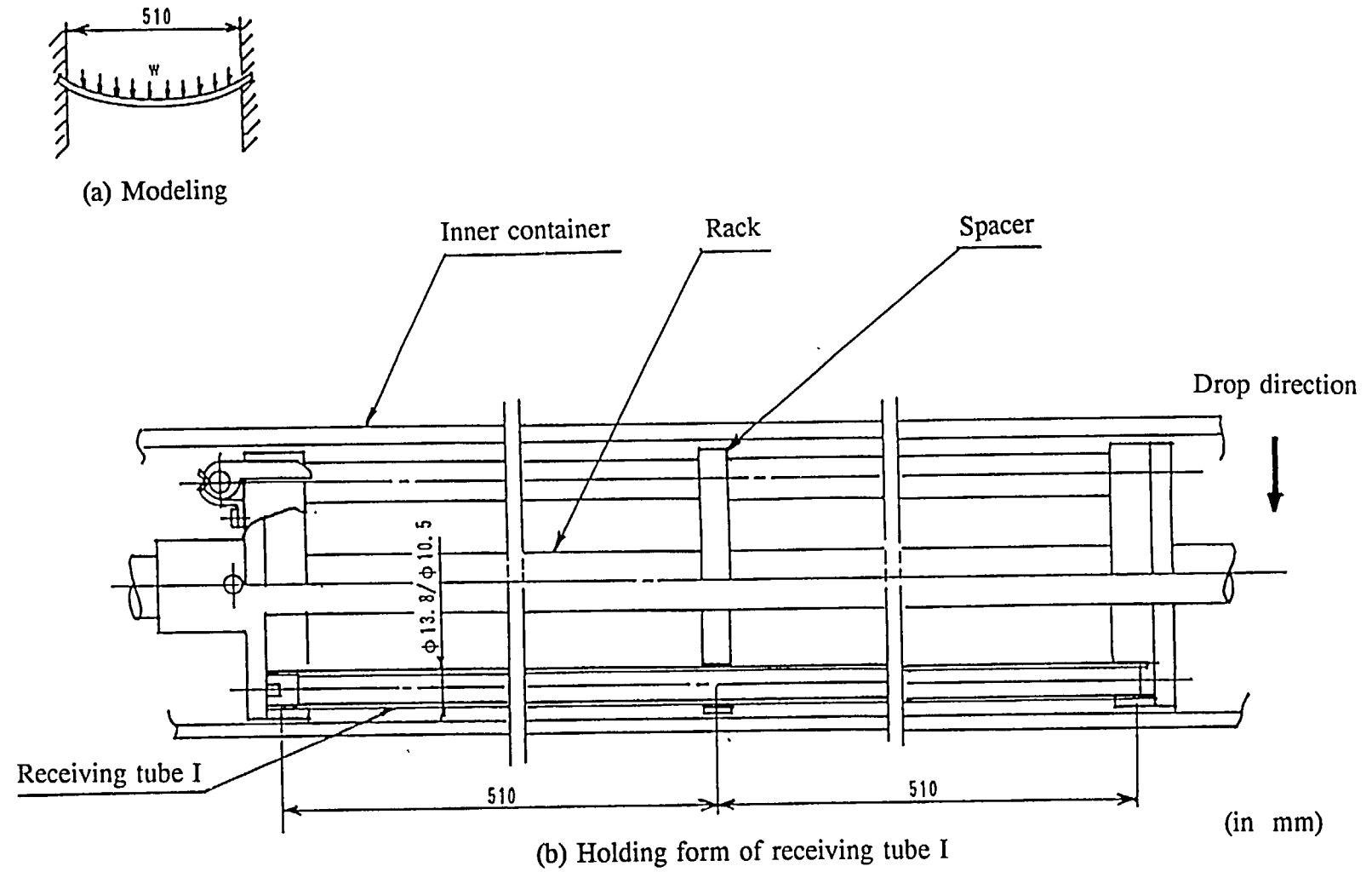


Fig. (II)-A.39 Horizontal Drop of Receiving Tube I

(f) Sampling valve lid and penetration hole lid

Two sampling lids and one penetration hole lid are installed in this packaging. They are much the same except for the length of the shielding lead plug. The heaviest rear sampling valve lid is thus analyzed. Assuming that the inertia force resulting from the impact acceleration during a horizontal drop is distributed near the center of the lid as shown in Fig. (II)-A.40, the bending stress generated in the lid is obtained, and indicates that the lid has sufficient strength.

The maximum bending stress generated in the flange is given by the expression 1) below.

$$\sigma = \frac{3pb^2}{8h^2} \times \left\{ 4(1 + \nu) \log_e \frac{a}{b} + 4 - (1 - \nu) \frac{b^2}{a^2} \right\}$$

p : Distributed load

$$p = \frac{WG}{\frac{\pi}{4}d^2}$$

W : Lid weight 6 kg
G : Acceleration during a horizontal drop 120 G
d : Diameter of the plug part 48.6 mm

$$p = \frac{9.807 \times 6 \times 120}{\frac{\pi}{4}48.6^2}$$
$$= 3.81 \text{ N/mm}^2$$

b : Radius of area subjected to a concentrated load 24.3 mm
h : Plate thickness of the flange 25 mm
a : Radius of the supporting point 60 mm
 ν : Poisson's ratio 0.3 mm

$$\sigma = \frac{3 \times 3.81 \times 24.3^2}{8 \times 25^2} \times \left\{ 4(1 + 0.3) \log_e \frac{60}{24.3} + 4 - (1 - 0.3) \frac{24.3^2}{60^2} \right\}$$
$$= 11.6 \text{ N/mm}^2$$
$$\approx 1.18 \text{ kg/mm}^2$$

1) Nihon Kikai Gakkai: Kikai Kogaku Benran, p. 4-115
(The Japan Society of Mechanical Engineers: Handbook of Mechanical Engineering, page 4-115)

The deformation of the O-ring groove part is given by the expression¹⁾ below.

$$\omega = \frac{Pb^4}{16D} \left[\frac{1}{2(1+\nu)} \left(1 - \frac{r^2}{a^2}\right) \left\{ 2(3+\nu) \frac{a^2}{b^2} - (1-\nu) \right\} - \left(1 + \frac{2r^2}{b^2}\right) \log_e \frac{a}{r} \right]$$

D : Flexural rigidity of the plate

$$D = \frac{Eh^3}{12(1-\nu^2)}$$

E	: Modulus of longitudinal elasticity	1.91 × 10 ⁵ N/mm ²
h	: Plate thickness of the flange	25 mm
ν	: Poisson's ratio	0.3
r	: Radius of the O-ring	36 mm

$$D = \frac{1.91 \times 10^5 \times 25^3}{12(1-0.3^2)}$$

$$= 2.73 \times 10^8 \text{ N}\cdot\text{mm}$$

$$\omega = \frac{3.81 \times 24.5^4}{16 \times 2.73 \times 10^8} \left[\frac{1}{2(1+0.3)} \left(1 - \frac{36^2}{60^2}\right) \left\{ 2(3+0.3) \frac{60^2}{24.3^2} - (1-0.3) \right\} - \left(1 + \frac{2 \times 36^2}{24.3^2}\right) \log_e \frac{60}{36} \right]$$

$$= 2.12 \times 10^{-3} \text{ mm}$$

The temperature of the flange (SUS304) is 75°C. If the yield stress of $\sigma_y = 180 \text{ N/mm}^2$ ($\approx 18.3 \text{ kg/mm}^2$) at a temperature of 80°C is assumed to be one of the criteria, the margin of safety (M.S.) is given by

$$M.S. = \frac{180}{11.6} - 1$$

$$= 15$$

The lid has sufficient strength to withstand the load applied during a horizontal drop. The degree of deformation (approximately 0.002 mm) of the O-ring groove part is less than the collapsed height (0.9 mm) of the O-ring used. Containment is thus maintained.

1) Nihon Kikai Gakkai: Kikai Kogaku Benran, p. 4-115
The Japan Society of Mechanical Engineers: Handbook of Mechanical Engineering, page 4-115)

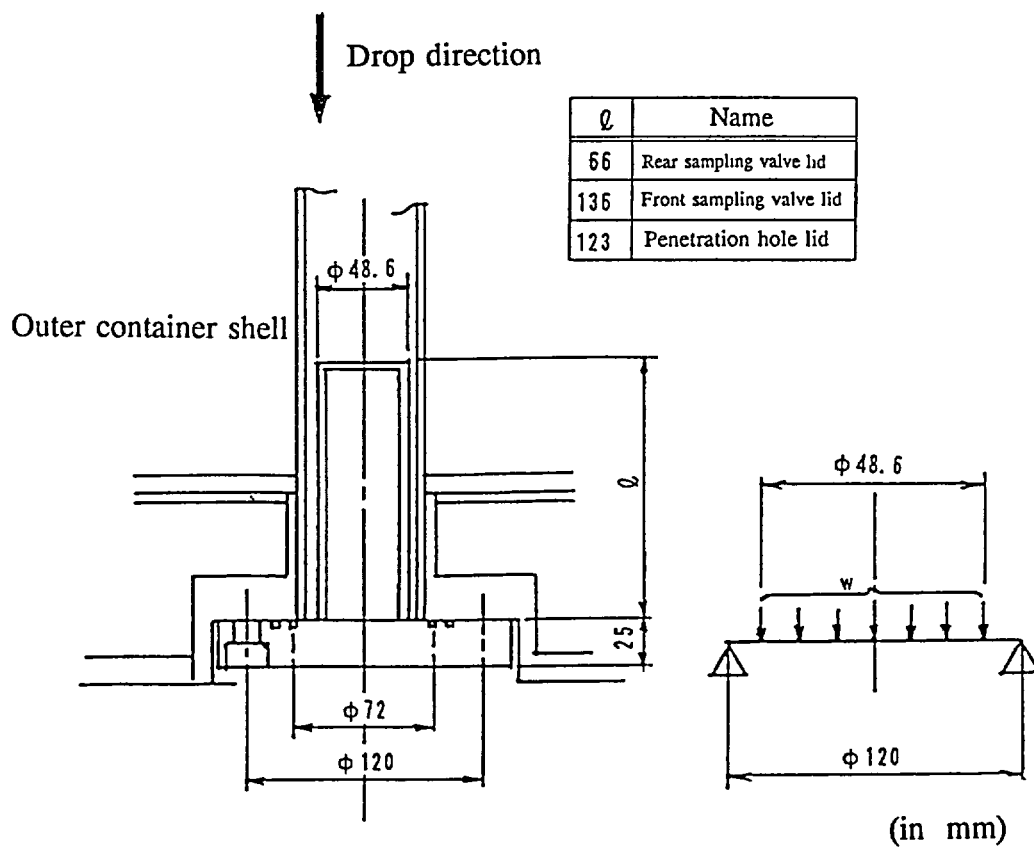


Fig. (II)-A.40 Sampling Valve Lid and Penetration Hole Lid (during a Horizontal Drop)

(g) Fastening bolts for the sampling valve lids and the penetration hole lid

The load that acts on the sampling valve lids and penetration hole lid is applied to their fastening bolts. At that time, the tensile stress generated in the bolts is obtained, and indicates that each bolt has sufficient strength. The ultimate stress generated in the fastening bolts is given by the expression below.

$$\sigma = \frac{WG}{nA}$$

W	: Lid weight	6 kg
G	: Impact acceleration	120 G
n	: Number of bolts	4
A	: Cross-sectional area of the bolt	

$$A = \frac{\pi d_B^2}{4}$$

d_B	: Diameter of the bolt thread (M12)	10.1 mm
-------	-------------------------------------	---------

$$\begin{aligned} A &= \frac{\pi}{4} \times 10.1^2 \\ &= 80 \text{ mm}^2 \end{aligned}$$

$$\begin{aligned} \sigma &= \frac{9.807 \times 6 \times 120}{4 \times 80} \\ &= 22.1 \text{ N/mm}^2 \\ &\approx 2.25 \text{ kg/mm}^2 \end{aligned}$$

The temperature of the fastening bolt (SUS630) is 75°C. If the yield stress of $\sigma_y = 682 \text{ N/mm}^2$ ($\approx 69.6 \text{ kg/mm}^2$) at a temperature of 80°C is assumed to be one of the criteria, the margin of safety (M.S.) is given by

$$\begin{aligned} M.S. &= \frac{682}{22.1} - 1 \\ &= 30 \end{aligned}$$

Therefore, the fastening bolt has sufficient strength to withstand the tensile load applied during a horizontal drop and does not break.

A.6.1.3 Corner Drop

The deformation and impact deceleration of the shock absorber during a 9-m corner drop are obtained by the calculation code SHOCK-2. This calculation indicates that only the shock absorber is deformed. As shown in Fig. (II)-A.41, the corner drop analysis determines the amount of deformation and impact deceleration of the shock absorber during a drop at an inclination angle of 23 degrees so that a line that aligns the center of gravity of the package with the corner that hits the target is perpendicular to the target.

As described previously, the boundary conditions are the form factor values shown in Fig. (II)-A.41. The numeric value below results when drop energy $E = 9.71 \times 10^8 \text{ N}\cdot\text{mm}$ is used.

Shock absorber deformation	210 mm
Impact deceleration	66 G

Therefore, only the shock absorber is deformed in the parts shown in Fig. (II)-A.41. Given the effect of the covering plate, to be on the safe side an acceleration of 75 G is assumed.

The axial impact acceleration and radial impact acceleration at that time are as follows:

Axial impact acceleration	$75 \times \cos 23^\circ = 69 \text{ G}$
Radial impact acceleration	$75 \times \sin 23^\circ = 29 \text{ G}$

These acceleration values do not exceed the impact acceleration during vertical and horizontal drops.

Impact acceleration during a vertical drop > Axial impact acceleration: $135 \text{ G} > 69 \text{ G}$
Impact acceleration during a horizontal drop > Radial impact acceleration: $120 \text{ G} > 29 \text{ G}$

Since the outer container, inner container, and fuel supporting can or receiving tube maintain their strength during vertical and horizontal drops with a stronger impact, they also maintain their strength during a corner drop.

The shielding plug lid fastening bolt and rotating plug lid fastening bolt are supported by the shock absorbers during a vertical drop as shown in Figs. (II)-A.24 and (II)-A.30. However, during a corner drop, the stress caused by the moment force shown in Fig. (II)-A.42 acts on each fastening bolt. Therefore, the stress state in the case of a corner drop differs from the stress state in the case of a vertical or horizontal drop.

The stresses generated in the shielding lid fastening bolt and rotating plug lid fastening bolt is thus obtained, and indicates that these bolts have sufficient strength.

Shape	See Fig. (II)-A.41.
Balsa wood	
Strain - stress curve	See Fig. (II)-A.3.
Shape coefficient	$K_1 = 1.0$ $K_2 = 1.0$ $K_3 = 1.0$ $K_4 = 0.75$
Drop energy	$E = 9.71 \times 10^8 \text{ N}\cdot\text{mm}$

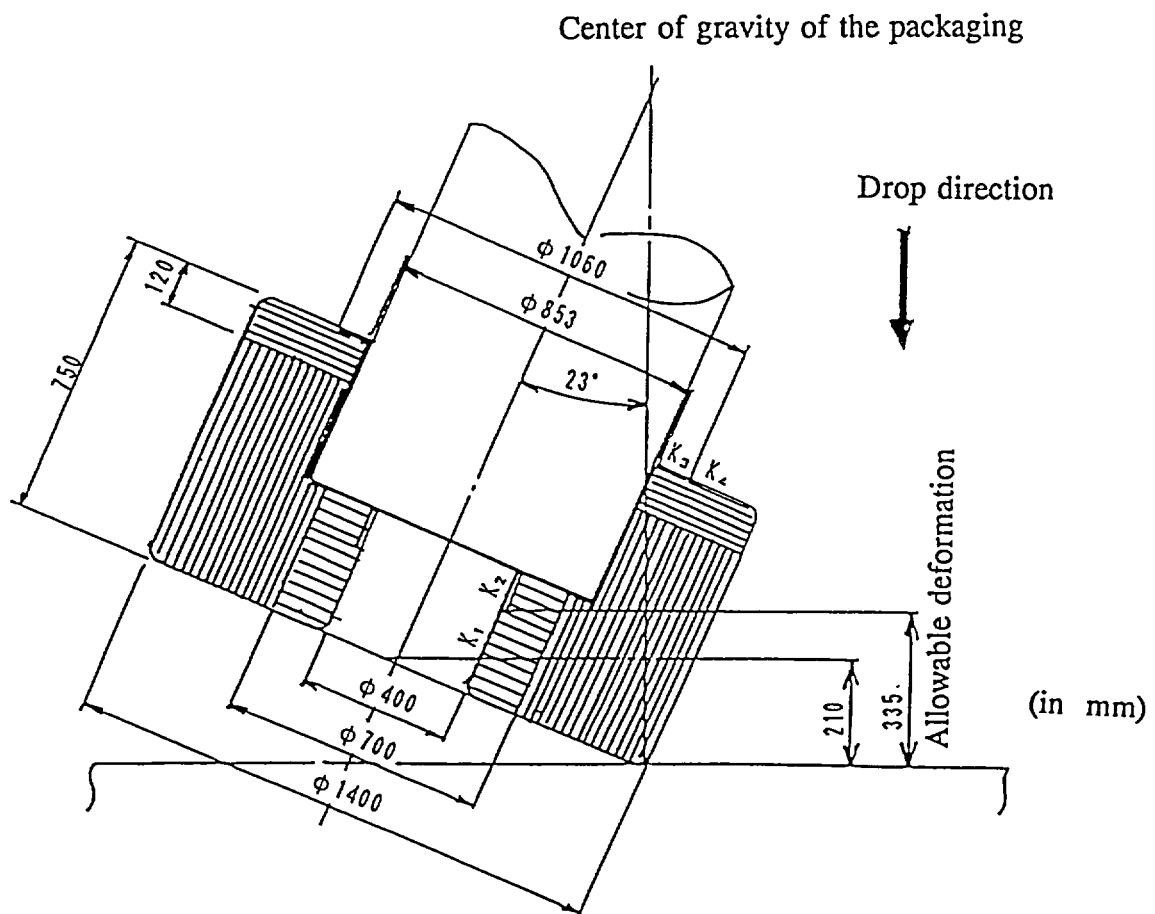


Fig. (II)-A.41 Corner Drop

(1) Shielding plug lid fastening bolt

During a corner drop, the load caused by the total weight of the shielding plug, shielding plug lid, rear lid, and contents acts on the shielding plug lid fastening bolt. If the rear lid unit is not constrained by the end plate of the shock absorber, to be on the safe side, an impact acceleration of 75 G acts on the package, with the A-A axis of the outer container corner part as the supporting point as shown in Fig. (II)-A.42. As a result, the moment of rotation acts on the fastening bolt.

This moment (M) is given by the expression below.

$$M = WG\ell_1 \cos A$$

W : Weight of the shielding plug, shielding plug lid, rear lid, and contents
W = 30 + 120 + 7 + 100
= 257 kg

G : Impact acceleration during a corner drop 75 G
 ℓ_1 : Moment arm 400 mm
A : Drop angle 23 degrees

$$M = 9.807 \times 257 \times 75 \times 400 \times \cos 23^\circ \\ = 6.96 \times 10^7 \text{ N}\cdot\text{mm}$$

In Fig. (II)-A.42, the inertia moment (I) of the bolt about the (A-A) axis is given by the expression below.

$$I = \sum_{i=1}^N (h_i^2 A_b + I_z) \quad 1)$$

h_i : Moment arm in the θ_i position
 $h_i = L_o + R (1 + \cos \theta_i)$

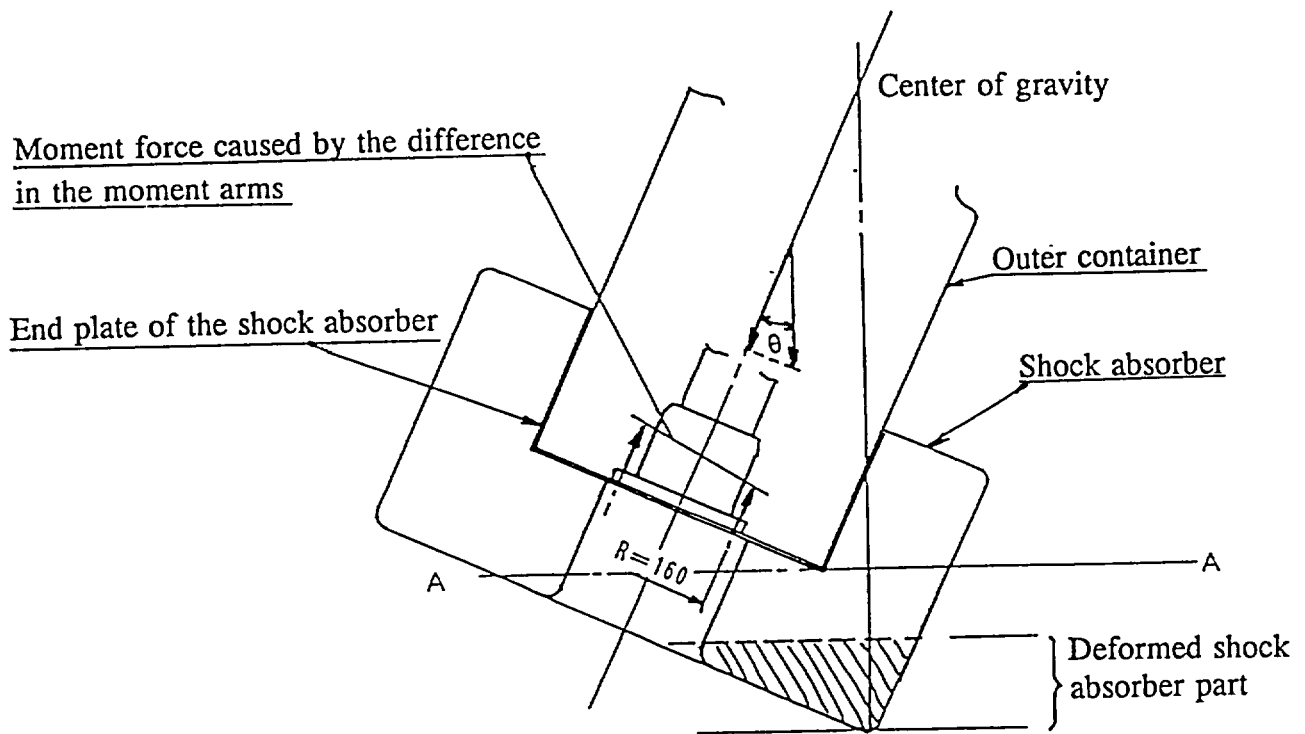
L_o : Distance between the (A-A) axis and lowest bolt 240 mm
R : Radius of a bolt circle 160 mm
 θ_i : Angle indicating the position of the i'th bolt
N : Number of bolts 16
 A_b : Cross-sectional area of the bolt thread (M20) 232 mm²
 I_z : Inertia moment about the center axis of each bolt $4.4 \times 10^3 \text{ mm}^4$

The expression below is given when the numeric values above are used.

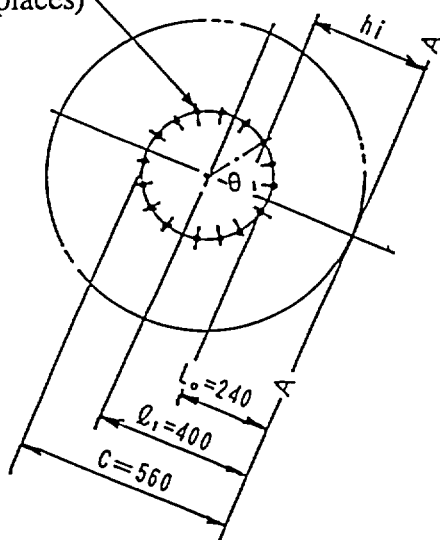
$$I = 6.43 \times 10^8 \text{ mm}^4$$

Therefore, the tensile stress (σ) generated in the fastening bolt is given by the expression below. As a result, the maximum tensile stress is generated in the bolt most distant from the A-A axis of the outer container corner part.

1) Nihon Kikai Gakkai: Kikai Kogaku Benran p. 4-50
(The Japan Society of Mechanical Engineers: Handbook of Mechanical Engineering, page 4-50)



Shielding plug lid fastening bolt
(M20 in 16 places)



(in mm)

Fig. (II)-A.42 Shielding Plug Lid Fastening Bolt

$$\sigma = \frac{MC}{I} \quad 1)$$

C : Distance of the bolt farthest from the (A-A) axis 560 mm

$$\begin{aligned} \sigma &= \frac{6.96 \times 10^7 \times 560}{6.43 \times 10^8} \\ &= 60.6 \text{ N/mm}^2 \\ &\approx 6.17 \text{ kg/mm}^2 \end{aligned}$$

The temperature of the fastening bolt (SUS630) is 73°C. If the yield stress of $\sigma_y = 682 \text{ N/mm}^2$ ($\approx 69.6 \text{ kg/mm}^2$) at a temperature of 80°C is assumed to be one of the criteria, to be on the safe side, the margin of safety (M.S.) is given by

$$\begin{aligned} M.S. &= \frac{682}{60.6} - 1 \\ &= 10 \end{aligned}$$

Therefore, the shielding plug lid fastening bolt has sufficient strength to withstand the tensile load during a corner drop.

The strain (ϵ) caused by the impact load is given by the expression below.

$$\epsilon = \frac{\sigma}{E} \quad 2)$$

σ : Stress generated in the bolt 60.6 N/mm²
 E : Modulus of longitudinal elasticity of the bolt material $2.13 \times 10^5 \text{ N/mm}^2$

Assuming that the initial length (ℓ) of the bolt is 45 mm, to be on the safe side, the elongation ($\Delta\ell$) of the bolt is given by

$$\begin{aligned} \Delta\ell &= \epsilon\ell \\ &= \frac{\sigma}{E} \cdot \ell \end{aligned}$$

ℓ : Initial length of the bolt 45 mm

$$\begin{aligned} \Delta\ell &= \frac{60.6}{2.13 \times 10^5} \times 45 \\ &= 0.01 \text{ mm} \end{aligned}$$

The collapsed height of the O-ring (8 mm in diameter) used for the shielding plug lid is 1.3 mm or more. Consequently, the containment is maintained even given the maximum elongation ($\Delta\ell = 0.01 \text{ mm}$) of the bolt.

-
- 1) R.J. Roark: Formulas for Stress and Strain, pages 100
 2) Nihon Kikai Gakkai: Kikai Kogaku Benran, p. 4-7
 (The Japan Society of Mechanical Engineers: Handbook of Mechanical Engineering, page 4-7)

(2) Strength of the rotating plug lid fastening bolt

The load from the total weight of the rotating plug lid, the rotating plug lid cover, the rotating plug, the front lid, and the contents acts on the rotating plug lid fastening bolt during a corner drop. If assuming, to be on the safe side, that the front lid unit is not constrained by the end plate of a shock absorber, an impact acceleration of 75 G acts on the package with the (A-A) axis of the outer container corner part as a supporting point as shown in Fig. (II)-A.43. As a result, the moment of rotation acts on the fastening bolt. This moment (M) is given by the expression below.

$$M = W \cdot \alpha \cdot \ell_o \cdot \cos A$$

W : Total weight of the rotating plug, the rotating plug lid cover, the rotating plug lid, the front lid, and the contents

$$\begin{aligned} W &= 125 + 75 + 220 + 15 + 100 \\ &= 535 \text{ kg} \end{aligned}$$

α : Impact acceleration during a corner drop 75 (G)
 ℓ_o : Moment arm 400 mm
A : Drop angle 23°

$$\begin{aligned} M &= 9.807 \times 535 \times 75 \times 400 \times \cos 23^\circ \\ &= 1.45 \times 10^8 \text{ N}\cdot\text{mm} \end{aligned}$$

The inertia moment of the bolt about the (A-A) axis shown in Fig. (II)-A.43 is given by

$$I = \sum_{i=1}^N (h_i^2 \cdot A_b + I_z)$$

h_i : Moment arm in θ_i position

$$h_i = L_o + R (1 - \cos \theta_i)$$

L_o : Distance between (A-A) axis and the lowest bolt 160 mm
R : Radius of bolt circle 240 mm
 θ_i : Angle indicating the position of i'th bolt

$$\theta_i = \frac{360}{N} \cdot i$$

N : Number of bolts 20
 A_b : Sectional area of the bolt thread (M20) 232 mm²
 I_z : Inertia moment about the center axis of each bolt 4.4×10^3 mm⁴

The expression below results when the numeric values above are used.

$$I = 8.76 \times 10^8 \text{ mm}^4$$

Therefore, the tensile stress (σ) generated in the fastening bolt is given by the expression below.

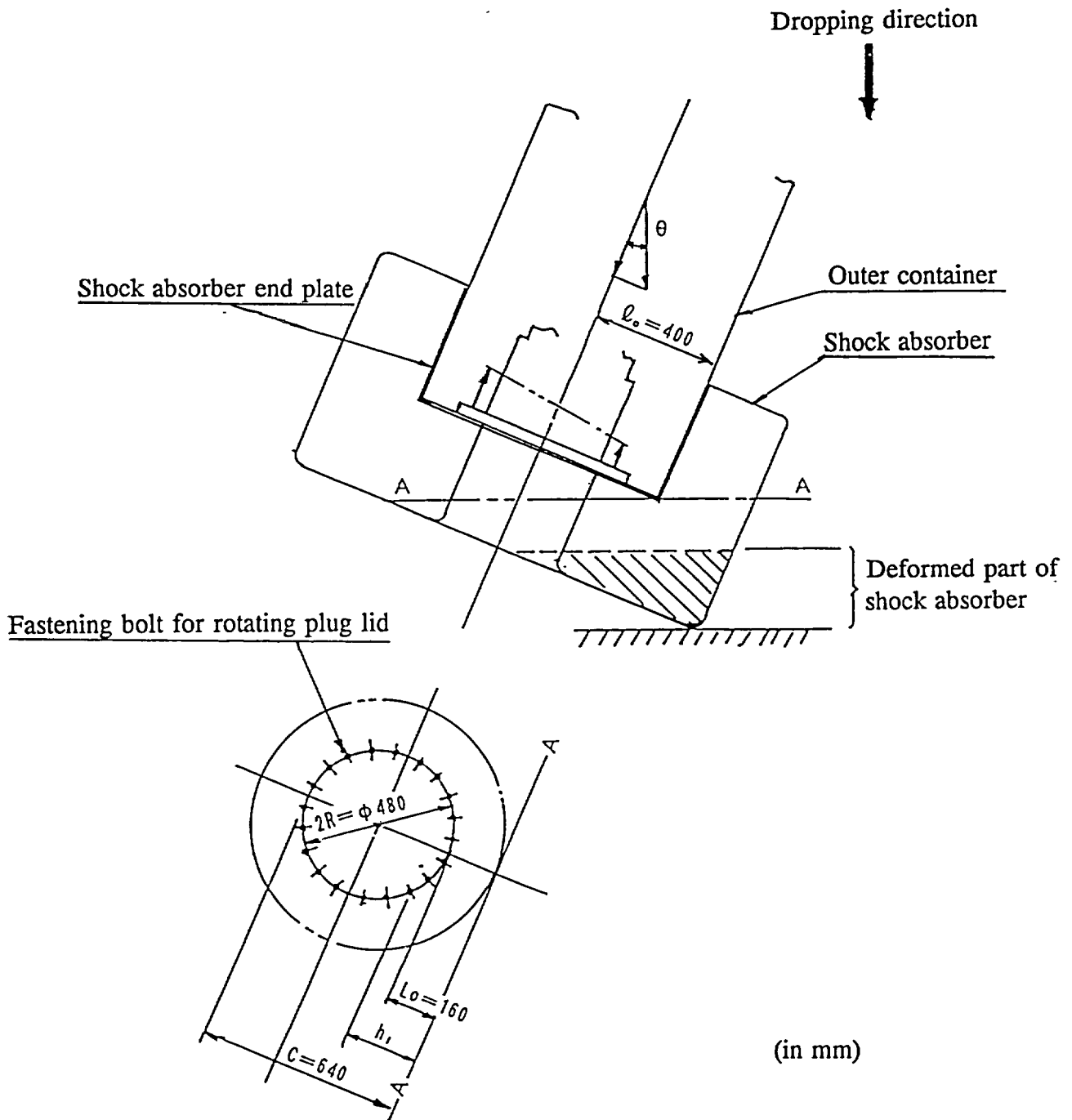


Fig. (II)-A.43 Fastening Bolt for Rotating Plug Lid

The maximum tensile stress is generated in the bolt at the greatest distance from the (A-A) axis of the outer container corner part.

$$\sigma = \frac{M \cdot C}{I}$$

C : Distance to the bolt furthest from (A-A) axis 640 mm

$$\begin{aligned}\sigma &= \frac{1.45 \times 10^8 \times 640}{8.76 \times 10^8} \\ &= 106 \text{ N/mm}^2 \\ &\approx 10.8 \text{ kg/mm}^2\end{aligned}$$

The temperature of the fastening bolt (SUS630) is 73°C. To be on the safe side, if the yield stress $\sigma_y = 682 \text{ N/mm}^2$ ($\approx 69.6 \text{ kg/mm}^2$) at a temperature of 80°C is assumed to be one of the criteria, the margin of safety (M.S.) is given by

$$\begin{aligned}M.S. &= \frac{682}{106} - 1 \\ &= 5.4\end{aligned}$$

The fastening bolt is thus not deformed or broken by the tensile load applied during a corner drop.

The strain (ϵ) resulting from the impact load is given

$$\epsilon = \frac{\sigma}{E}$$

σ : Stress occurring in the bolt 106 N/mm²
 E : Modulus of the longitudinal elasticity of the bolt material $2.13 \times 10^5 \text{ N/mm}^2$

Assuming that the initial length (ℓ) of a bolt is 45 mm to be on the safe side, the bolt elongation ($\Delta \ell$) at that time is given by the expression below.

$$\begin{aligned}\Delta \ell &= \epsilon \cdot \ell \\ &= \frac{\sigma}{E} \cdot \ell\end{aligned}$$

ℓ : Initial length of the bolt 45 mm

$$\begin{aligned}\Delta \ell &= \frac{106}{2.13 \times 10^6} \times 45 \\ &= 0.02 \text{ mm}\end{aligned}$$

Since the collapsed height of an O-ring (8 mm in diameter) used in the rotating plug lid is more than 1.3 mm, containment is maintained even if the maximum elongation ($\Delta \ell = 0.02 \text{ mm}$) of the bolt is assumed.

A.6.1.4 Oblique drop

This subsection evaluates the oblique drop (when the drop direction is in between a corner drop and a vertical drop, and between a corner drop and a horizontal drop).

The axial and radial acceleration components during an oblique drop are lower than those during vertical and horizontal drops. During severer vertical and horizontal drops, the outer container, inner container, and fuel supporting can or receiving tube maintain their strength. Like the above, therefore, they also maintain their strength during an oblique drop.

Therefore, this subsection concentrates on an analysis showing that the shock absorber deformation during an oblique drop does not reach the outer container.

When a package drops at angle α formed by the G-A line and the line perpendicular to the target during an oblique drop as shown in Fig. (II)-A.44, the drop energy can be divided into the deforming energy at point A and the rotating energy of the package. The rotating energy is absorbed by the shock absorber at another edge.

The drop energy is given by the expression below when it is converted into kinetic energy for evaluation.

$$E = W \cdot H$$

$$E = \frac{1}{2} \cdot M \cdot V^2 \quad 1)$$

Assuming that the packaging is a rigid body, the inertia moment can be derived from the angular motion equations at point A as shown below.

$$I \cdot \omega = M \cdot V \cdot e$$

I : Inertia moment of the packaging at point A

$$I = I_0 + M \cdot \ell^2$$

I_0 : Inertia moment of packaging at point G

$$I_0 = M \left(\frac{R^2}{4} + \frac{L^2}{12} \right) \quad 2)$$

M : Packaging mass

$$M = W$$

W : Package weight . 11,000 kg

$$M = 11,000$$

$$= 11.0 \times 10^3 \text{ kg}$$

ℓ : Distance between points G and A 1776 mm

R : Radius of a shock absorber 700 mm

L : Total length of the package 3264 mm

1) Nihon Kikai Gakkai: Kikai Kogaku Benran, p. 3-21 (The Japan Society of Mechanical Engineers: Handbook of Mechanical Engineering, page 3-21)

2) Maruzen: Kikai Sekkei Benran, p. 71, 1979
(Handbook of Mechanical Design: page 71, Maruzen, 1979)

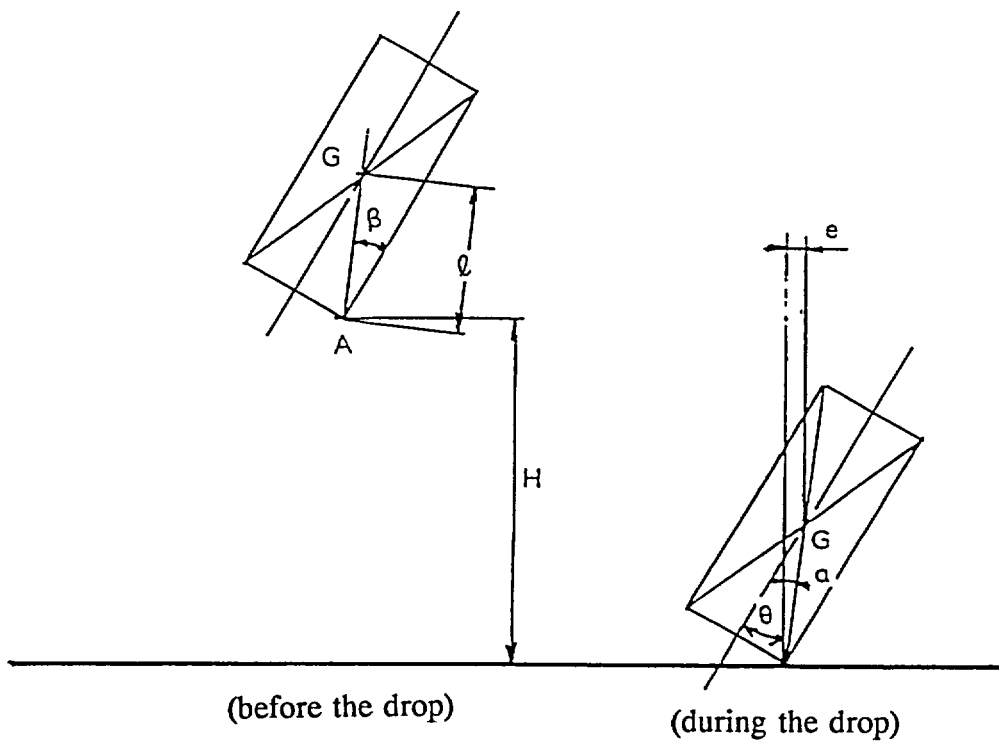


Fig. (II)-A.44 Oblique Drop Model

$$I_0 = 11.0 \times \left(\frac{700^2}{4} + \frac{3264^2}{12} \right)$$

$$= 1.11 \times 10^7 \text{ N}\cdot\text{sec}^2\cdot\text{mm}$$

- ω : Revolving angular speed of the packaging after it makes contact with the target
 v : Speed just before contact with the target
 e : Distance between the center of gravity (G) and the line perpendicular to the target
 $e = \ell \cdot \sin\alpha$
 α : Angle of G-A line to the perpendicular line

Rotating energy E_R is given by

$$E_R = \frac{1}{2} I \cdot \omega^2 \quad 1)$$

$$= E \left\{ \frac{\sin^2 \alpha}{L + \left(\frac{I_0}{M \cdot \ell^2} \right)} \right\}$$

Therefore, the impact energy E_s exerted at point A is

$$E_s = E - E_R$$

$$= \left\{ 1 - \frac{\sin^2 \alpha}{1 + \left(\frac{I_0}{M \cdot \ell^2} \right)} \right\}$$

$$= E \left\{ \frac{\cos^2(\theta - \beta) + \frac{I_0}{M \cdot \ell^2}}{1 + \left(\frac{I_0}{M \cdot \ell^2} \right)} \right\}$$

where

- θ : Angle formed by the packaging's center line and the line perpendicular to the target
 β : Angle formed by the packaging's center line and the G-A line to the target 23°

The evaluations are performed for inclined angle θ every 15 degrees within a range of 15° to 75° degrees. Assuming that the impact energy E_s is absorbed by a shock absorber, the deformation and impact deceleration are calculated in the same manner as during corner drop by the calculation code, SHOCK-2. Table (II)-A.23 and Fig. (II)-A.45 provide the resulting information.

As shown in this table, deformation is limited to the shock absorber. The shock absorber deformation does not reach the outer container body.

- 1) Nihon Kikai Gakkai: Kikai Kogaku Benran, p. 3-30
 (The Japan Society of Mechanical Engineers: Handbook of Mechanical Engineering, page 3-30)

Table (II)-A.23 Impact Force and Deformation during an Oblique Drop

Drop angle	Impact energy (Es) = Energy to be absorbed by a shock absorber	Impact Deceleration G	Deformation	Allowable degree of deformation of a shock absorber
15°	$7.17 \times 10^8 \text{ N} \cdot \text{mm}$	96 G	170 mm	About 300 mm
30°	$7.50 \times 10^8 \text{ N} \cdot \text{mm}$	90 G	217 mm	About 400 mm
45°	$7.07 \times 10^8 \text{ N} \cdot \text{mm}$	79 G	255 mm	About 410 mm
60°	$5.99 \times 10^8 \text{ N} \cdot \text{mm}$	71 G	265 mm	About 390 mm
75°	$4.55 \times 10^8 \text{ N} \cdot \text{mm}$	69 G	217 mm	About 340 mm

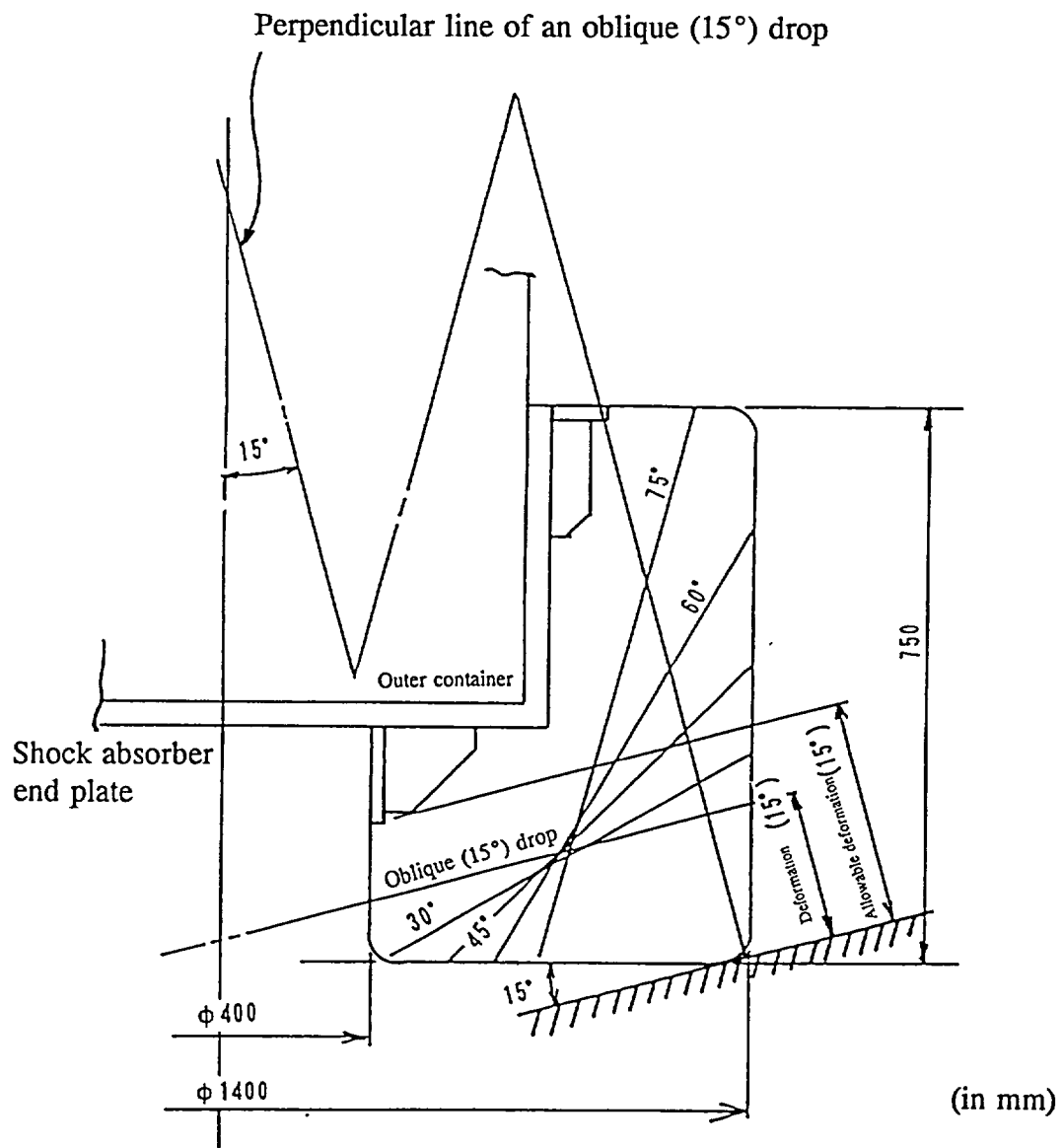


Fig. (II)-A.45 Deformation during Oblique Drop

A.6.1.5 Summary and examination of results

From the calculations in subsections A.6.1.1 through A.6.1.4, deformation occurs only in the shock absorbers of this package regardless of the attitude from which the package is dropped from a height of 9 m. The shock absorber deformation does not affect the outer container. Table (II)-A.24 summarizes the deformation of the shock absorber for each drop attitude.

Table (II)-A.24 Shock Absorber Deformation in Drop Test I

Drop attitude	Shock absorber thickness at the shock absorber end plate (mm)	Allowable deformation (mm)	Deformation by drop test I (mm)
Vertical drop	320	185	110
Horizontal drop	273	273	160
Corner drop	400	335	210

The containment system such as lid units and inner shell remains sound and maintains its containment, even if these parts are subject to a maximum acceleration resulting from drops in each attitude. The secondary containment system such as a fuel supporting can or receiving tubes also remains sound. During the front-end-first vertical drop, the locking plate and inner container screw that fix the inner container are damaged, but the inner container remains sound and stays at its position in the inner shell. The contents also remain at their positions even after drop test I is conducted.

A.6.2 Mechanical Test and Drop Test II (1 m Drop)

This subsection performs an evaluation under the assumption that drop test II is conducted immediately after drop test I. As described previously, the increase in temperature in the O-ring part of the containment boundary during a thermal test may be accelerated when the shock absorber deformation during the second drop test is added to the shock absorber deformation during drop test I. This would cause the maximum damage. During drop test I, the deformation resulting from each drop attitude remains only in the shock absorber since the drop is onto a horizontal plane. However, during drop test II, the outer shell part of the outer container, as well as the shock absorber, may directly drop on a mild steel bar, measuring more than 150 mm in diameter and 200 mm in height. As a result of such a collision, if the outer shell part, resin layer part, and cement layer part are penetrated, the shielding lead might melt. This subsection, therefore, examines the influence on the outer container's outer shell part when the part is dropped on a mild steel bar.

Table (II)-A.25 lists the impact acceleration values during drop tests I and II using a 1/2-scale model. As shown in this table, for each drop attitude, the impact acceleration during drop test II is lower than that during drop test I. The relative relationship also holds true for the actual package.

During drop test I, the outer container, inner container, and fuel supporting can or receiving tubes maintain their strength in any drop attitude, so they also maintain their strength during drop test II. The amount of shock absorber deformation at each drop attitude is shown below.

(a) Horizontal drop

During a horizontal drop, the outer shell part of the outer container or the front or rear shock absorber installed on each end of the outer shell part may collide with the mild steel bar. The maximum stress is generated in the outer shell part when the center portion of the outer container's outer shell part (i.e., the gravity center position of the package) directly collides with the mild steel bar.

The analysis presented in this subsection assumes that the center portion drops on the mild steel bar. The amount of shock absorber deformation when either of the shock absorbers drops on the mild steel bar is also shown.

(a.1) Drop on the center portion of outer container's outer shell (Drop on the center of gravity)

As described previously, when the outer shell part of the outer container is penetrated by a mild steel bar, the lead might be melted during the subsequent thermal test. This subsection proves that even if the center portion of the package's outer shell drops on a mild steel bar, the outer shell part will not be penetrated. The outer shell part also maintains sufficient strength against the stress resulting from the bending moment generated in the outer shell of the outer container by the drop impact.

Table (II)-A.25 Acceleration during Drop Tests I and II in a 1/2-Scale Model, and the Corresponding Maximum Stress Generated in the Outer Shell of Outer Container

Drop attitude	Vertical drop		Horizontal drop		Corner drop		Remarks
	Acceleration (G)	Maximum stress* (N/mm ²)	Acceleration (G)	Maximum stress* (N/mm ²)	Acceleration (G)	Maximum stress* (N/mm ²)	
Drop test I	236	88.3	231	272	160	42.3	
Drop test II							
Center-of-gravity drop	75***	18.6***	193**	152**	53	15.7	
Eccentric drop	34	15.7	99	47.1	-	-	

* The maximum stress: is represented by values obtained when the maximum measured value of the strain gauge installed in the axial direction of the outer container is multiplied by Young's modulus of stainless steel.

** Direct drop of the center portion of the outer container on the mild steel bar. The outer shell part of the outer container was not penetrated by the mild steel bar. Only a concave measuring 8.5 mm in depth was formed.

*** The steel plate (8 mm) that coats the fir-plywood is not penetrated. A concave measuring, 24 mm in depth, was formed. The center of the outer shell is the resin layer (which has heat dispersion fins), and its end is the resin layer (without heat dispersion fins).

A cement layer is provided between the resin layer and the lead shield. They have a strength that exceeds the compression strength ($\sigma = 12.7 \text{ N/mm}^2 \approx 1.3 \text{ kg/mm}^2$) of lead. (Compression strength of resin $\sigma_r = 47.1 \text{ N/mm}^2 \approx 4.8 \text{ kg/mm}^2$, compression strength of cement $\sigma_c = 60.8 \text{ N/mm}^2 = 6.2 \text{ kg/mm}^2$). To prevent penetration by a mild steel bar, the necessary plate thickness of the shell which is backed up with lead can be obtained by Nelms's formula;

$$t = \left(\frac{W}{\sigma_u} \right)^{0.71} \quad (1)$$

where

t : Necessary plate thickness
W : Package weight 11,000 kg = 24251 LB
 σ_u : Tensile strength of the outer shell material
496 N/mm² \approx 51 kg/mm² \approx 72536 LB/in²

and thus

$$t = \left(\frac{24251}{72536} \right)^{0.71}$$

$$= 0.46 \text{ inch}$$

$$= 11.7 \text{ mm}$$

The plate thickness used for the outer shell is 16 mm or more. Therefore, a mild steel bar will not penetrate the outer shell during drop test II.

Next, assume that the load applied at that time acts on the outer shell as shown in Fig. (II)-A.46. The stress generated in the outer shell is given by the expression below.

$$\sigma = \frac{M}{Z}$$

M : Bending moment generated in the outer shell during the drop test

$$M = \frac{W}{8} \cdot \ell$$

W : Load

$$W = \frac{\pi}{4} \cdot d^2 \cdot \sigma$$

d : Diameter of the mild steel bar 150 mm

σ : Compression strength of the mild steel bar = Tensile strength
402 N/mm² \approx 41 kg/mm²

1) H.A. Nelms: Structural Analysis of Shipping Cask Effects of Jacket Principal Properties and Curvature on Puncture Resistance ORNL-TM-1312 Vol3.

$$W = \frac{\pi}{4} \times (150)^2 \times 402$$

$$= 7.10 \times 10^6 \text{ N}$$

ℓ : Length of the outer container 2564 mm

$$M = \frac{1}{8} \times 7.10 \times 10^6 \times 2564$$

$$= 2.28 \times 10^9 \text{ N}\cdot\text{mm}$$

Z : Section modulus of the outer container's outer shell

$$Z = \frac{\pi}{32} \cdot \frac{d_2^4 - d_1^4}{d_2}$$

d_2 : Outer diameter of the outer shell 800 mm

d_1 : Inner diameter of the outer shell 768 mm

$$Z = \frac{\pi}{32} \times \frac{800^4 - 768^4}{800}$$

$$= 7.57 \times 10^6 \text{ mm}^3$$

$$\sigma = \frac{2.28 \times 10^9}{7.57 \times 10^6}$$

$$= 301 \text{ N/mm}^2$$

$$\approx 30.6 \text{ kg/mm}^2$$

The temperature of the outer shell (SUS304) is 72°C. If the value $\sigma_{UD} = 496 \text{ N/mm}^2$ ($\approx 50.6 \text{ kg/mm}^2$) at a temperature of 80°C is assumed to represent the dynamic tensile strength, the margin of safety (M.S.) is given by

$$M.S. = \frac{496}{301} - 1$$

$$= 0.7$$

Therefore, the outer shell has sufficient strength to withstand the drop impact, and is not damaged.

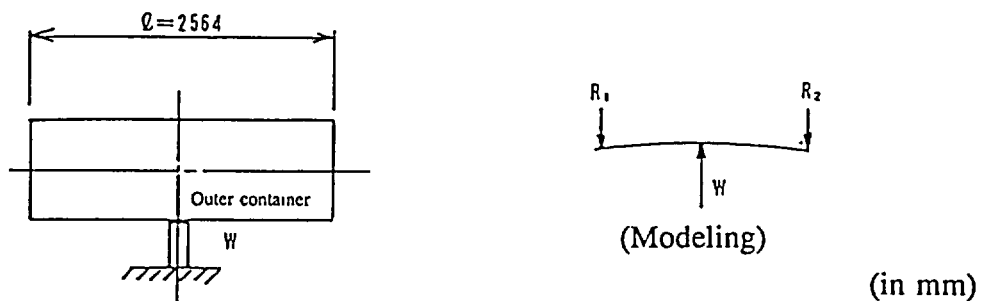


Fig. (II)-A.46 Drop Test II on the Center of the Outer Shell

(a.2) Drop of package's shock absorber on a mild steel bar

As described in step (a.1), the outer shell part of an outer container is constituted by stainless steel measuring 16 mm or more in thickness, and is not penetrated by the mild steel bar. The condition under which maximum damage is caused during drop test II is the deformation of a shock absorber that causes maximum damage during the subsequent thermal test.

The penetration hole part of this package uses O-rings. The maximum allowable service temperature is 200°C. Since the thermal conductivity of the shock absorber is lower than that of metal, the temperature near the O-ring will rise during a thermal test if the vicinity of the place where the O-ring is used collides with the mild steel bar during the preceding drop test.

If this package collides with the mild steel bar during a horizontal drop, the collision point is shifted off the center of gravity of the package as shown in Fig. (II)-A.47 (eccentric impact). In this case, some of this package's weight contributes to the weight applied to the collision point. This weight is called reduced impact weight. The reduced impact weight increases as the impact point gets nearer to the center of gravity. Therefore, as shown in Fig. (II)-A.47, the deformation of the shock absorber becomes larger when the impact point is not located near the rear sampling valve lid, but rather near the penetration hole lid or front sampling valve lid. The deformation of the shock absorber during a horizontal drop when the impact point is located near the penetration hole lid is obtained below.

The impact energy that acts on the impact point during a collision is based on this reduced impact weight. This package's remaining drop energy is consumed as the rotating energy of the container.

$$E_k = E_s + E_r$$

where

E_k	:	Drop energy of the package	N.mm
E_s	:	Impact energy	N.mm
E_r	:	Rotating energy	N.mm

The drop energy E_k and impact energy E_s of this package are given by the expression below.

$$E_k = W \cdot H$$

$$E_s = W' \cdot H$$

W	:	Package weight	11,000 kg
H	:	Drop height	1000 mm
W'	:	Reduced impact weight ¹⁾	

1) Nihon Kikai Gakkai: Kikai Kogaku Benran, p. 3-41, 1979
(The Japan Society of Mechanical Engineers: Handbook of Mechanical Engineering, page 3-41, 1979)

$$W' = \frac{W}{1 + \frac{P^2}{k^2}} \quad 1)$$

- P : Distance between the package's center of gravity and the impact point 1091 mm
k : Rotating radius around the center of gravity of the package

$$k = \sqrt{\frac{d^2}{16} + \frac{l^2}{12}}$$

- d : Outer diameter of the outer container 800 mm
l : Length of the outer container 2564 mm
and thus

$$k = \sqrt{\frac{800^2}{16} + \frac{2564^2}{12}}$$

$$= 767 \text{ mm}$$

$$W' = \frac{9.807 \times 11000}{1 + \left(\frac{1091^2}{767^2}\right)}$$

$$= 3.17 \times 10^4 \text{ N}$$

The impact energy is given by

$$E_s = 3.57 \times 10^4 \text{ M}$$

$$= 3.57 \times 10^7 \text{ N}\cdot\text{mm}$$

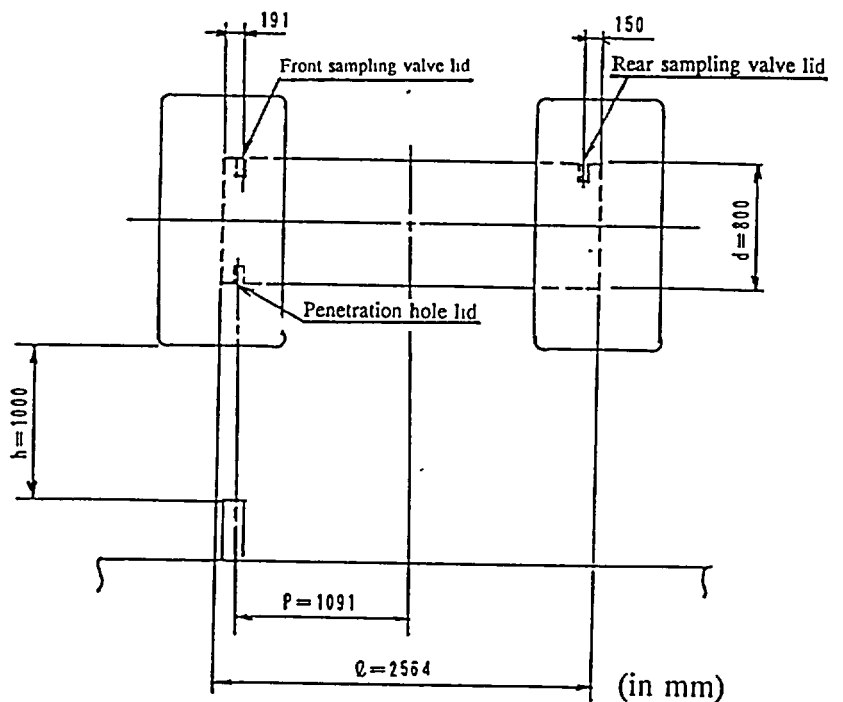


Fig. (II)-A.47 Horizontal Drop on the Shock Absorber

- 1) Nihon Kikai Gakkai: Kikai Kogaku Benran, p. 3-41, 1979
(The Japan Society of Mechanical Engineers: Handbook of Mechanical Engineering, page 3-41, 1979)

As shown in Fig. (II)-A-46, the mild steel bar may make contact with the fire-ly wood and felt wool in the center portion during a vertical drop. Therefore, each portion is evaluated to indicate that the deformation does not affect the outer container.

(b) Vertical drop

$$= 37 \text{ mm} \\ = 273 - 180 - 70$$

(Actual thickness of the shock absorber) - (Deformation during drop test I) - (Deformation during drop test II)

container body. as close as 37 mm from the penetration hole in part. The deformation does not affect the simply rigid, when drop test I and II overlap. The shock absorber remains undeformed assumption that the degree of the deformation by the two tests of the shock absorber is The thickness of the shock absorber that remains undeformed is obtained as follows on the

$$= 76 \text{ mm}$$

$$\frac{\frac{\pi}{2} \times 120^2 \times 10^3}{3.27 \times 10^6 - 1.2 \times 0.4 \times 120 \times 3 \times 30 \times 420 \times \pi}$$

h	:	Depth of deformation	up to 101 = 30 mm
a	:	Tensile strength of shock absorber's cover plate	400 N/mm ² (30°C)
t	:	Thickness of the shock absorber's cover plate	3 mm
C ₂	:	Constant	0.8
C ₁	:	Constant	1.2
δ	:	Shock absorber deformation	10.8 N/mm ² = 1.1 kg/mm ²
σ _c	:	Compressive bearing stress of plate wood (at right angles to the grain orientation)	120 mm
b	:	Diameter of the mild steel bar	
E _a	:	Absorbed energy	

$$E_a = \frac{\pi}{2} \cdot \sigma_c \cdot \delta + C_1 \cdot C_2 \cdot \pi \cdot \delta \cdot t \cdot a$$

is thus given by the expression below. The energy above is absorbed as deformation at an impact point. The cover plate is deformed by the mild steel bar, and the plate wood is deformed. The absorbed energy

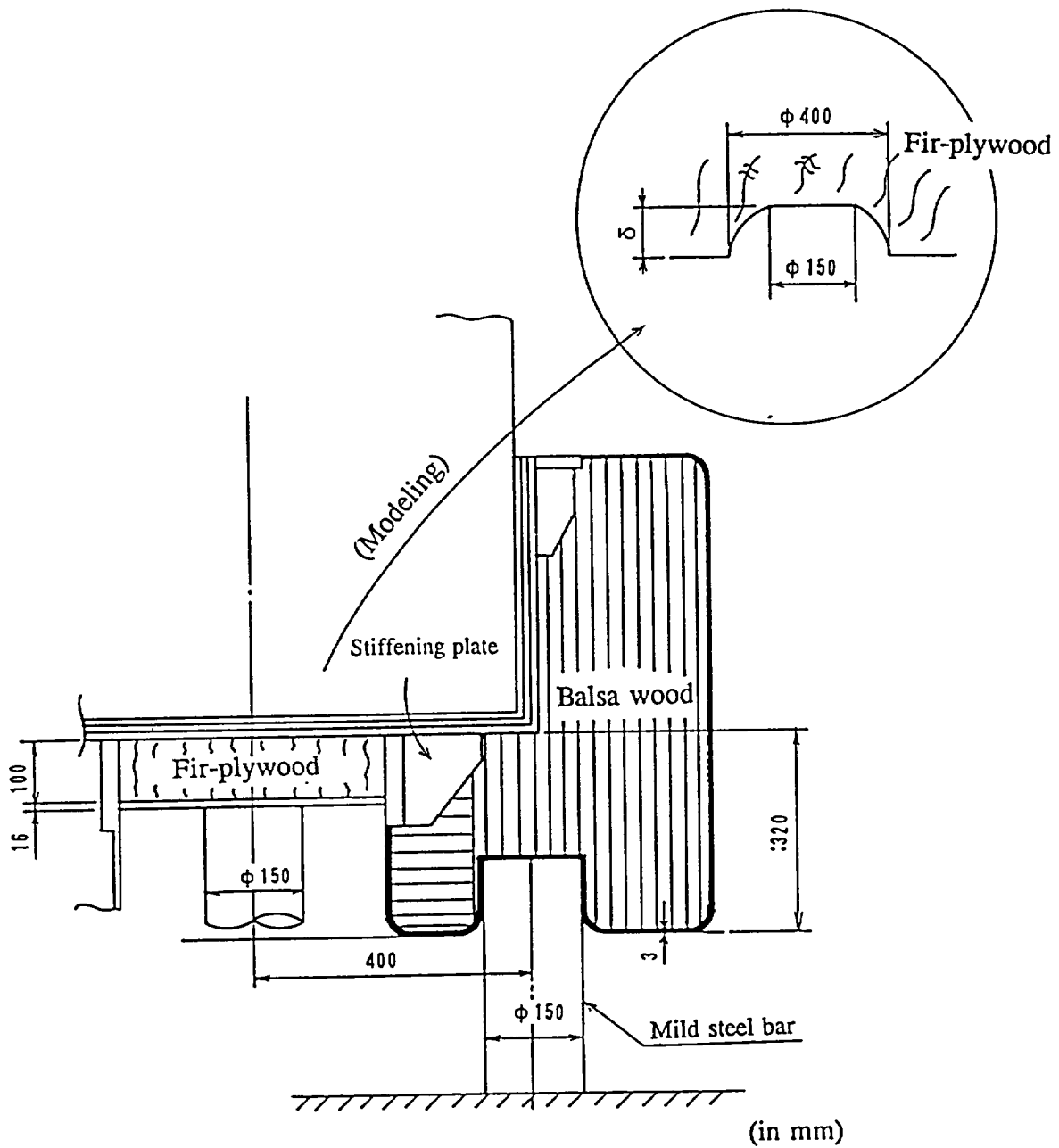


Fig. (II)-A.48 Vertical Drop on the Shock Absorber

(b.1) Vertical drop on the center of the fir-plywood as the impact point (center-of-gravity drop)

Fir-plywood is protected by a 16 mm-thick steel plate and is not penetrated for the same reason as previously described in step (a.1).

The drop energy of this package is absorbed by the deformation of the plate and fir-plywood. In this case, the deformation is obtained by assuming that the drop energy is absorbed only by the fir-plywood deformation shown in Fig. (II)-A.48. To be on the safe side, the energy absorbed by the deformation of the steel plate is not considered.

$$W \cdot h = \frac{1}{3} \cdot \pi \cdot \delta \cdot \sigma_f \cdot (R^2 + Rr + r^2) \quad 1)$$

W	:	Package weight	11,000 kg
h	:	Drop height	1000 mm
R	:	Radius of cone deformation (See Fig. (II)-A.48)	200 mm
r	:	Radius of cone deformation (See Fig. (II)-A.48)	75 mm
σ_f	:	Compressive deforming stress of fir-plywood	29.4 N/mm ² \approx 3.0 kg/mm ²
δ	:	Deformation	

$$\delta = \frac{W \cdot h}{\frac{\pi}{3} \cdot \sigma_f \cdot (R^2 + Rr + r^2)}$$

$$\begin{aligned} \delta &= \frac{9.807 \times 11000 \times 1000}{\frac{\pi}{3} \times 29.4 \times (200^2 + 200 \times 75 + 75^2)} \\ &= 58 \text{ mm} \end{aligned}$$

The degree of the deformation (58 mm) is smaller than the plate thickness (100 mm) of the fir-plywood. The deformation does not thus affect the front and rear lid units of the outer container.

(b.2) Vertical drop in which the end part of the shock absorber is the impact point (eccentric drop)

The balsa wood can be divided into two areas--the inside where the grain of wood is oriented at right angles to the drop direction, and the outside where it is oriented parallel to the drop direction, as shown in Fig. (II)-A.48. The stiffening plate of a shock absorber's inner shell is installed on the inside part of the balsa wood. This limits the degree of penetration of the mild steel bar into the shock absorber.

1) Nihon Kikai Gakkai: Kikai Kogaku Benran, p. 2-23
(The Japan Society of Mechanical Engineers: Handbook of Mechanical Engineering, page 2-23)

The case where drop test II is conducted on the end plate of the shock absorber to allow easier penetration of the mild steel bar is evaluated next.

As in step (a), impact energy E_s is first obtained since it is an eccentric impact.

$$W' = \frac{W}{1 + \frac{P^2}{k^2}}$$

- W' : Reduced impact weight
 P : Distance between the package's center of gravity and impact point 400 mm
 k : Rotating radius around the center of gravity of the package 767 mm

$$W' = \frac{9.807 \times 11000}{1 + \left(\frac{400^2}{767^2}\right)}$$

$$= 8.48 \times 10^4 \text{ N}$$

and thus impact energy E_s is given by

$$\begin{aligned}
 E_s &= W' \cdot H \\
 &= 8.48 \times 10^4 \times 1000 \\
 &= 8.48 \times 10^7 \text{ N}\cdot\text{mm}
 \end{aligned}$$

As in step (b), the deformation is also given by the expression below.

$$E_s = \frac{\pi}{4} \cdot d^2 \cdot \sigma_B \cdot \delta + C_1 \cdot C_2 \cdot \pi \cdot d \cdot t \cdot \sigma \cdot h$$

- σ_B : Compressive deforming stress of balsa wood (parallel to the grain orientation)
 19.6 N/mm² \approx 2.0 kg/mm²

$$\begin{aligned}
 \delta &= \frac{8.48 \times 10^7 - 1.2 \times 0.8 \times \pi \times 150 \times 3 \times 496 \times 30}{\frac{\pi}{4} \times 150^2 \times 19.6} \\
 &= 184 \text{ mm}
 \end{aligned}$$

When drop tests I and II overlap, the thickness of the shock absorber that remains undeformed is as follows:

$$\begin{aligned}
 &(\text{Axial thickness of the shock absorber}) - (\text{Deformation during drop test I}) - (\text{Deformation during drop test II}) \\
 &= 320 - 110 - 184 \\
 &= 26 \text{ mm}
 \end{aligned}$$

Therefore, the deformation is limited to the shock absorber and does not affect the container body.

(c) Corner drop

The degree of deformation of the shock absorber during drop test II when the package is dropped on a mild steel bar at the angle (drop angle of 23 degrees) of the corner drop is obtained to indicate that the deformation does not affect the outer container. All the drop energy is absorbed by the deformation of the shock absorber and steel covering plate since it is a corner drop (center-of-gravity drop). As in step (a.2), therefore, the expression below holds true.

$$E_s = \frac{\pi}{4} \cdot d^2 \cdot \sigma_B \cdot \delta + C_1 \cdot C_2 \cdot \pi \cdot d \cdot t \cdot \sigma \cdot h$$

E_s : Absorbed energy

$$\begin{aligned} E_s &= W \cdot H \\ &= 1.08 \times 10^8 \text{ N}\cdot\text{mm} \end{aligned}$$

The deformation of balsa materials is given by

$$\begin{aligned} \delta &= \frac{1.08 \times 10^8 - 1.2 \times 0.8 \times \pi \times 150 \times 3 \times 496 \times 30}{\frac{\pi}{4} \times 150^2 \times 24.5} \\ &= 200 \text{ mm} \end{aligned}$$

The thickness of the shock absorber that remains undeformed is obtained on the assumption that the deformation of the shock absorber is simply added, when drop tests I and II overlap. As shown in Fig. (II)-A.49, the expression below is given.

$$\begin{aligned} &(\text{Drop-direction thickness of the shock absorber}) - (\text{Deformation during drop test I}) - \\ &(\text{Deformation during drop test II}) \\ &= 520 - 210 - 200 \\ &= 110 \text{ mm} \end{aligned}$$

Therefore, the deformation does not affect the outer container.

The allowable thickness of the shock absorber after drop test I (corner drop) is minimized at the end part of the outer container, as shown in Fig. (II)-A.49. The case in which it is assumed that this end part collides with the mild steel bar is also examined.

The drop in this case is an eccentric drop as shown in Fig. (II)-A.49. As in step (a.2), the impact energy (E_s) during an eccentric drop is given by

$$\begin{aligned} E_s &= W' \cdot H \\ W' &= \frac{W}{1 + \left(\frac{p^2}{k^2}\right)} \end{aligned}$$

W'	: Reduced impact weight	
P	: Distance between the package's center of gravity and the impact point	160 mm
k	: Rotating radius around the center of gravity of the package	767 mm

$$W' = \frac{9.807 \times 11000}{1 + \left(\frac{160^2}{767^2}\right)}$$

$$= 1.03 \times 10^5 \text{ N}$$

$$E_s = 1.03 \times 10^5 \times 1000$$

$$= 1.03 \times 10^8 \text{ N}\cdot\text{mm}$$

In the same manner as previously described, the deformation of the shock absorber is given as follows:

$$\delta = \frac{1.03 \times 10^8 - 1.2 \times 0.8 \times \pi \times 150 \times 3 \times 496 \times 30}{\frac{\pi}{4} \times 150^2 \times 24.7}$$

$$= 188 \text{ mm}$$

Even if drop test I (corner drop) and drop test II overlap as shown in Fig. (II)-A.49, the deformation does not affect the outer container.

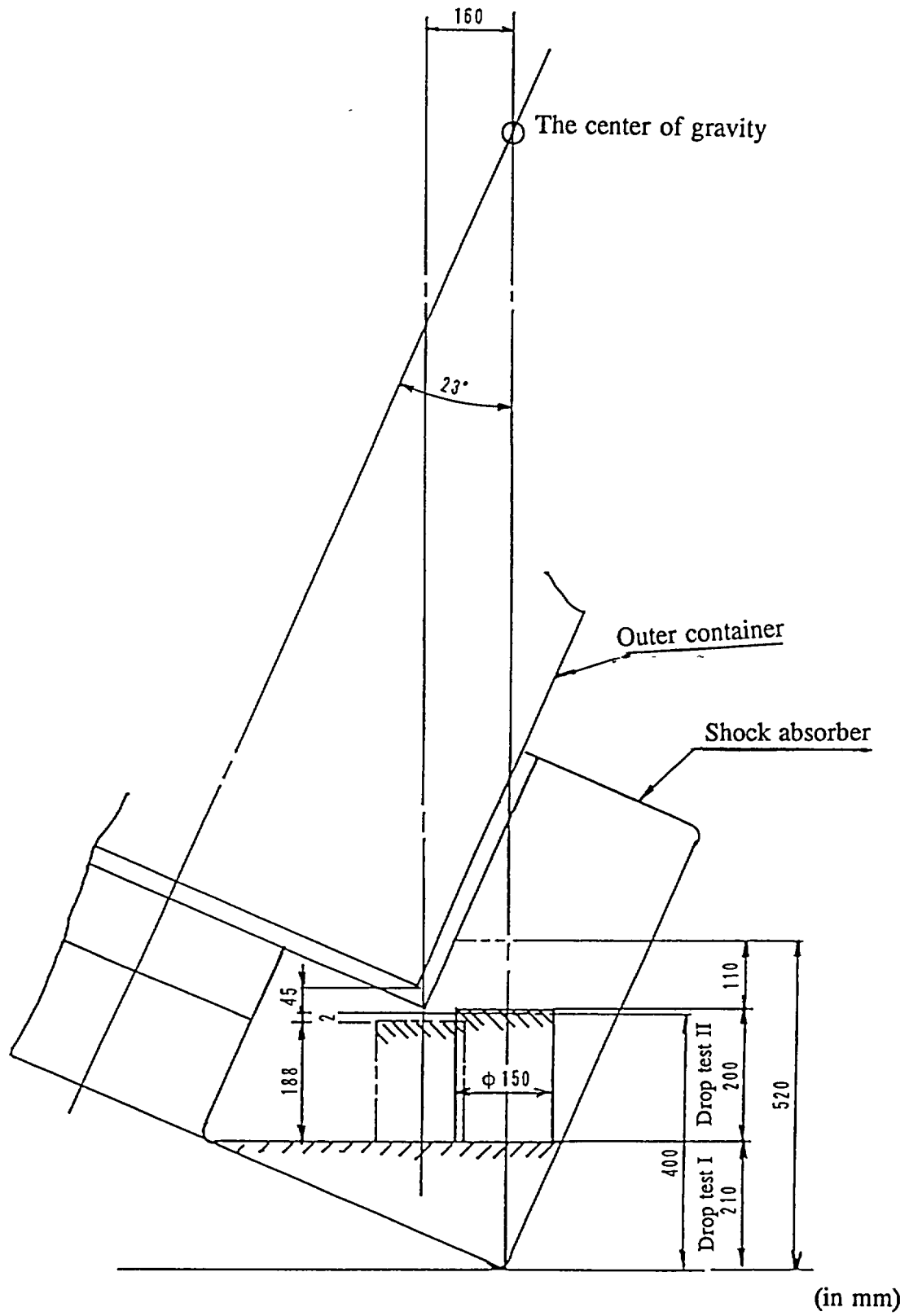


Fig. (II)-A.49 Corner Drop onto the Mild Steel Bar

A.6.2.1 Summary of the results

The outer container's outer shell consists of stainless steel with a thickness of 16 mm or more, and is not penetrated by a mild steel bar during drop test II. The steel plate that covers the fir-plywood is also not penetrated during a center-of-gravity vertical drop because of this 16 mm thickness. The remaining thickness of undeformed fir-plywood is 42 mm. Assuming that the steel plate covering the balsa wood is penetrated by a mild steel bar because it is 3 mm thick, the following evaluation is performed. Table (II)-A.26 lists the value obtained when the deformation during drop test I is added to the deformation of this balsa wood (i.e., the value when drop test II is added to drop test I). The value obtained when this value is subtracted from the initial thickness of the shock absorber is also listed in Table (II)-A.26. The maximum damage during subsequent thermal tests likely results in a temperature increase near an O-ring that forms the containment boundary of the outer container's lid units. As described in Section (II)-B, "Thermal Analysis," the balsa wood has an effective insulating performance and is treated so that it is flame resistant. Therefore, the temperature of the O-ring rises as a result of the heat input during thermal testing when the plate of the balsa wood near the O-ring is thinner.

Table (II)-A.26 Deformation of the Balsa Wood Shock Absorber during Drop Tests I and II

Drop attitude	Thickness of the shock absorber (mm)	Total deformation during drop tests I and II (mm)	Thickness of the undeformed shock absorber (mm)
Vertical drop	320	294	26
Horizontal drop	273	236	37
Corner drop	520	410	110

As shown in Table (II)-A.26, the maximum damage conditions would arise during vertical drop test II, which is a drop near the O-ring of the front or rear lid, when this test is immediately performed after the balsa wood has been deformed by a vertical drop from a height of 9 m. Therefore, in the thermal analysis under accident test conditions, the deformation state after vertical drop is modeled. Trunnions, lifting lug, and base plates are installed on the outer shell part of the outer container. When the mild steel bar strikes against one of these parts, the energy is absorbed in this part. Also since it is an eccentric drop, the bending moment occurring in the outer shell part becomes smaller than in the case of a drop on the center part of the outer container described in step (a.1). This indicates that the outer container remains sound. The fusible plug installed in the outer shell is a hole with a 12 mm diameter. The fusible plug is much smaller than the mild steel bar having a diameter of 150 mm, so the effect of the plug can be ignored.

Because the drop height is 1 m, which is lower than the 9 m of drop test I and because of the partial deformation (column of 150 mm in diameter) by the mild steel bar, the drop in each attitude has a lower impact deceleration than during drop test I. Analysis results have already shown that the outer container, inner container, and fuel supporting can or receiving tube maintain their strength during drop test I. They also maintain their strength during drop test II. The evaluation below is thus performed on the assumption that the contents remain unaffected.

A.6.3 Thermal Test

A.6.3.1 Summary of temperatures and pressures

Section B.5 describes the evaluation of the temperatures and pressures of this package for the thermal test that is conducted after the mechanical test. Table (II)-A.27 summarizes the results. The results of the evaluation carried out during the thermal test show that severe thermal conditions arise when Contents I (260 W) are loaded. In this case, the maximum temperature of the rotating plug lid and shielding plug lid is 125°C. The maximum temperature of the sampling valve lids and the penetration hole lid is 120°C.

The temperatures above are lower than the maximum normal operating temperature (200°C) of the O-ring used for each lid. Containment is thus maintained. The temperature of the shielding lead is 193°C. The shielding lead does not melt because this temperature is less than its melting point (327°C).

Table (II)-A.27 Maximum Temperatures and Pressures under Thermal Test Conditions

Parts	Maximum temperature	Maximum pressure
Outer shell	656°C	-
Resin layer (heat dispersion fin)	405°C	-
Lead shield	193°C	-
Rotating plug lid and shielding plug lid (outer shell lids)	125°C	-
Penetration hole lid	120°C	-
Inner shell	193°C	80 kPa
Inner container	284°C	-
Fuel supporting can	332°C	230 kPa
Receiving tube	332°C*	660 kPa

* When Contents VI is loaded.

Eight fusible plugs are installed in the outer shell. The fusible plugs, which are made of bismuth, melt under these thermal test conditions because their melting point is 271°C. These fusible plugs emit steam consisting of water vapor due to high temperature and carbonic acid gas generated by a change in organization of the cement layer filled between the resin layer and the lead shield to prevent an increase in the internal pressure of the outer container's shell part.

The maximum temperature of the resin layer is 405°C. At this temperature, the resin is carbonized and gas is generated. This gas also escapes through the fusible plug holes to prevent an increase in the internal pressure. During shield analysis, the shielding calculation under accident test conditions is performed on the assumption that this resin is lost.

Moreover, ten fusible plugs are installed in each of the covered plates of the front and rear shock absorbers. These fusible plugs allow the gas generated in the balsa wood and fir-plywood to escape to prevent an excessive increase of pressure in the shock absorbers.

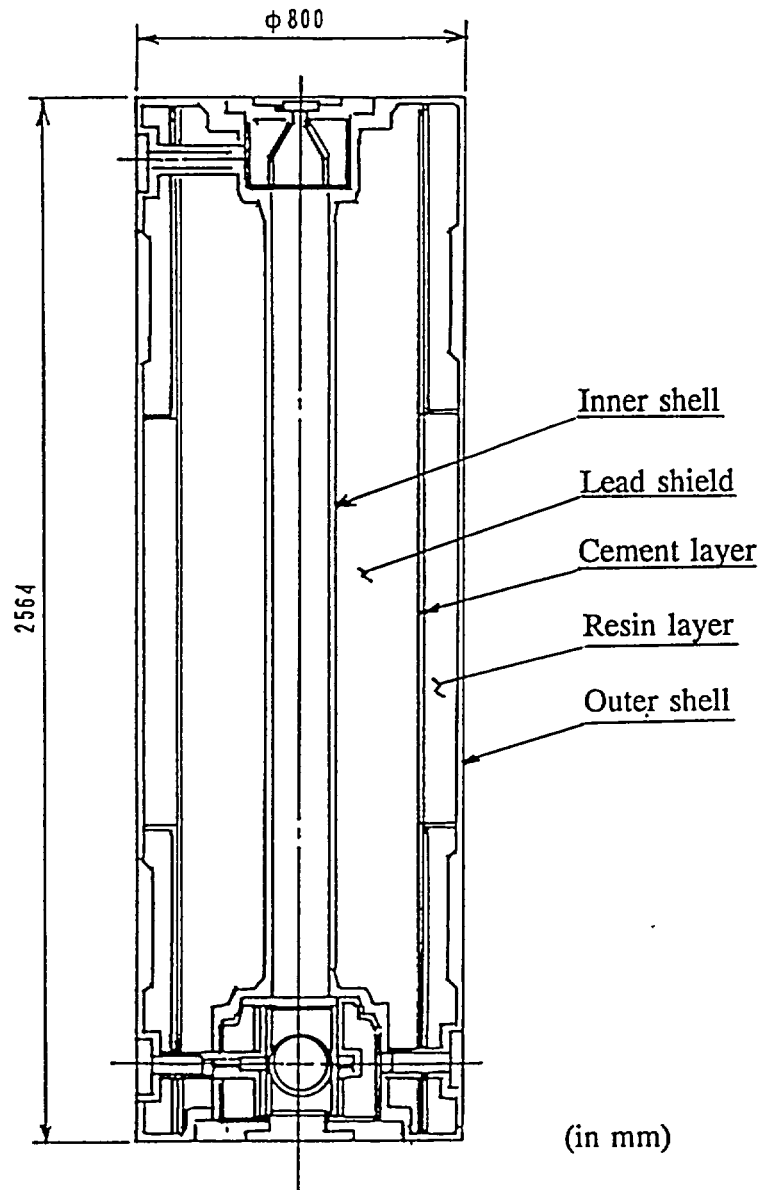


Fig. (II)-A.50 Packaging (Thermal Test)

A.6.3.2 Thermal Expansion

(1) Thermal stress

Thermal expansion occurs as the temperature of this packaging increases during a thermal test. The temperature increase is different in each part. Therefore, the thermal stress is the problem. Fig. (II)-A.50 shows the shape of the packaging.

Under thermal test conditions, the outer shell of the packaging reaches a high temperature. No constraining force is applied even when the resin layer (burns partially) and lead expand. Therefore, the thermal stress that occurs because of the temperature difference of the inner and outer shells is the problem.

Thermal analysis indicates that the temperature difference of the inner and outer shells increases when Contents II are loaded. As shown in Fig. (II)-A.52, half of the container on the rotating plug side is modeled, to be on the safe side, (because the shielding plug side has greater strength) to evaluate the elasticity and plasticity by the calculation code, ANSYS.

As the results of the thermal analysis show that the temperature difference of the inner and outer shells is the largest under the conditions shown in Fig. (II)-A.52, the thermal stress is evaluated under the same conditions. The modulus of longitudinal elasticity, the coefficient of thermal expansion, and Poisson's ratio apply the values shown in Table (II)-A.28, and the stress - strain curve apply the values in Fig. (II)-A.51¹⁾.

1) Battele: Structure Analysis Handbook, 1979

Table (II)-A.28 Physical Property Value of the Inner and Outer Shells at High Temperatures

Temperature	Modulus of the longitudinal elasticity	Coefficient of thermal expansion	Poisson's ratio
150°C	$1.92 \times 10^5 \text{ N/mm}^2$	$17.05 \times 10^{-6} \text{ 1/}^\circ\text{C}$	0.32
200	1.83×10^5	17.25×10^{-6}	0.32
250	1.81×10^5	17.43×10^{-6}	0.33
300	1.78×10^5	17.62×10^{-6}	0.33
350	1.73×10^5	17.80×10^{-6}	0.33
400	1.68×10^5	17.99×10^{-6}	0.34
450	1.64×10^5	18.18×10^{-6}	0.34
500	1.59×10^5	18.36×10^{-6}	0.35
550	1.54×10^5	18.57×10^{-6}	0.35
600	1.50×10^5	18.72×10^{-6}	0.36
650	1.45×10^5	18.87×10^{-6}	0.37
700	1.40×10^5	18.97×10^{-6}	0.38

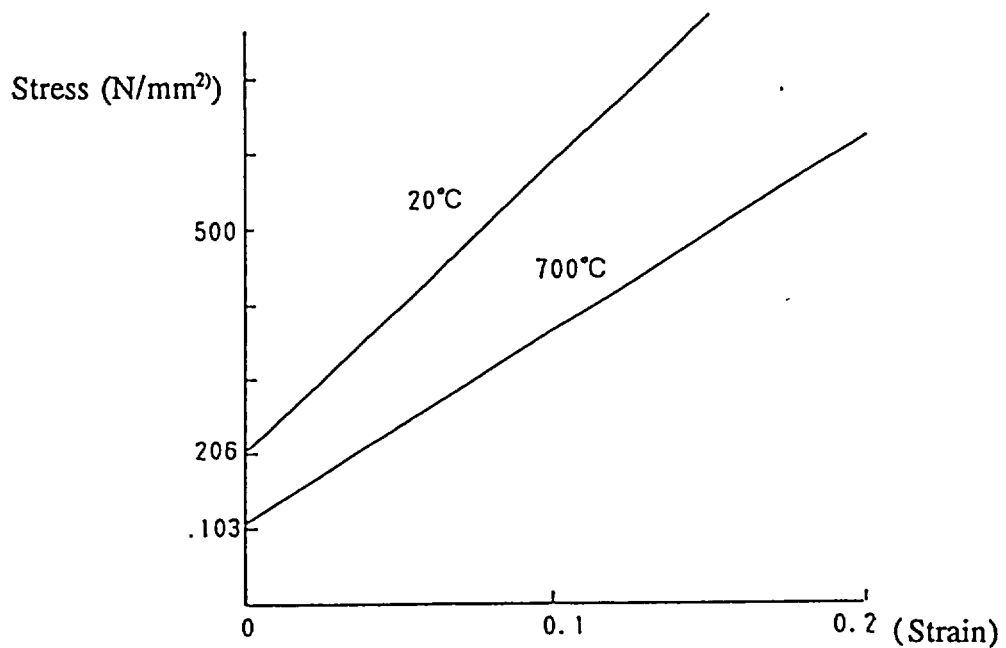


Fig. (II)-A.51 Stress - Strain Curve

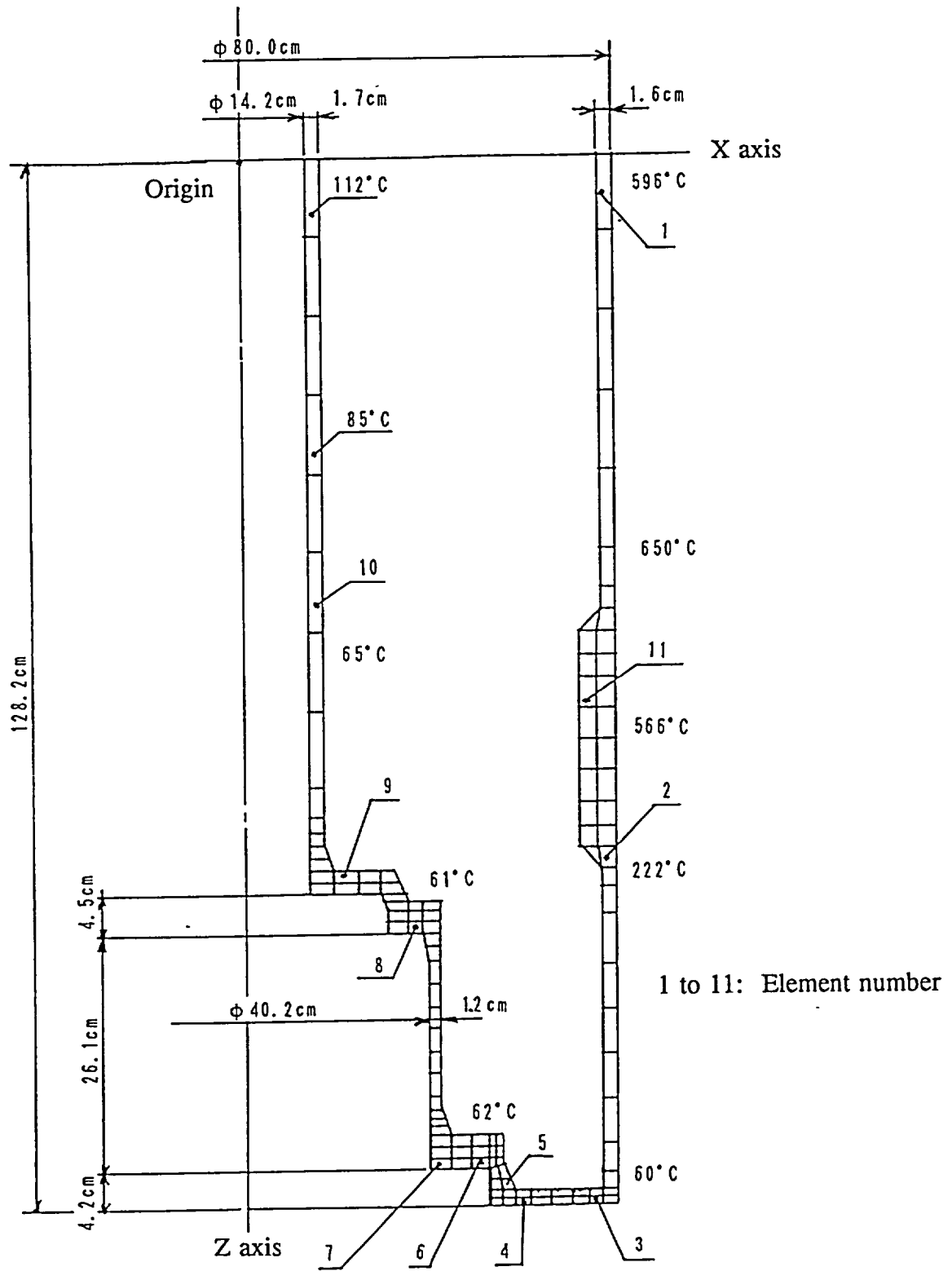


Fig. (II)-A.52 Analysis Model of the Thermal Stress

Table (II)-A.29 lists the calculation results by the code, ANSYS.

Table (II)-A.29 Calculation Results of the Thermal Stress

	Stress	Displacement*
1	-24.5 N/mm ² (-2.5 kg/mm ²)	0.1 mm
2	40.2 N/mm ² (-4.1 kg/mm ²)	9.66 mm
3	199 N/mm ² (20.3 kg/mm ²)	9.60 mm
4	-258 N/mm ² (-26.3 kg/mm ²)	4.83 mm
5	340 N/mm ² (34.7 kg/mm ²)	3.11 mm
6	-32.3 N/mm ² (-3.3 kg/mm ²)	3.11 mm
7	-25.5 N/mm ² (-2.6 kg/mm ²)	2.54 mm
8	60.8 N/mm ² (6.2 kg/mm ²)	2.30 mm
9	172 N/mm ² (17.5 kg/mm ²)	1.72 mm
10	116.7 N/mm ² (11.9 kg/mm ²)	1.32 mm
11	-114 N/mm ² (-11.6 kg/mm ²)	8.4 mm

* Displacement in the Z-axis direction

The maximum stress occurs in element number 5. The stress is $\sigma = 340 \text{ N/mm}^2$ ($\approx 34.7 \text{ kg/mm}^2$). The stress that is generated is secondary stress, so the tensile strength value represents the design criterion value. The temperature of element number 5 is 62° . Therefore, if the value ($\sigma_u = 485 \text{ N/mm}^2 \approx 49.5 \text{ kg/mm}^2$) at a temperature of 100°C is assumed to represent the tensile strength of the material (SUS304) to be on the safe side, the margin of safety (M.S.) is given by

$$M.S. = \frac{485}{340} - 1$$

$$= 0.43$$

The inner shell thus maintains sufficient strength. The maximum stress on the outer shell occurs in element number 11. The temperature of this element number is 566°C . If the value ($\sigma_u = 254 \text{ N/mm}^2$) ($\approx 26 \text{ kg/mm}^2$) at a temperature of 700°C is assumed to represent the design criterion value of the tensile strength of the material, the margin of safety (M.S.) is given by

$$M.S. = \frac{254}{114} - 1$$

$$= 1.2$$

Therefore, the outer shell also maintains sufficient strength. As shown in Fig. (II)-A.53, the strain of the rotating plug lid and O-ring plane is the displacement difference of element numbers 6 and 7. This is given by

$$\delta = 3.11 - 2.54$$

$$= 0.54\text{mm}$$

The strain is smaller than the collapsed height (1.3 mm) of the O-ring used. Containment is thus maintained.

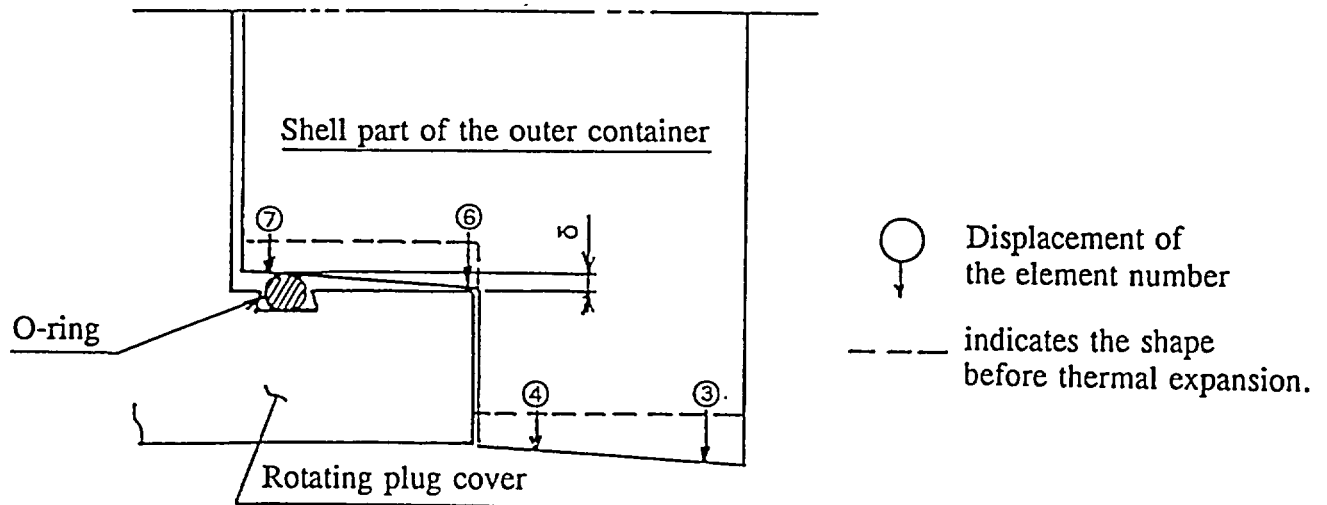


Fig. (II)-A.53 Thermal Stress Evaluation Results

(2) Stress by internal pressure

As a result of the thermal evaluation under thermal test conditions (see Table (II)-A.27), the maximum pressure in the inner shell is 80 kPa(G). The maximum pressures in the fuel supporting can, receiving tube are 230 kPa(G) and 660 kPa(G), respectively. To be on the safe side, the stress calculation is performed with a design pressure in the inner shell of 196 kPa(G) ($\approx 2.0 \text{ kg/cm}^2\text{G}$), a design pressure in the fuel supporting can of 294 kPa(G) ($\approx 3.0 \text{ kg/cm}^2\text{G}$), and a design pressure in the receiving tube of 686 kPa(G) ($\approx 7.0 \text{ kg/cm}^2\text{G}$).

In evaluating the containment system, the lead shield is omitted to be on the safe side, and the stainless steel alone is assumed to be able to withstand the pressure. The stress of the parts below is obtained next.

- (a) Inner shell
- (b) Rear lid unit
- (c) Front lid unit
- (d) Penetration hole lid part
- (e) Fuel supporting can
- (f) Receiving tube

(a) Inner shell

Since the center portion of the inner shell is longer in axial direction than across the diameter, the conditions are the same as when internal pressure acts on an infinite circular model. In this case, the stress generated in the inner shell is given by the expression below.

$$\sigma = p \cdot \frac{\frac{k^2}{R^2} + 1}{k^2 - 1} \quad 1)$$

k : Coefficient based on radius = $\frac{b}{a}$
 a : Inner radius 71 mm (See Fig. (II)-A.54.)
 b : Outer radius 81 mm

$$k = \frac{88}{71}$$

$$= 1.24$$

R : Coefficient based on the radius

$$R = \frac{r}{a}$$

r : Radius of the calculation point

where

$$r = a = 71 \text{ mm}$$

$$R = 1$$

p : Internal pressure 196 kPa = 0.196 N/mm²

and thus

the maximum stress generated in the inner shell is given by

$$\sigma = 0.196 \times \frac{\frac{1.24^2}{1} + 1}{1.24^2 - 1}$$

$$= 0.9 \text{ N/mm}^2$$

$$\approx 0.09 \text{ kg/mm}^2$$

The temperature of the inner shell (SUS304) is 193°C. If the value $\sigma_y = 144 \text{ N/mm}^2$ ($\approx 14.7 \text{ kg/mm}^2$) at a temperature of 200°C is assumed to represent the design criterion value of the yield stress, the margin of safety (M.S.) is given by

$$M.S. = \frac{144}{0.9} - 1$$

$$= 159$$

Therefore, the inner shell maintains sufficient strength.

1) Maruzen: Kikai Sekkei Jishu, p. 793
 (Handbook of Mechanical Design: Maruzen, page 793)

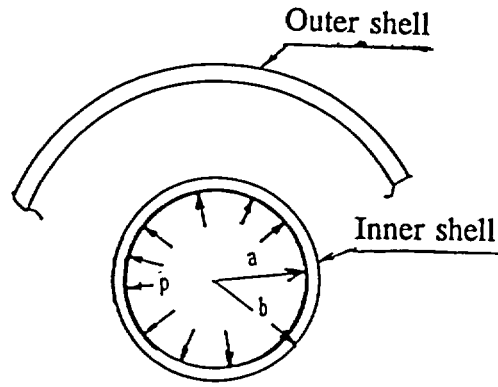


Fig. (II)-A.54 Analysis Model of the Inner Shell

(b) Rear lid unit

The analysis model for this evaluation has the same shape as the model used during drop tests. The model is an analysis model whose load conditions are changed as shown in Fig. (II)-A.55. The deformation and stress when an internal pressure of 196 kPa(G) is applied are elasticity-calculated by the calculation code, ANSYS. Table (II)-A.30 list the physical property value of the stainless steel under thermal test conditions.

Table (II)-A.31 lists the calculation results for the main parts.

Table (II)-A.30 Physical Property Value of the Rear Lid Unit (Temperature: 200°C)

	SUS304	SUS630
Modulus of longitudinal elasticity	$1.83 \times 10^5 \text{ N/mm}^2$	$2.06 \times 10^5 \text{ N/mm}^2$
Poisson's ratio	0.3 -	0.3 -

Table (II)-A.31 Calculation Results for Main Parts of the Rear Lid Unit

Parts	Stress	Displacement
1	0.78 N/mm^2 (0.08 kg/mm ²)	0.059 mm
2	1.7 N/mm^2 (0.17 kg/mm ²)	0.057 mm
3	1.6 N/mm^2 (0.16 kg/mm ²)	0.054 mm
4	1.6 N/mm^2 (0.16 kg/mm ²)	0.053 mm
5	0.78 N/mm^2 (0.08 kg/mm ²)	0.034 mm
6	1.3 N/mm^2 (0.13 kg/mm ²)	0.033 mm
7	0.2 N/mm^2 (0.02 kg/mm ²)	0.003 mm
8	0.2 N/mm^2 (0.02 kg/mm ²)	0.012 mm
9	0.3 N/mm^2 (0.03 kg/mm ²)	0.02 mm
10	3.2 N/mm^2 (0.33 kg/mm ²)	0.087 mm

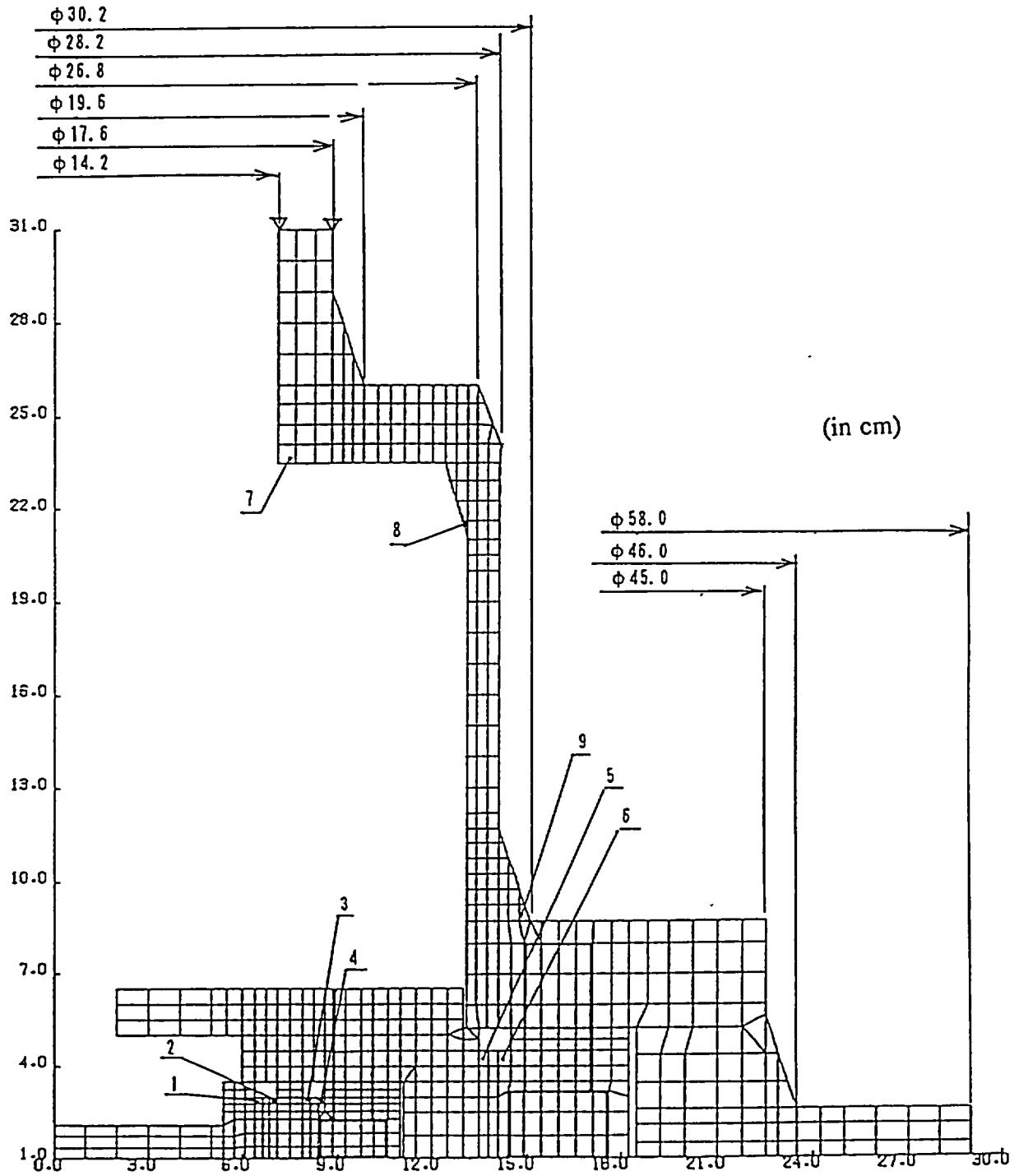


Fig. (II)-A.55 Rear Lid Unit (thermal test)

The temperature of the shielding plug lid (SUS304) (the temperature of the outer shell lid) is 125°C. If the value $\sigma_y = 144 \text{ N/mm}^2$ ($\approx 14.7 \text{ kg/mm}^2$) at a temperature of 200°C is assumed to represent the design criterion value of the yield stress, the margin of safety (M.S.) is given by

$$M.S. = \frac{144}{3.9} - 1$$

$$= 36$$

The deformation of the O-ring packing part is less than 0.06 mm. Moreover, the collapsed height of the O-ring to be used is more than 0.9 mm. Containment is thus maintained.

(c) Front lid unit

As in the drop test, the elasticity is evaluated by the calculation code, ANSYS, based on the assumption that an internal pressure of 196 kPa(G) is applied using the analysis model shown in Fig. (II)-A.56. As in step (a), the physical property value of the stainless steel is the same as the value shown in Table (II)-A.30. Table (II)-A.32 lists the calculation results for the main parts.

Table (II)-A.32 Calculation Results for Main Parts of the Front Lid Unit

	Stress	Displacement
1	2.1 N/mm ² (0.21 kg/mm ²)	0.014 mm
2	0.4 N/mm ² (0.04 kg/mm ²)	0.014 mm
3	1.7 N/mm ² (0.17 kg/mm ²)	0.013 mm
4	2.3 N/mm ² (0.23 kg/mm ²)	0.005 mm
5	3.9 N/mm ² (0.04 kg/mm ²)	0.005 mm
6	0.3 N/mm ² (0.03 kg/mm ²)	0.0004 mm
7	3.9 N/mm ² (0.4 kg/mm ²)	0.004 mm
8	3.2 N/mm ² (0.33 kg/mm ²)	0.005 mm
9	3.0 N/mm ² (0.31 kg/mm ²)	0.012 mm
10	0.2 N/mm ² (0.02 kg/mm ²)	0.004 mm

The maximum stress occurs at the position of element number 5. The margin of safety in this part can thus be calculated. The temperature of the rotating plug lid (SUS304) (the temperature of the outer shell lid) is 125°C. If the value $\sigma_y = 144 \text{ N/mm}^2$ ($\approx 14.7 \text{ kg/mm}^2$) at a temperature of 200°C is assumed to represent the design criterion value of the yield stress, the margin of safety (M.S.) is given by

$$M.S. = \frac{144}{3.9} - 1$$

$$= 36$$

The deformation of an O-ring packing part is less than 0.02 mm. Moreover, the collapsed height of the O-ring to be used is more than 0.9 mm. Containment is thus maintained.

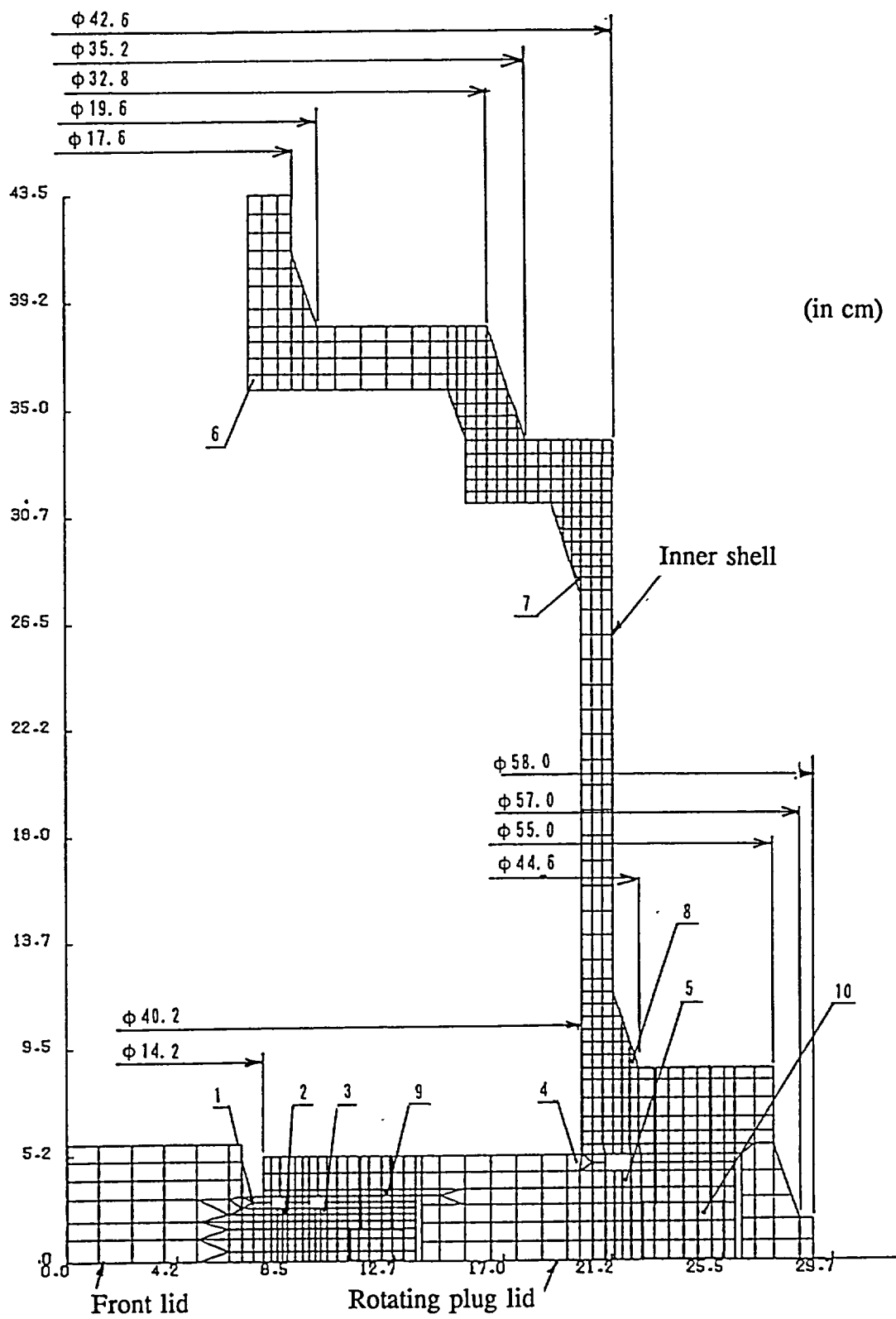


Fig. (II)-A.56 Front Lid Unit (Thermal Test)

(d) Penetration hole lid

Assuming that pressure resistance is maintained by only the lid and flange parts as shown in Fig. (II)-A.57, the elasticity is evaluated by the calculation code, ANSYS, when an internal pressure of 196 kPa(G) acts on these parts. Table (II)-A.33 lists the physical property value under thermal test conditions. Table (II)-A.34 lists the calculation results for the main parts.

**Table (II)-A.33 Physical Property Value of the Penetration Hole Lid Unit
(Temperature: 200°C)**

	SUS304	SUS630
Modulus of longitudinal elasticity	$1.83 \times 10^5 \text{ N/mm}^2$	$2.06 \times 10^5 \text{ N/mm}^2$
Poisson's ratio	0.3 -	0.3 -

Table (II)-A.34 Calculation Results for the Main Parts of the Penetration Hole Lid

Parts	Stress	Displacement
1	1.1 N/mm ² (0.11 kg/mm ²)	0.002 mm
2	1.0 N/mm ² 0.10 kg/mm ²	0.001 mm
3	1.0 N/mm ² 0.10 kg/mm ²	0.004 mm
4	0.4 N/mm ² 0.04 kg/mm ²	0.007 mm
5	0.2 N/mm ² 0.02 kg/mm ²	0.006 mm
6	0.1 N/mm ² 0.01 kg/mm ²	0.005 mm

The temperature of the penetration hole lid unit is 120°C. If the value at a temperature of 200°C is assumed to represent the design criterion value of the yield stress, the margin of safety (M.S.) is given by

$$\begin{aligned} M.S. &= \frac{144}{1.1} - 1 \\ &= 130 \end{aligned}$$

The deformation of the O-ring packing part is less than 0.01 mm. Moreover, the collapsed height of the O-ring packing to be used is more than 0.9 mm. Containment is thus maintained.

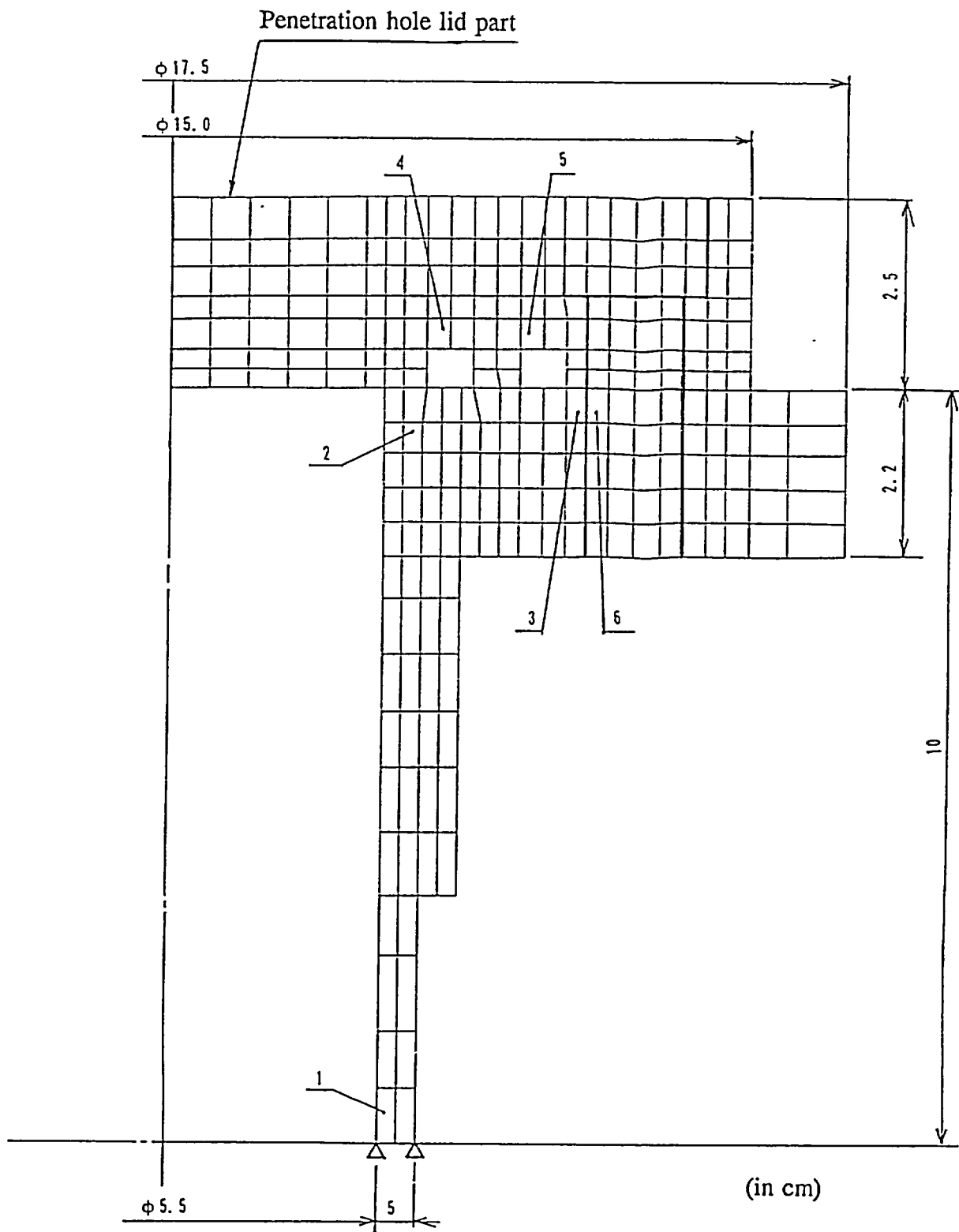


Fig. (II)-A.57 Analysis Model of Penetration Hole Lid

(e) Fuel supporting can

The fuel supporting can is a tube with circular plates installed on both ends as shown in Fig. (II)-A.58. The bottom plate is thinner than the lid plate. Therefore, the stresses generated in the tube and at the bottom plate of the fuel supporting can may be determined.

The stress generated in the tube is given by the expression provided below when the tube is thin and cylindrical.

$$\sigma = \frac{P \cdot R}{t} \quad 1)$$

p	:	Internal pressure	294 kPa(B) = 0.294 N/mm ²
R	:	Radius of the tube	42.6 mm
t	:	Plate thickness	2 mm

$$\begin{aligned}\sigma &= \frac{0.294 \times 42.6}{2} \\ &= 6.3 \text{ N/mm}^2 \\ &\approx 0.64 \text{ kg/mm}^2\end{aligned}$$

The bending stress resulting from the internal pressure generated in bottom plate is given

$$\sigma = \frac{3W}{8\pi \cdot m \cdot t^2} (3m + 1) \quad 1)$$

W : Load

$$\begin{aligned}W &= P \cdot \pi \cdot R^2 \\ &= 0.294 \times \pi \times 42.6^2 \\ &= 1.68 \times 10^3 \text{ N}\end{aligned}$$

m	:	Reciprocal of Poisson's ratio	3.3
t	:	Bottom plate thickness	3 mm

$$\begin{aligned}\sigma &= \frac{3 \times 1.68 \times 10^3}{8 \times \pi \times 3.3 \times 3^2} (3.3 \times 3 + 1) \\ &= 73.6 \text{ N/mm}^2 \\ &\approx 7.49 \text{ kg/mm}^2\end{aligned}$$

The temperature of the fuel supporting can is 332°C. If the value $\sigma_y = 118 \text{ N/mm}^2 \approx 12.1 \text{ kg/mm}^2$ at a temperature of 400°C is assumed to represent the design criterion value of the yield stress, the margin of safety (M.S.) is given by

-
- 1) Maruzen: Kikai Sekkei Benran, p. 791 (Handbook of Mechanical Design: Page 791, Maruzen)
 - 2) R.J. Roark: Formulas for Stress and Strain, P212, McGraw Hill Book, 1965

$$M.S. = \frac{118}{73.4} - 1$$

$$= 0.6$$

The fuel supporting thus maintains sufficient strength.

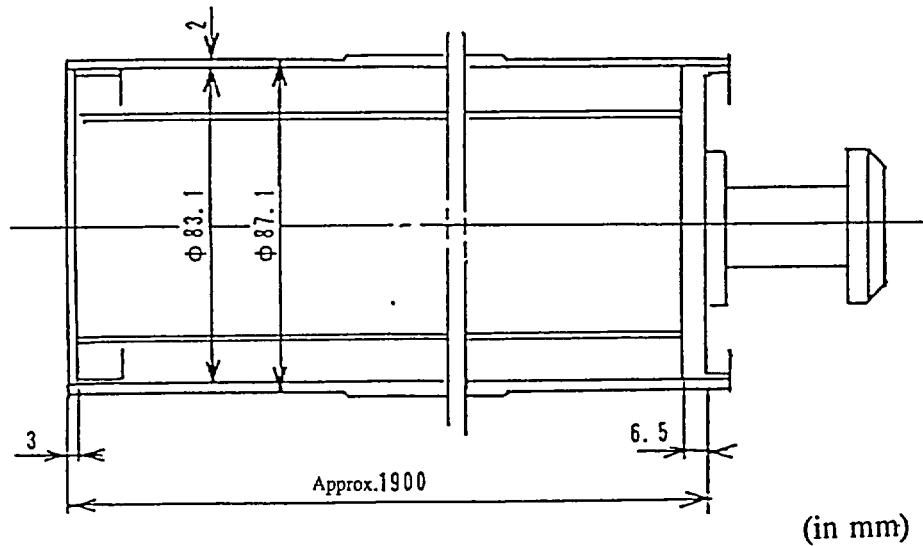


Fig. (II)-A.58 Fuel Supporting Can

(f) Receiving tube

In receiving tube I (13.8 mm/10.5 mm in diameter) and receiving tube II (22 mm/19 mm in diameter), one end plug is welded, while the other end plug is welded after it is screwed in. Receiving tube II (shown in Fig. (II)-A.59), which has a larger inner diameter and a smaller plate thickness than receiving tube I is examined below.

The end plug has a thicker plate than the pipe part and is sufficiently strong. Therefore, the stress generated in the pipe when internal pressure is applied is determined.

$$\sigma = \frac{P \cdot R}{t}$$

p	: Internal pressure	686 kPa = 0.686 N/mm ²
R	: Radius of the pipe	11 mm
t	: Plate thickness of the pipe	1.5 mm

$$\sigma = \frac{0.686 \times 11}{1.5}$$

$$= 5.03 \text{ N/mm}^2$$

$$\approx 0.52 \text{ kg/mm}^2$$

The temperature of receiving tube II is 332°C. If the value $\sigma_y = 123 \text{ N/mm}^2$ ($\approx 12.6 \text{ kg/mm}^2$) at a temperature of 350°C is assumed to represent the design criterion value of the yield stress, the margin of safety (M.S.) is given by

$$\begin{aligned} M.S. &= \frac{123}{5.03} - 1 \\ &= 23 \end{aligned}$$

Therefore, receiving tube II maintains sufficient strength.

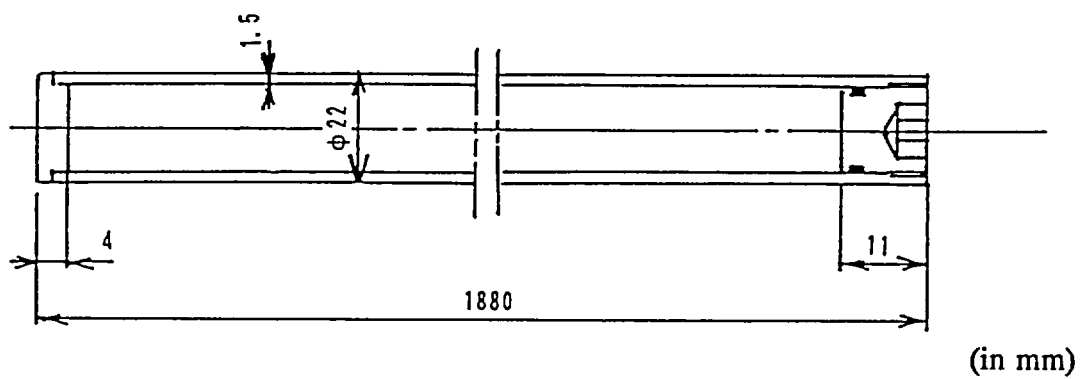


Fig. (II)-A.59 Receiving Tube II

A.6.3.3 Comparison with the Allowable Stress

Table (II)-A.35 compares the actual stress generated and the design criterion value.

Table (II)-A.35 Comparison with the Allowable Stress (2)

(No. 1)

Condi- tions	Evaluation item	Design criterion	Design cri- terion value	Evaluation result	Margin of safety	Re- marks
Accident test conditions	Drop test I					
	Rear-end-first vertical drop					
	Shock absorber	Thickness	185 mm	110 mm	Meets the criterion.	
	Outer shell	σ_{UD}	595 N/mm ²	380 N/mm ²	0.6	
	Inner shell	σ_y	174 N/mm ²	66 N/mm ²	1.6	
	Shielding plug lid					
	Plug receiving part	σ_{UD}	595 N/mm ²	422 N/mm ²	0.4	
	Fastening bolt	σ_y	682 N/mm ²	161 N/mm ²	3.2	
	Sampling valve lid fastening bolt	$0.6\sigma_y$	409 N/mm ²	24.8 N/mm ²	15	
	Inner container	P_k	6.37x10 ⁵ N	4.63x10 ⁴ N	13	P_k : Buck- ling load
	Fuel supporting can I	P_k	2.17x10 ⁵ N	3.31x10 ⁴ N	5.6	
	Rear lid of fuel supporting can	σ_{UD}	524 N/mm ²	372 N/mm ²	0.4	
	Rack supporting rod	σ_{UD}	524 N/mm ²	164 N/mm ²	2.2	
	Rack end plate	σ_{UD}	524 N/mm ²	376 N/mm ²	0.4	
	Receiving tube	P_k	1.87x10 ³ N	1.32x10 ³ N	0.4	
	Front-end-first vertical drop					
	Rotating plug lid receiving part	σ_{UD}	595 N/mm ²	549 N/mm ²	0.08	
	Rotating plug lid fastening bolt	σ_y	682 N/mm ²	93.2 N/mm ²	6.3	
	Inner container	P_k	6.37x10 ⁵ N	8.61x10 ⁴ N	6.4	
	Horizontal drop					
Shock absorber	Thickness	273 mm	160 mm	Meets the criterion		
Outer shell	σ_{UD}	595 N/mm ²	460 N/mm ²	0.3		

Table (II)-A.35 Comparison with the Allowable Stress (2)

(No. 2)

Condi- tions	Evaluation item	Design criterion	Design cri- terion value	Evaluation result	Margin of safety	Re- marks
Accident test conditions	Inner shell	σ_y	174 N/mm ²	101 N/mm ²	0.7	
	Fuel supporting can spacer	$0.6\sigma_{UD}$	314 N/mm ²	203 N/mm ²	0.5	
	Receiving tube	σ_{UD}	524 N/mm ²	291 N/mm ²	0.8	
	Sampling valve lid					
	Penetration hole lid	σ_y	180 N/mm ²	11.6 N/mm ²	15	
	Sampling valve lid fastening bolt					
	Penetration hole lid fastening bolt	σ_y	682 N/mm ²	22.1 N/mm ²	30	
	Corner drop					
	Shock absorber	Thickness	335 mm	210 mm	Meets the criterion	
	Shielding plug lid fastening bolt	σ_y	682 N/mm ²	60.6 N/mm ²	10	
	Rotating plug lid fastening bolt	σ_y	682 N/mm ²	106 N/mm ²	5.4	
	Oblique drop					
	Shock absorber (60 degrees)	Thickness	390 mm	295 mm	Meets the criterion.	
	Drop test II					
	Outer shell	Plate thickness σ_{UD}	16 mm 496 N/mm ²	11.7 mm 301 N/mm ²	Meets the criterion. 0.7	

Table (II)-A.35 Comparison with the Allowable Stress (2)

(No. 3)

Condi- tions	Evaluation item	Design criterion	Design cri- terion value	Evaluation result	Margin of safety	Re- marks
Accident test conditions	Thermal test					
	Thermal expansion					
	Inner shell	σ_U	485 N/mm ²	340 N/mm ²	0.43	
	Outer shell	σ_U	254 N/mm ²	114 N/mm ²	1.2	
	Stress calculation					
	Inner shell	σ_y	144 N/mm ²	0.9 N/mm ²	159	
	Shielding plug lid	σ_y	144 N/mm ²	3.2 N/mm ²	44	
	Rotating plug lid	σ_y	144 N/mm ²	3.9 N/mm ²	36	
	Penetration hole lid	σ_y	144 N/mm ²	1.1 N/mm ²	130	
	Fuel supporting can	σ_y	118 N/mm ²	73.4 N//m ²	0.6	
	Receiving tube	σ_y	123 N/mm ²	5.03 N/mm ²	23	
	Water immersion					
	Rotating plug	σ_y	174 N/mm ²	2.55 N/m ²	67	

A.6.4 Water Immersion

The maximum radioactivity of this package is 2.04 pBq. A water immersion test at a 200-m depth is not required because the maximum radioactivity is less than 37 pBq. The effect of water immersion when water pressure (147 kPa(G)) at a depth of 15 m acts on the packaging was examined. In this case, the water immersion test was conducted after external heat was applied under the thermal accident test conditions described in section B.5 of Chapter (II) following drop tests I and II. As the applied pressure, the internal pressure caused by the decay heat of the internal contents was ignored to be on the safe side, and only an external pressure of 147 kPa(G) was assumed to be applied. The box portion on the rotating plug side that is most significantly influenced by the external pressure was evaluated. (See Fig. (II)-A.60.) The critical pressure at which the box on the rotating plug side buckles as a result of external pressure is given by the expression below.¹⁾

$$P_k = \left\{ \frac{E}{4(1 - \nu^2)} \right\} \left(\frac{t}{r} \right)^3$$

P_k	:	Critical pressure at which the cylindrical shell buckles as a result of external pressure only without the influence of axial force	
E	:	Modulus of longitudinal elasticity	$1.91 \times 10^5 \text{ N/mm}^2$
ν	:	Poisson's ratio	0.3
t	:	Plate thickness	12 mm
r	:	Mean radius of the cylindrical shell	207 mm
ℓ	:	Length	

$$\ell \geq 4.90 \sqrt{t \cdot r}$$

To be on the safe side, assume that ℓ is an infinite length. In this case, the expression below results.

$$\begin{aligned} P_k &= \left\{ \frac{1.91 \times 10^5}{4(1 - 0.3^2)} \right\} \left(\frac{12}{207} \right)^3 \\ &= 10.2 \text{ N/mm}^2 \\ &\approx 1.04 \text{ kg/mm}^2 \end{aligned}$$

No buckling occurs because the criterion value is 0.147 N/mm^2 , which is less than the above critical pressure. The stress on the cylindrical shell when the box on the rotating plug side is subject to external pressure (0.147 N/mm^2) is given by the expression below.

1) Maruzen: Kikai Sekkei Benran, p. 792
(Handbook of Mechanical Design: Page 792, Maruzen)

$$\sigma_{\theta} = - \frac{k^2 + \frac{k^2}{R^2}}{k^2 - 1} P_b \quad 1)$$

σ_{θ} : Circumferential stress of the cylinder
 P_b : Pressure 0.147 N/mm²
 R : Constant

$$R = \frac{r}{a}$$

r : Mean radius of the box 207 mm
 a : Inner radius of the box 201 mm

$$R = 1.03$$

k : Constant

$$k = \frac{b}{a}$$

b : Outer radius of the box 213 mm

$$k = 1.06$$

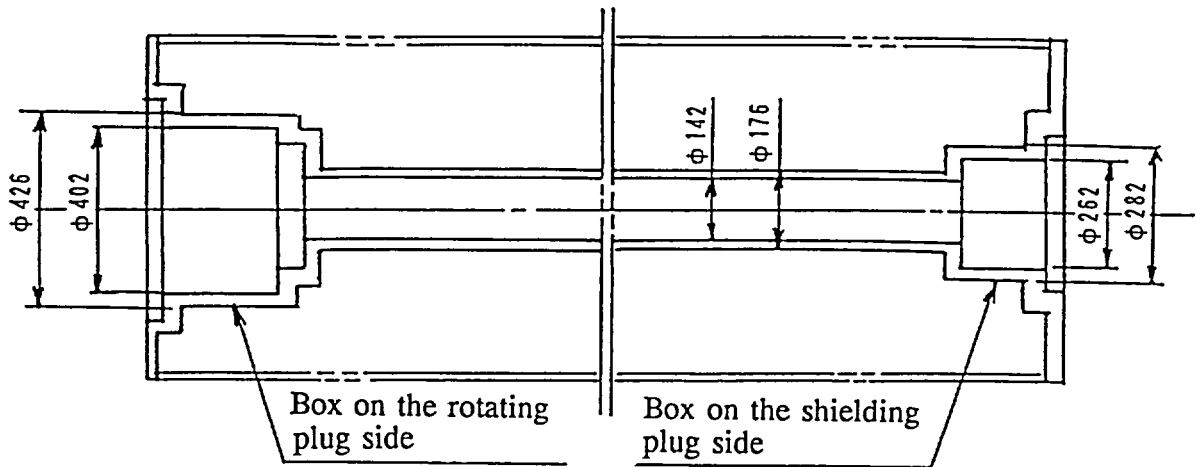
$$\begin{aligned} \sigma_{\theta} &= - \frac{1.06^2 + \frac{1.06^2}{1.03^2}}{1.06^2 - 1} \times 0.147 \\ &= -2.6 \text{ N/mm}^2 \\ &\approx -0.26 \text{ kg/mm}^2 \end{aligned}$$

The temperature of the box (SUS304) on the rotating plug side (the temperature of the inner shell) is 85°C. If the value $\sigma_y = 174 \text{ N/mm}^2$ ($\approx 17.8 \text{ kg/mm}^2$) at a temperature of 90°C is assumed to represent the design criterion value of the yield stress, the margin of safety (M.S.) is given by

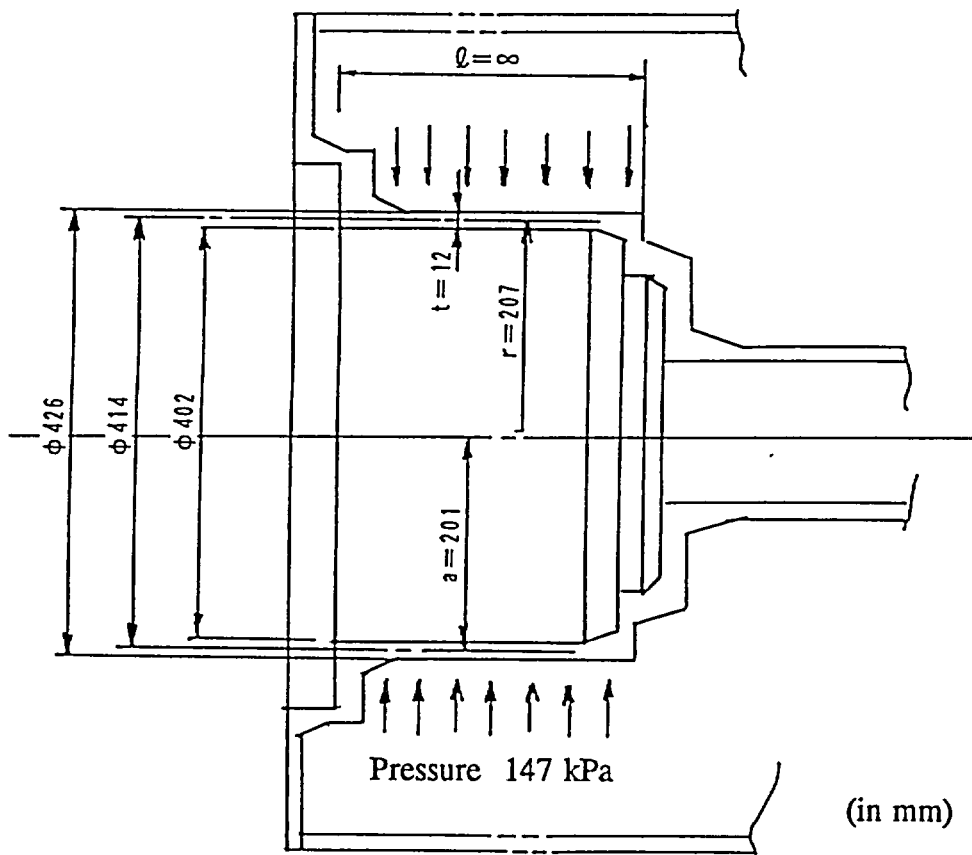
$$\begin{aligned} M.S. &= \frac{174}{2.6} - 1 \\ &= 66 \end{aligned}$$

Therefore, the box on the rotating plug side has sufficient strength, and is not damaged.

1) Nihon Kikai Gakkai: Kikai Kogaku Benran, p. 4-92
 (The Japan Society of Mechanical Engineers: Handbook of Mechanical Engineering, page 4-92)



(a) Inner shell part of the outer container



(b) Rotating plug part

Fig. (II)-A.60 Water Immersion Test

A.6.5 Summary and Evaluation of Results

The damage under accident test conditions is summarized for every test item.

(1) Drop test I (9-m free drop)

The degree of deformation of a shock absorber obtained with each drop attitude does not exceed the allowable degree and does not affect the outer container. Using the value obtained when the effect of the steel plate covering the balsa wood is added to the impact deceleration resulting from the deformation of this shock absorber, the stress of the outer container is evaluated. The results show that each part maintains sufficient strength. Even including the degree of the displacement in the boundary of containment, the deformation does not exceed the collapsed height of the O-ring. However, the locking plate that supports and fixes the shielding plug onto the rear lid or the inner container screw that connects the inner container to the shielding plug is damaged during a front-end-first vertical drop. However, the locking plate and inner container screw form no boundary of containment. An evaluation of the package's behavior after these are damaged indicates that this package maintains its performance.

(2) Drop test II (1-m drop)

An evaluation has been made on the assumption that the deformation of a shock absorber during drop test II is added to the deformation resulting from drop test I. This test also evaluates the results arising from a drop attitude, (that is, a vertical drop from a height of 1 m when the balsa wood is the impact point), in which the maximum damage is caused during a subsequent thermal test, because this test leaves only the thin part of an undeformed shock absorber near the O-ring.

These are the most severe conditions for a thermal test, and therefore thermal analyses are carried out under these conditions.

A 1/2-scale model drop test has been executed to confirm that the impact deceleration in all the drop attitudes is lower than in drop test I.

The above results show that this package has the requisite resistance and sufficient strength.

(3) Thermal test

The thermal stress that is generated in the containment system (i.e., the outer container, fuel supporting can, and receiving tube) is obtained analytically and does not exceed the allowable stress. Therefore, the containment system also maintains sufficient strength.

The above results show that this package maintains sufficient strength during a thermal test.

(4) Water immersion test

An evaluation of the outside containment system (i.e., the outer container) reveals that the stress that is generated during a water immersion test does not exceed the allowable stress. This means that the containment system maintains sufficient strength. No water penetrates the containment system.

The results of the preceding structural evaluation are applied to a thermal analysis, containment analysis, shield analysis, and criticality analysis as follows:

(a) Thermal analysis

A shock absorber functions as a heat insulator under normal test conditions, and the internal temperature rises as the thickness of the shock absorber increases. Therefore, this thermal analysis is performed on the assumption that the shock absorber is not deformed by a free drop.

Under accident test conditions, the analysis is conducted on the deformation that is most easily subject to the heat input when this package is subject to fire.

That is, deformation, which reduces the thickness of the shock absorber covering all the openings of the package and extending over the entire deformed area, is assumed. In other words, the deformation that results when a vertical drop is applied to the balsa wood already deformed by a vertical drop during drop test I is used in the evaluation.

(b) Containment analysis

The preceding structural evaluation indicates that the containment system (i.e., the outer container's inner shell and lid units) remains sound. The secondary containment system (i.e., the fuel supporting can and receiving tube) also remains sound. Therefore, in the containment analysis, the leakage of a radioactive material is evaluated on the assumption that the containment system remains sound.

(c) Shield analysis

Under normal test conditions, a shock absorber is deformed by a free drop. Moreover, the outer dimensions of the package contract. This analysis is performed this effect into consideration.

Under accident test conditions, an evaluation is performed on packaging without shock absorbers. For the neutron shield analysis in the radial direction, the analysis is performed under the assumption that the resin layer has been lost.

(d) Criticality analysis

Under normal and accident test conditions, this analysis is performed on only the package body without the shock absorbers in order to be on the safe side. The results of the water immersion test conducted in the structural evaluation reveal that the outer container maintains sufficient strength. No water penetrates the inner shell in this case. To be on the safe side, this evaluation is performed on the assumption that water does penetrate.

A.7 Special-Form Nuclear Fuel Materials

This packaging does not apply to this section because it is not for special-form nuclear fuel materials.

A.7.1 Outline (Omitted)

A.7.2 Impact (Omitted)

A.7.3 Percussion (Omitted)

A.7.4 Heating (Omitted)

A.7.5 Bending (Omitted)

A.7.6 Water Immersion (Omitted)

A.7.7 Summary and Evaluation of Results (Omitted)

A.8 Radioactive Contents

The radioactive contents of this package are irradiated fuel pins generated by the fuel material irradiation experiment for fast breeder development, and structural materials (stainless steel) such as a fuel cladding tube, wrapper tubes, and material test-pieces irradiated by a fast breeder reactor. The stress generated in a fuel supporting can or receiving tube holding fuel pins is obtained by the method described in subsection A.6.1.1 Table (II)-A.36 provides the results. These receiving containers have sufficient strength during a drop test under accident test conditions.

Therefore, no fission product escapes to the outside of the fuel supporting can or receiving tube.

The structural materials of the fuel cladding tube, wrapper tube, or material test-piece are directly stored in the inner container. The contents are made of metal so that the activated materials cannot escape from the inner container.

Table (II)-A.36 Comparison of the Radioactive Contents with the Design Criterion Values

Condi- tion	Evaluation item	Design criterion	Design cri- terion value	Evaluation result	Margin of safety
Accident test conditions	Drop test I				
	Vertical drop				
	Fuel supporting can I	P_k	$2.17 \times 10^5 \text{ N}$	$3.31 \times 10^4 \text{ N}$	5.6
	Rear lid of the fuel supporting can	σ_{UD}	524 N/mm^2	372 N/mm^2	0.4
	Receiving tube	P_k	$1.87 \times 10^3 \text{ N}$	$1.32 \times 10^3 \text{ N}$	0.4
	Horizontal drop				
	Fuel supporting can spacer	$0.6 \sigma_{UD}$	314 N/mm^2	203 N/mm^2	0.54
Receiving tube	σ_{UD}	524 N/mm^2	291 N/mm^2	0.8	

A.9 Fissile Package

This section describes the change in shape regarding the criticality when this package is subject to test conditions established by "the rules for transporting nuclear fuel materials and the like outside of a factory or business site" and "notification that prescribes details of engineering standards on the transport of nuclear fuel materials and the like outside of a factory or business site."

A.9.1 Normal Test Conditions

(1) Water spray test

As described in subsection A.5.2, this packaging is made of a stainless steel with a smooth-finish surface. Therefore, it prevents water from being collected and retained, and has no water absorbency. This packaging is not deformed even under water spray test conditions.

(2) Drop test onto a corner or onto each of the quarters of each rim from a height of 0.3 m

When the corner drop test from a height of 0.3 m is conducted, only the corner of either of the shock absorbers installed on both ends of this packaging becomes deformed. The degree of deformation ($h_{0.3}$) is obtained by the method described in subsection A.6.1.3.

$$h_{0.3} = 68 \text{ mm}$$

(3) Free drop test

Assuming the deformation that occurs in the package by free drop onto a corner or onto each of the quarters of each rim in step (2), the degree of deformation ($h_{0.3+0.6}$) and impact deceleration ($G_{0.3+0.6}$) during a free drop test from a height of 0.6 m are obtained by the method described in subsection A.6.1.3. Table (II)-A.37 lists that obtained results.

Table (II)-A.37 Calculation Results of a Free Drop (0.3 m + 0.6 m)

Item	Degree of deformation (mm)	Deceleration (G)
Vertical drop	21	62
Horizontal drop	68	29
Corner drop	99	24

(4) Stacking test

As described in subsection A.5.4, this packaging is not deformed even under stacking test conditions.

(5) Penetration test

As described in subsection A.5.5, a concave dent measuring approximately 2.7 mm appears on the outer shell of the packaging body when a penetration test is conducted. However, the area of this dent is limited. Therefore, the change in shape does not affect the conditions of the criticality analysis.

(6) Summary and evaluation of results

Even if the tests in steps (1) through (5) are conducted, items ((a) through (d)) below, which are established by law, are satisfied, and the shape of the packaging or other conditions related to the criticality analysis are maintained.

- (a) A dent measuring approximately 2.7 mm appears on the outer shell and its shape provides the basis for the criticality analysis. However, the dent accounts for less than 1% of the criticality analysis volume. No dent exceeding 5% of this volume appears.
- (b) No dent appears in any other part besides the one described in step (a), and no dent measuring 10 cm³ appears in the structural part.
- (c) Deformation occurs only in the shock absorber, and the containment system remains sound, so no water penetrates the system. The criticality analysis assumes that there is no shock absorber.
- (d) Since the criticality analysis dimensions (800 mm in diameter × 2564 mm in length) are unaffected even after tests under normal test conditions are conducted, there are no changes which increase the neutron multiplication factor significantly.

A.9.2 Accident Test Conditions

The results prescribe that the more severe test of the two-test series shown below be conducted. In this subsection, both cases are examined. In either case, the critical shape does not change.

Case (1)

Normal test conditions (A.9.1) + drop test I + drop test II + thermal test + 0.9-m water immersion test

Case (2)

Normal test conditions (A.9.1) + 15-m immersion test

A.9.2.1 Case (1)

The deformed value is obtained under test conditions, which have been specified to provide the maximum deformation.

(1) Water spray test

As described in subsection A.5.2, this packaging is made of stainless steel with a smooth-finish surface. Therefore, it prevents water from being collected and retained, and has no water absorbency. This packaging is not deformed even under water spray test conditions.

(2) Drop test onto a corner or onto each of the quarters of each rim from a height of 0.3 m

A corner of the shock absorber becomes deformed as a result of a corner drop test from a height of 0.3 m. The deformation value ($h_{0.3}$) at that time is as follows: (See subsection A.9.1(2).)

$$h_{0.3} = 68 \text{ mm}$$

(3) Free drop test

Given the deformation occurring in the package because of a free drop onto a corner or onto each of the quarters of each rim from a height of 0.3 m, the deformation value ($h_{0.3+0.6}$) of the shock absorber resulting from a 0.6-m free drop is as follows: (See subsection 9.1(3).)

1) Vertical drop	Deformation value	21 mm
2) Horizontal drop	Deformation value	68 mm
3) Corner drop	Deformation value	99 mm

(4) Stacking test

As described in subsection A.5.4, this packaging is not deformed even under stacking test conditions.

(5) Penetration test

As described in subsection A.5.5, a concave dent measuring approximately 2.6 mm appears in the outer shell of the packaging body when a penetration test is conducted. However, the area of this dent is limited. Therefore, the change in shape does not affect the conditions of the criticality analysis.

(6) 9-m free drop test

After a free drop (0.3 m and 0.6 m) under normal test conditions, a package subjected to a 9-m free drop at three different attitudes, as shown below, is evaluated.

- 1) Vertical drop
- 2) Horizontal drop
- 3) Corner drop

1) Vertical drop

Table (II)-A.38 lists the deformation value ($h_{0.3+0.6+9.0}$) and impact deceleration ($G_{0.3+0.6+9.0}$) (during a drop test) obtained in the same manner as in subsection A.6.1.1 when a 9-m vertical drop test is conducted after the free drops (0.3 m and 0.6 m) under normal test conditions. Table (II)-A.39 lists the results evaluated in the same manner as in subsection A.6.1.1 when the containment system (i.e., the lid units and the inner shell), and the secondary containment system (i.e. the fuel supporting cans or the receiving tubes) are subject to the impact acceleration resulting from a drop in this drop attitude.

2) Horizontal drop

Table (II)-A.38 lists the deformation value ($h_{0.3+0.6+9.0}$) and impact deceleration ($G_{0.3+0.6+9.0}$) (during a drop test) obtained in the same manner as in subsection A.6.1.2 when a 9-m horizontal drop test is conducted after the free drops (0.3 m and 0.6 m) under normal test conditions. Table (II)-A.39 lists the results evaluated in the same manner as in subsection A.6.1.2 when the containment system (i.e. the lid units and the inner shell), and the secondary containment system (i.e. the fuel supporting cans or the receiving tubes) are subject to the impact acceleration resulting from a drop in this drop attitude.

3) Corner drop

Table (II)-A.38 lists the deformation value ($h_{0.3+0.6+9.0}$) and impact deceleration ($G_{0.3+0.6+9.0}$) (during a drop test) obtained in the same manner as in subsection A.6.1.3, when a 9-m drop test is conducted after the free drops (0.3 m and 0.6 m) under normal test conditions. Table (II)-A.39 lists the results evaluated in the same manner as in subsection A.6.1.3 when the containment system (i.e. the lid units) is subject to the impact acceleration resulting from a drop at this attitude.

Table (II)-A.38 Calculation Results of a free Drop (0.3 m + 0.6 m + 9.0 m)

Item	Degree of deformation (mm)	Deceleration (G)
Vertical drop	117	139
Horizontal drop	182	132
Corner drop	242	82

Table (II)-A.39 Comparison with the Allowable Stress

(No. 1)

Condi- tions	Evaluation item	Design criterion	Design cri- terion value	Evaluation result	Margin of safety	Re- marks
Accident test conditions	Drop test I					
	Rear-end-first vertical drop					
	Shock absorber					
	Outer shell	σ_{UD}	595 N/mm ²	391 N/mm ²	0.52	
	Inner shell	σ_y	174 N/mm ²	68 N/mm ²	1.5	
	Shielding plug lid					
	Plug receiving part	σ_{UD}	595 N/mm ²	435 N/mm ²	0.37	
	Fastening bolt	σ_y	682 N/mm ²	166 N/mm ²	3.1	
	Sampling valve lid fastening bolt	$0.6\sigma_y$	409 N/mm ²	25.5 N/mm ²	15	
	Inner container	P_k	6.37x10 ⁵ N	4.77x10 ⁴ N	12	P _k : Buck- ling load
	Fuel supporting can I	P_k	2.17x10 ⁵ N	3.41x10 ⁴ N	5.4	
	Rear lid of fuel supporting can	σ_{UD}	524 N/mm ²	383 N/mm ²	0.36	
	Rack supporting rod	σ_{UD}	524 N/mm ²	169 N/mm ²	2.1	
	Rack end plate	σ_{UD}	524 N/mm ²	387 N/mm ²	0.35	
	Receiving tube	P_k	1.87x10 ³ N	1.36x10 ³ N	0.38	
	Front-end-first vertical drop					
	Rotating plug lid receiving part	σ_{UD}	595 N/mm ²	565 N/mm ²	0.05	
	Rotating plug lid fastening bolt	σ_y	682 N/mm ²	96.0 N/mm ²	6.1	
	Inner container	P_k	6.37x10 ⁵ N	8.87x10 ⁴ N	6.1	

Table (II)-A.39 Comparison with the Allowable Stress

(No. 2)

Condi- tions	Evaluation item	Design criterion	Design cri- terion value	Evaluation result	Margin of safety	Re- marks
Accident test conditions	Horizontal drop					
	Outer shell	σ_{UD}	595 N/mm ²	506 N/mm ²	0.17	
	Inner shell	σ_y	174 N/mm ²	111 N/mm ²	0.57	
	Fuel supporting can spacer	$0.6\sigma_{UD}$	314 N/mm ²	223 N/mm ²	0.40	
	Receiving tube	σ_{UD}	524 N/mm ²	320 N/mm ²	0.63	
	Sampling valve lid fastening bolt	σ_y	180 N/mm ²	12.8 N/mm ²	13	
	Penetration hole lid fastening bolt	σ_y	682 N/mm ²	24.3 N/mm ²	27	
	Corner drop					
	Shielding plug lid fastening bolt	σ_y	682 N/mm ²	66.3 mm	9.3	
	Rotating plug lid fastening bolt	σ_y	682 N/mm ²	116 N/mm ²	4.9	

(7) Drop test II

Drop test II is conducted on the part of the shock absorber that has become deformed during the drop test I mentioned above. The deformation value is obtained in the same way in subsection A.6.2.

The drop energy (E_k) generated during drop test II on the packaging corner is given by

$$E_k = 1.03 \times 10^8 \text{ N}\cdot\text{mm} \\ \approx 1.05 \times 10^7 \text{ kg}\cdot\text{mm}$$

When the deformation energy of the shock absorber's cover plate is subtracted from the drop energy, the expression below results.

$$E_k = 8.19 \times 10^7 \text{ N}\cdot\text{mm} \\ \approx 8.35 \times 10^6 \text{ kg}\cdot\text{mm}$$

The shock absorption material (balsa wood) and the inner steel plate of the shock absorber become deformed by this energy.

The energy absorption value (E_b) of the balsa wood deformation is given by the expression below.

$$E_b = \frac{\pi}{4} \cdot (150)^2 \times \sigma_b \times h$$

where

$$\begin{array}{ll} \sigma_b & : \quad \text{Deformed stress of the balsa wood} \\ & \quad \quad \quad 24.5 \text{ N/mm}^2 \approx 2.5 \text{ kg/mm}^2 \\ h & : \quad \text{Deformation value} \\ & \quad \quad \quad 158 \text{ mm} \end{array}$$

$$E_b = 6.84 \times 10^7 \text{ N}\cdot\text{mm} \\ \approx 6.98 \times 10^6 \text{ kg}\cdot\text{mm}$$

The energy absorption value (E_s) of the deformation of the shock absorber's inner steel plate is given by the expression below

$$E_s = \sigma_s(V_1 - V_2)$$

where

$$\begin{array}{ll} \sigma_s & : \quad \text{Crushing stress (yield stress) of the inner steel plate} \\ & \quad \quad \quad 206 \text{ N/mm}^2 \approx 21 \text{ kg/mm}^2 \\ V_1, V_2 & : \quad \text{Volume of the deformed portion} \end{array}$$

$$V_1 = R_1^3 \tan A \left(\sin B_1 - \frac{\sin^3 B_1}{3} - B_1 \cos B_1 \right)$$

$$B_1 = \cos^{-1} \left(1 - \frac{Z}{R_1 \sin A} \right)$$

$$V_2 = R_2^3 \tan A \left(\sin B_2 - \frac{\sin^3 B_2}{3} - B_2 \cos B_2 \right)$$

$$B_2 = \cos^{-1} \left(1 - \frac{Z - 13}{R_2 \sin A} \right)$$

A	: Drop angle	23°
R ₁	: Outer radius of the inner steel plate	426.5 mm
R ₂	: Inner radius of the inner steel plate	416.5 mm
Z	: Deformation value	

If each numeric value is calculated so that E_s is $E_k - E_b$, the deformation value (Z) will be as shown below.

$$Z = 16 \text{ mm}$$

Fig. (II)-A.61 shows the deformation values of the shock absorber mentioned above.

As described in subsection A.6.2, the stress generated in the outer shell does not exceed the design criterion value. The evaluation conditions related to the criticality analysis are therefore maintained.

1) Nihon Kikai Gakkai: Kikai Kogaku Benran, p. 2-23, Kaitei 6 pan
(The Japan Society of Mechanical Engineers: Handbook of Mechanical Engineering, page 2-23, Sixth Edition)

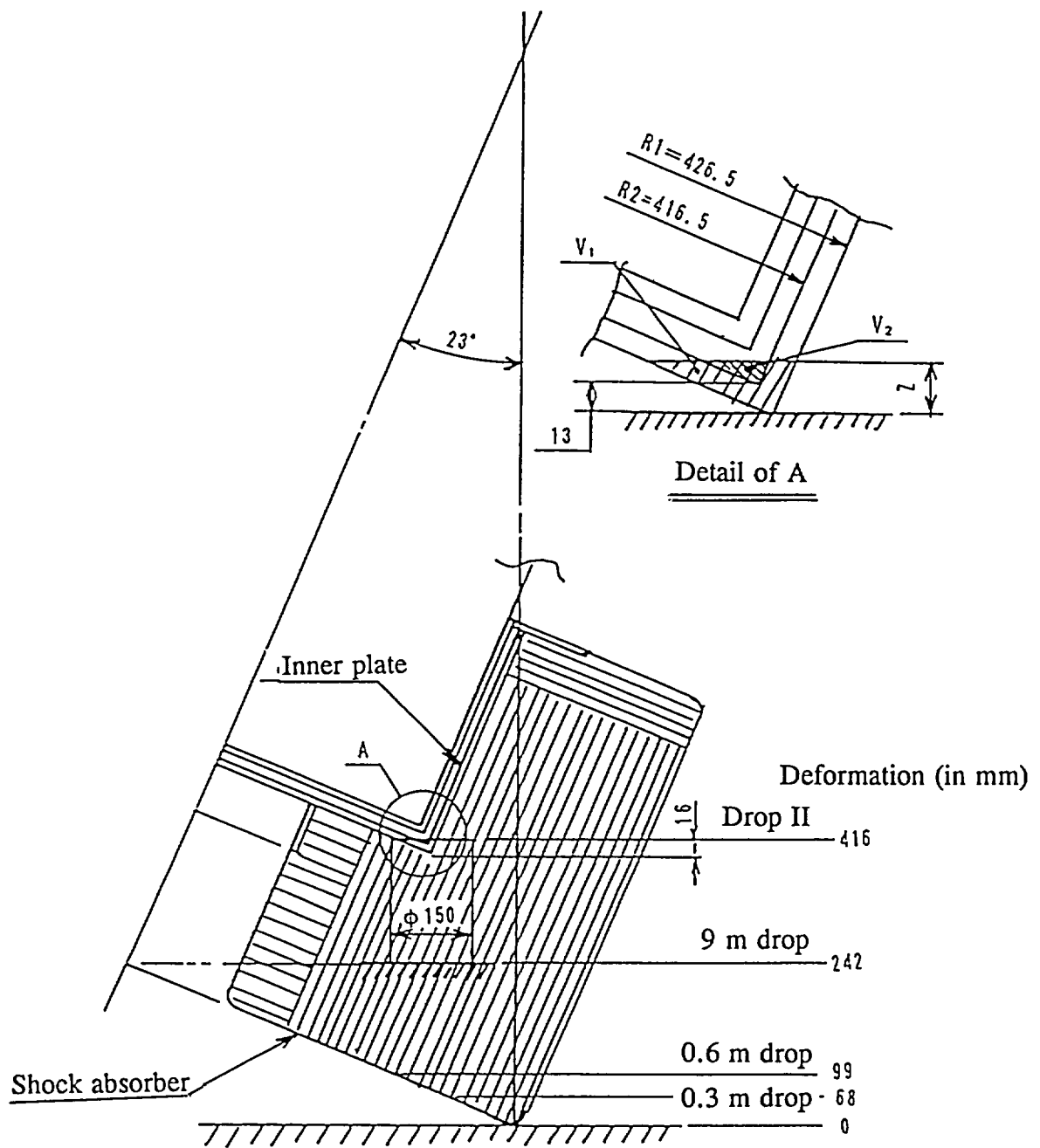


Fig. (II)-A.61 Free Drop onto a Corner or onto Each of the Quarters of Each Rim

(8) Thermal test

This evaluation is performed under thermal test conditions assuming that the insulating cement filled into the inner plate of a shock absorber is partially lost during a drop test and that the steel plate touches the outer container.

Applying the thermal analysis model shown in Fig. (II)-A.62, the maximum temperature at each part and the time it takes to reach it are obtained in the same manner as in section B.5. Table (II)-A.40 lists the resulting information.

The shielding lead does not melt even if a thermal test is conducted. The temperature of the packing is also less than the allowable service temperature.

Thermal stress is generated by the temperature difference between the inner and outer shells. As a result of the evaluation (Contents I - eccentric) in this section, the maximum temperature of the inner and outer shells is the same as the temperature of Contents I (vertical drop) in the same receiving state, shown in section B.5. Therefore, the maximum thermal stress in this case is also generated in the inner shell as described in subsection A.6.3.2. The margin of safety is approximately 0.4. This packaging is thus not damaged by thermal stress and remains sound. Therefore, the shape related to the criticality is not changed.

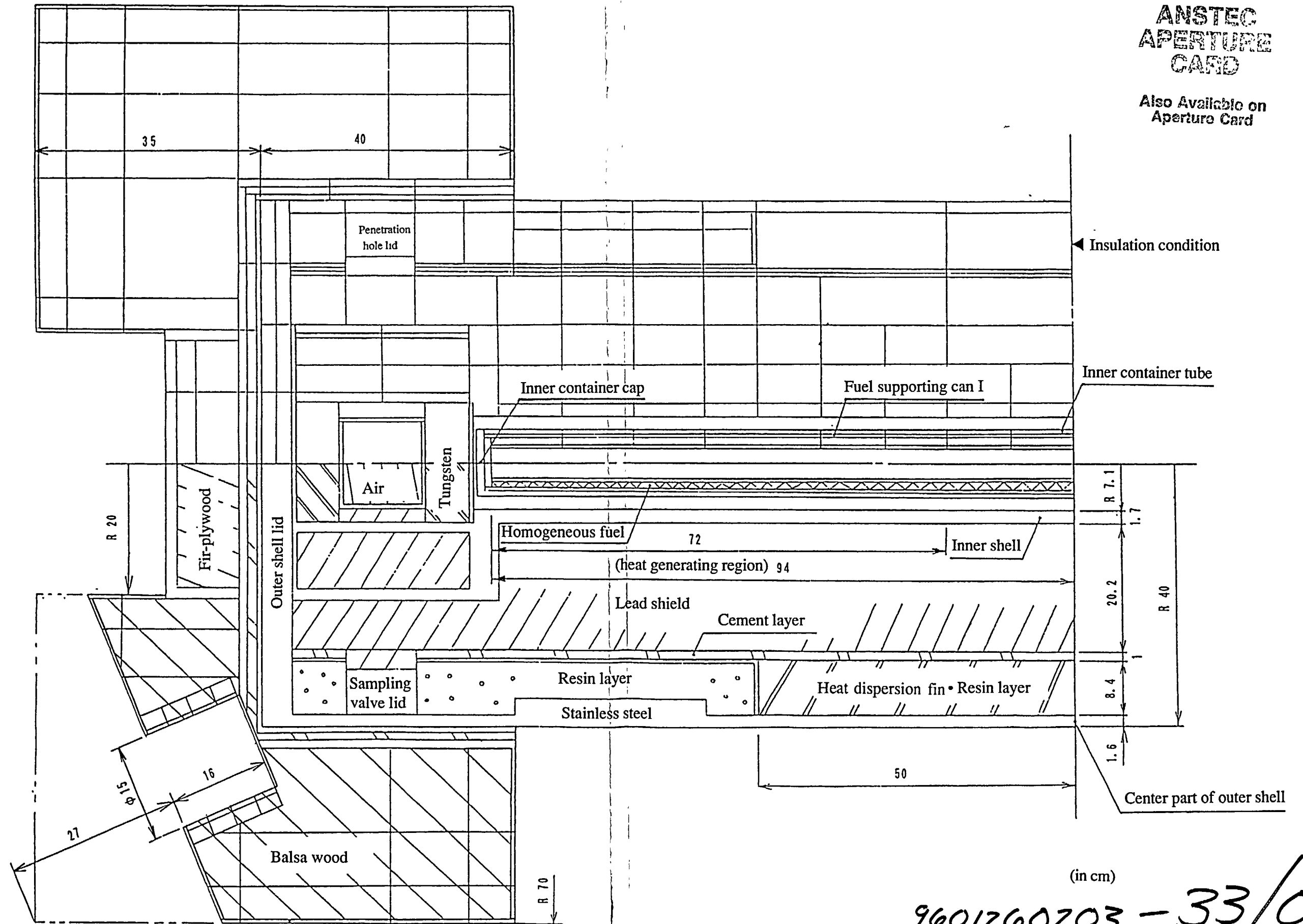
Table (II)-A.40 Maximum Temperature under Accident Test Conditions (Contents I)

Parts	Temperature	Time elapsed after a fire
Shock absorber's steel plate	781°C	0.5 h
Shock absorber's steel plate *1	796°C	0.5 h
Outer shell	656°C	0.5 h
Outer shell lid	125°C	8.0 h
Sampling valve lid	120°C	2.7 h
Penetration hole lid	120°C	2.7 h
Lead shield	193°C	1.2 h
Tungsten	132°C	7.2 h
Inner shell	193°C	1.3 h
Inner container cylinder	278°C	3.7 h
Inner container cap	254°C	7.0 h
Fuel supporting can I	328°C	4.0 h
Fuel pin	397°C	4.0 h
O-ring	125°C	8.0 h

*1 Indicates the portion damaged as a result of an accidental drop.

**ANSTEC
APERTURE
CARD**

Also Available on
Aperture Card



(in cm)

9601260203 - 33/01

Shock absorber steel plate

Fig. (II)-A.62 Thermal Analysis Model under the Accident Test Condition (Contents I/eccentric)

(9) 0.9-m water immersion test

As described in A.6.4, "Water Immersion Test", no water penetrates this packaging even if a 0.9-m water immersion test is conducted.

A.9.2.1 Case (2)

To determine the actual degree of deformation, the test conditions specified to maximize the deformation value shall be applied.

(1) Water spray test

As described in subsection A.5.2, this packaging is made of a stainless steel with a smooth-finish surface. Therefore, it prevents the collection and retention of water, and exhibits no water absorbency. This packaging is not deformed even by a water spray test.

(2) Drop test onto a corner or onto each of the quarters of each rim from a height of 0.3 m

If a corner drop test from the height of 0.3 m is conducted, only the corners of the shock absorbers installed on both ends of this packaging become deformed. The deformation value ($h_{0.3}$) is obtained by the method described in subsection A.6.1.3.

$$h_{0.3} = 68 \text{ mm}$$

(3) Free drop test

Given the deformation that occurs in the package after a free drop onto a corner or onto each of the quarters of each rim from a height of 0.3 m in the above subsection (2), the deformation value ($h_{0.3+0.6}$) and impact deceleration resulting from a free drop test from a height of 0.6 m are as follows: (See subsection A.9.1(3).)

1) Vertical drop	Deformation value	21 mm
2) Horizontal drop	Deformation value	68 mm
3) Corner drop	Deformation value	99 mm

(4) Stacking test

As described in subsection A.5.4, this packaging is not deformed even after a stacking test.

(5) Penetration test

As described in subsection A.5.5, a concave dent measuring approximately 2.6 mm is generated in the outer shell of the packaging body when a penetration test is conducted. However, the area of this dent is limited. Therefore, the change in shape does not affect the conditions of the criticality analysis.

(6) 15-m water immersion test

As described in subsection A.6.4, this packaging is not deformed even after a 15-m water immersion test is conducted.

A.9.2.3 Summary and evaluation of results

(1) 9-m free drop test

Compared with the values obtained during a 9-m free drop test, the deformation value and impact deceleration (about 3% during a vertical drop, about 10% during a horizontal drop, and about 24% during a corner drop) increase. However, the stress generated in the containment system (i.e., lid units and inner shell) and in the secondary containment system (i.e., a fuel supporting can or receiving tube) does not exceed the design criterion. The containment of this packaging is thus maintained, and the shape of the packaging or other conditions related to the criticality analysis are also maintained.

(2) Drop test II

During a corner drop, which causes the largest deformation value as compared with A.6.2, "Drop Test II", deformation is limited to the shock absorber. The packaging body is not deformed. Therefore, the shape of the packaging or other conditions related to the criticality analysis are maintained.

(3) Thermal test

The shielding lead does not melt even during a thermal test. The temperature of the packaging also remains lower than the operating temperature.

Thermal stress is generated by the temperature difference between the inner and outer shells. As a result of the evaluation (Contents I - eccentric) conducted in this section, the maximum temperature of the inner and outer shells is the same as that of Contents I (vertical drop) in the same receiving state in section B.5. Therefore, the maximum thermal stress in this case is generated in the inner shell as described in subsection A.6.3.2. The margin of safety is approximately 0.4. This packaging is thus not damaged by thermal stress and remains sound. Therefore, the shape of the packaging or other conditions related to the criticality analysis are maintained.

(4) 15-m water immersion test

As described in A.6.4, "Water Immersion Test", the containment system exhibits sufficient pressure resistance at a depth of 15 m in water. As a result, no water penetrates the packaging.

Judging from the results obtained above, even if the tests in cases (1) and (2) are conducted repeatedly in the predetermined order, the shape of the packaging or other conditions related to the criticality analysis are maintained.

A.10 Appendix

1. Correction of the Impact Deceleration

1.1 Vertical drop

The following are believed to influence the deceleration of a covering plate during a vertical drop. The impact deceleration that is generated is obtained by the deformation of these portions.

- (a) Compressive deformation of the pipe in the bolt tightening hole of the shock absorber
- (b) Compressive deformation of the steel plate on the side wall of the center cavity of the shock absorber
- (c) Compressive deformation of the shock absorber covering plate

(a) Compression of the pipe in the bolt tightening hole

If the pipe is compressed in the axial direction, the compressive crushing stress is given as follows by E.C. Lusk:

$$\sigma_{mc} = 47.74 \sigma_y \left(\frac{t}{S}\right)^2 \quad 1)$$

where

σ_{mc}	:	Nominal compressive crushing stress	
σ_y	:	Yield stress of the material	206 N/mm ² = 21 kg/mm ²
t	:	Pipe thickness	1.65 mm
S	:	Inner diameter of the pipe	57.2 mm

$$\begin{aligned} \sigma_{mc} &= 47.74 \times 206 \times \left(\frac{1.65}{57.2}\right)^2 \\ &= 8.18 \text{ N/mm}^2 \end{aligned}$$

The crushing stress (F_1) of the pipe in the bolt tightening hole of the shock absorber is given by the expression below.

$$F_1 = n \cdot \sigma_{mc} \frac{\pi(d_o)^2}{4}$$

where

n	:	Number of bolt tightening holes	12
d_o	:	Outer diameter of the pipe	60.5 mm

The expression below results when each numeric value is used.

1) R.J.Burion E.C Lusk : Compact Metallic Impact for Shipping Containers CONF-710801

$$F_1 = 12 \times 8.183 \times \frac{60.5^2}{4} \times \pi$$

$$= 2.82 \times 10^5 \text{ N}$$

(b) Steel plate on the side wall of the center cavity of the shock absorber

As in step (a), the load (F_2) applied during the deformation of the steel plate on the side wall of the center cavity of the shock absorber is given by

$$\sigma_{mc} = 47.74 \sigma_y \left(\frac{t}{s}\right)^2$$

t : Thickness of the steel plate on the side wall of the center cavity 3 mm
s : Diameter of the cavity 400 mm

$$\sigma_{mc} = 47.74 \times 206 \left(\frac{3}{400}\right)^2$$

$$= 5.53 \times 10^{-1} \text{ N/mm}^2$$

$$F_2 = \sigma_{mc} \cdot \pi \cdot \left(\frac{S + 2t}{2}\right)^2$$

$$= 5.53 \times 10^{-1} \times \pi \times \left(\frac{406}{2}\right)^2$$

$$= 7.16 \times 10^4 \text{ N}$$

(c) Covering plate

The surface opposite to the collision surface becomes bent or deformed because it has only a thin plate ($t = 3$ mm). Therefore, the constraining force against the covering plate on the side surface is weak. However, assuming that the covering plate is completely constrained, force (F_3) is given as follows, as in steps (a) and (b):

$$F_3 = 6.87 \times 10^4 \text{ N}$$

Therefore, based on steps (a), (b), and (c), the resistance force (F) with respect to the compression is given by

$$F = F_1 + F_2 + F_3$$

$$= 2.82 \times 10^5 + 7.16 \times 10^4 + 6.87 \times 10^4$$

$$= 4.22 \times 10^5 \text{ N}$$

The impact deceleration (G) is given by the expression below.

$$G = \frac{F}{W}$$

$$= \frac{4.22 \times 10^5}{9.807 \times 11000}$$

$$= 3.91 \text{ g}$$

The impact deceleration calculated by the code, SHOCK-2, is 130 G. Therefore, the strength of each part of this packaging is evaluated on the assumption that the force obtained when the deceleration calculated above is added is applied.

$$G = 130 + 3.91$$

$$\approx 135 \text{ g}$$

1.2 Horizontal drop

(a) Side plate

The deformation value calculated by the code, SHOCK-2, is 160 mm. The load that is generated from the side plate is obtained when this deformation occurs.
(Fig. (II)-A-App.-1)

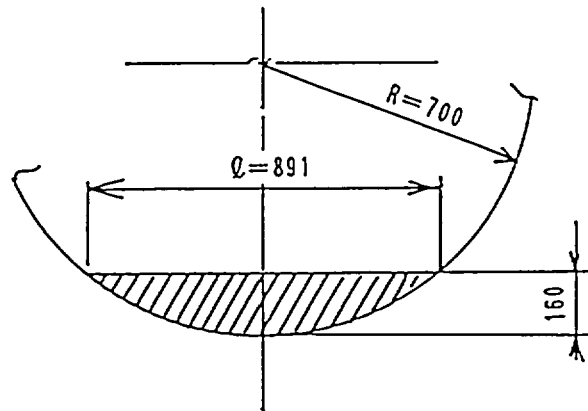


Fig. (II)-A-App.1 Shock Absorber Side Plate

The expression below results when, to be on the safe side, the maximum length of the deformed portion is assumed.

$$F = \sigma \cdot t \cdot \ell$$

σ	: Yield stress of the side plate	$206 \text{ N/mm}^2 \approx 21 \text{ kg/mm}^2$
t	: Total thickness of the side plate (corresponding to the front and rear shock absorbers)	$(3 + 3) \times 2 = 12 \text{ mm}$
ℓ	: Length of the deformed portion	891 mm

$$\begin{aligned} F &= 206 \times 12 \times 891 \\ &= 2.20 \times 10^6 \text{ N} \end{aligned}$$

The impact deceleration (G) is given by the expression below.

$$\begin{aligned} G &= \frac{F}{W} \\ &= \frac{2.20 \times 10^6}{9.807 \times 11000} \\ &= 20.5 \text{ g} \end{aligned}$$

The impact deceleration calculated by the code, SHOCK-2, is 98 g. Therefore, the strength of each part of this packaging is evaluated on the assumption that the force obtained when the deceleration calculated above is added is applied.

$$\begin{aligned} G &= 98 + 20.5 \\ &= 118.5 \\ &\approx 120 \text{ g} \end{aligned}$$

1.3 Corner drop

The impact deceleration calculated by the code, SHOCK-2, is 66 G. Given the influence of the steel plate, the strength of each part of this packaging is evaluated on the assumption that an impact deceleration of 9 G is added and that an impact acceleration of 75 G is applied in the same manner as in the case of the horizontal drop.

2. Analysis Model and Input of the ANSYS Calculation Code

2.1 Drop analysis

Figs. (II)-A-App.2 and 3 show the analysis models of shielding plug lid and rotating plug lid units. The rear lid is tightened to the shielding plug lid with a bolt via the O-ring packing. The shielding plug lid is tightened to the upper flange of an inner shell with a bolt via the O-ring packing.

Similarly, the front lid is tightened to the rotating plug lid with a bolt via the O-ring packing. The rotating plug lid is tightened to the lower flange of an inner shell with a bolt via the O-ring packing. Since the analysis model is a two-dimensional axisymmetric model, the modulus of longitudinal elasticity and the specific gravity are inputted after a correction to ensure that the bolt and its bolt tightening hole portion have an equal amount of rigidity. Tables (II)-A-App.1 and 2 list the correction results.

2.2 Pressure-resistant analysis

The analysis models of the shielding plug lid and rotating plug lid units are the same as the model used for the drop analysis. Fig. (II)-A-App.4 shows the analysis model of a penetration hole lid part. The modulus of longitudinal elasticity of the materials used for the shielding plug lid and rotating plug lid units takes the value obtained when the drop analysis model is corrected on the basis of the value shown in Table. (II)-A-App.3.

2.3 Thermal stress analysis

Since the temperature gradient is low, the thermal stress evaluation under normal test conditions used a cylindrical model as shown in Fig. (II)-A-App.5(a), with particular attention paid to the section of the center portion of the packaging shell.

The thermal stress evaluation under accident test conditions (thermal test) was performed with a model of the inner and outer shells from one end to the center thereof, as shown in Fig. (II)-App.5(b).

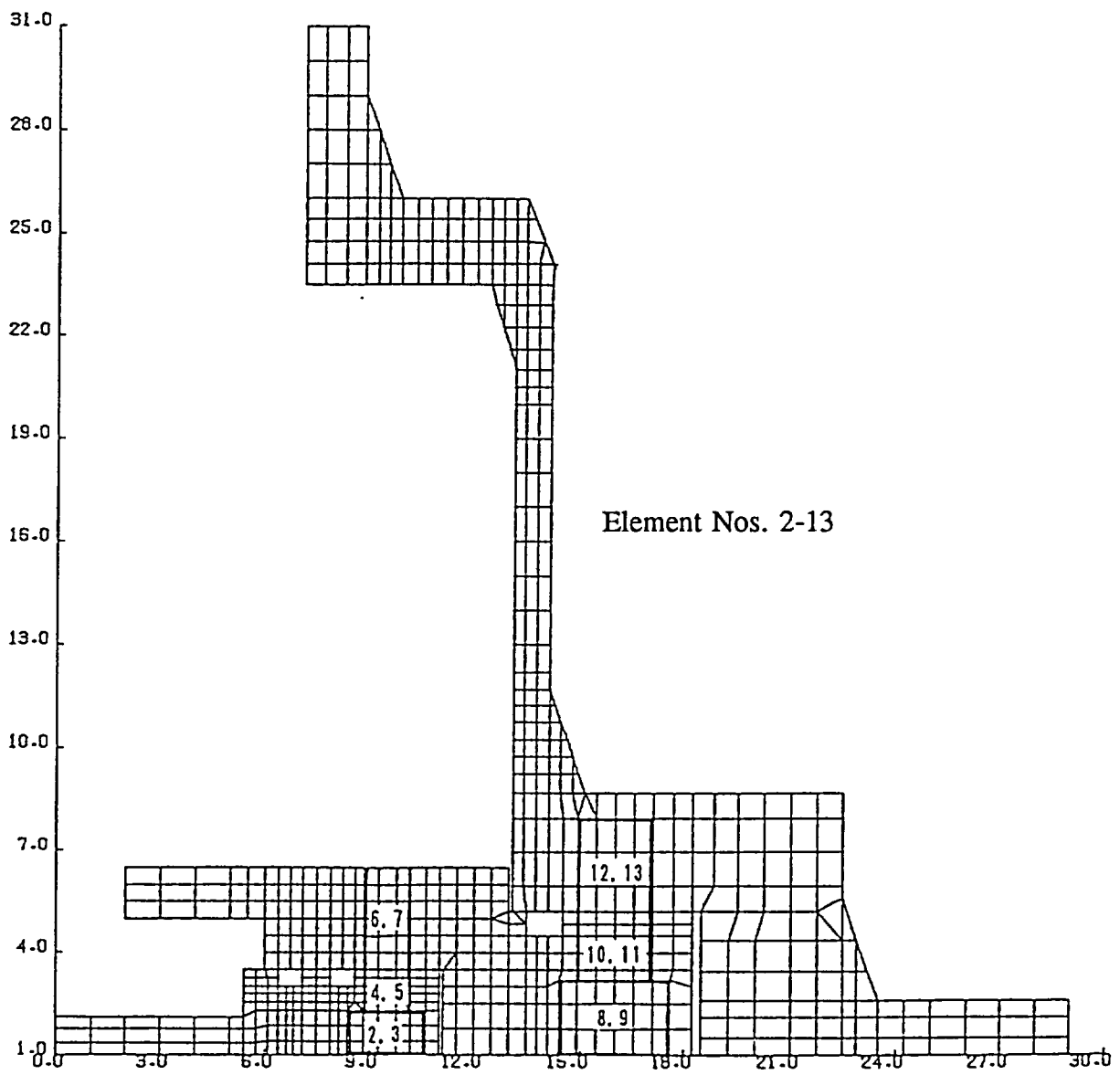


Fig. (II)-A-App.2 Analysis Model of Rear Lid Unit

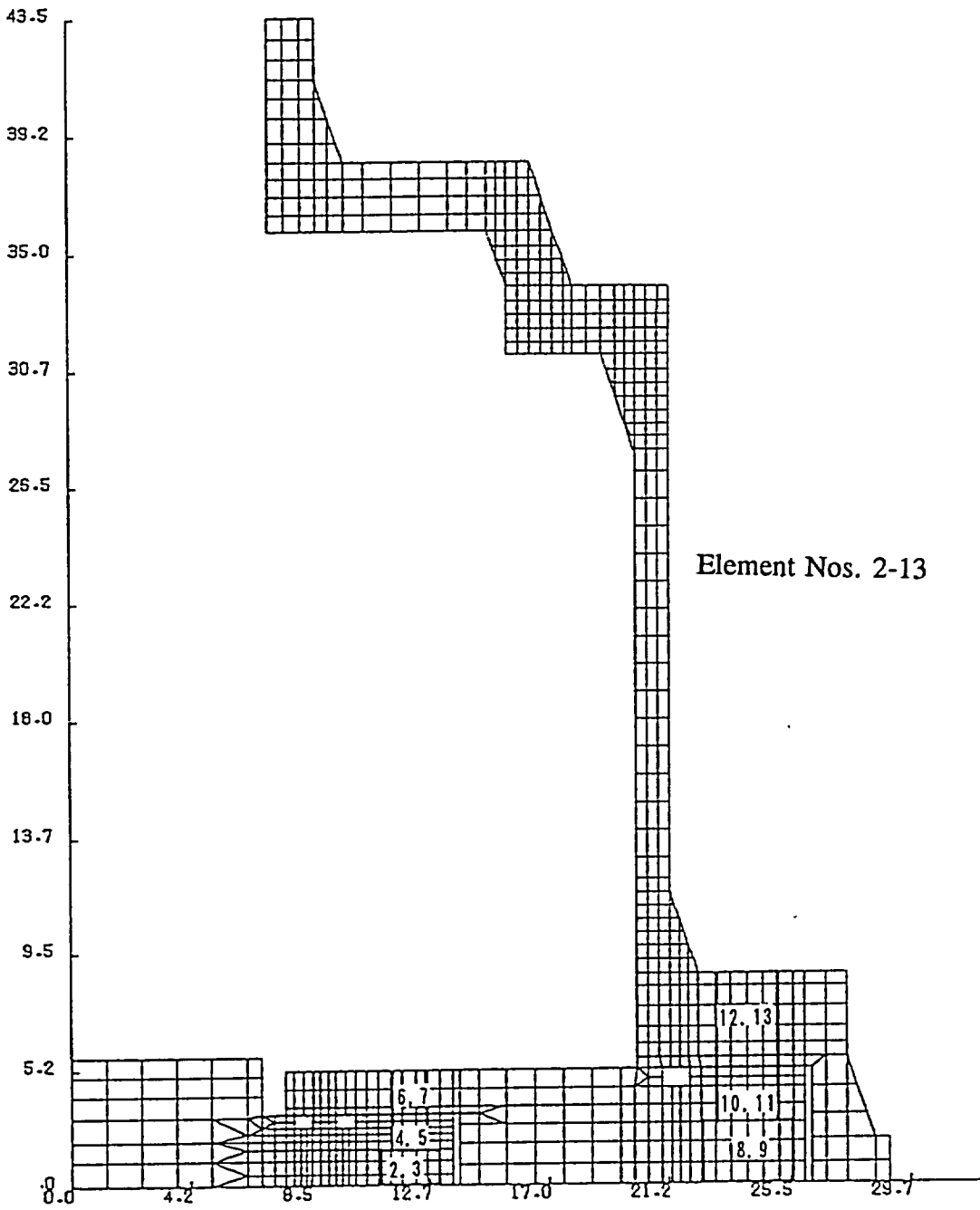


Fig. (II)-A-App.3 Analysis Model of Front Lid Unit

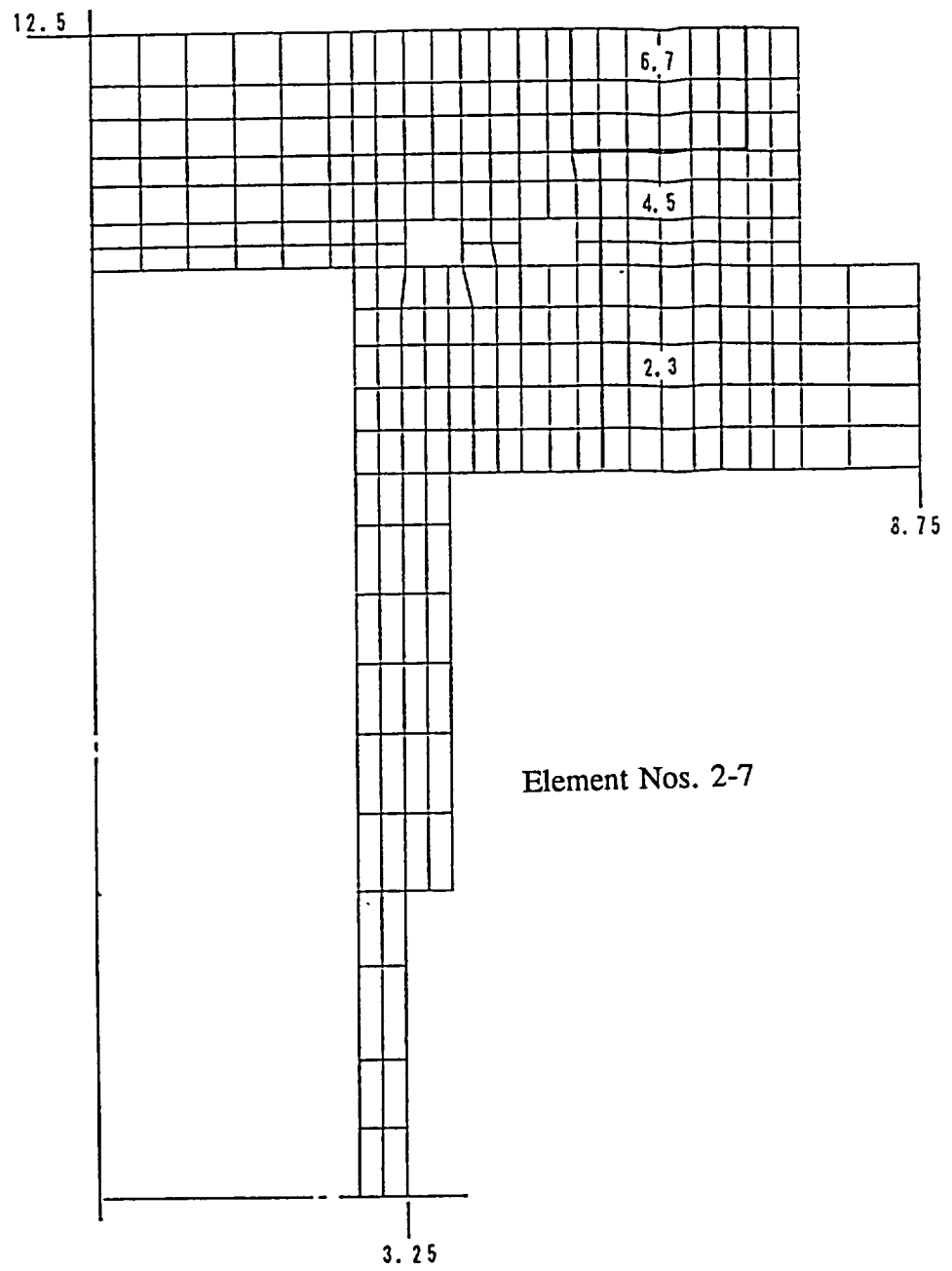
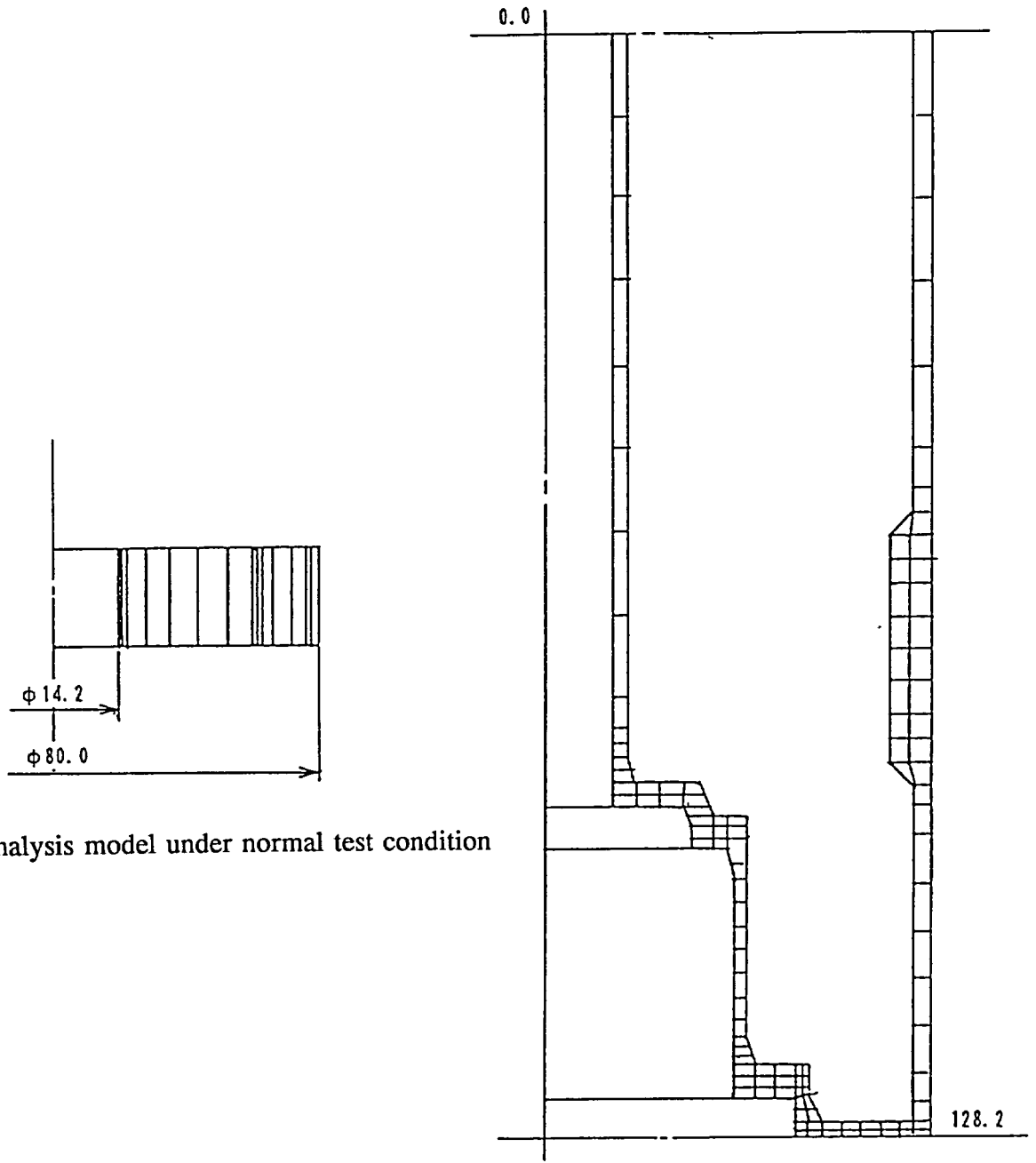


Fig. (II)-A-App.4 Analysis Model of Penetration Hole Lid



(a) Analysis model under normal test condition

(b) Analysis model under accident test conditions

Fig. (II)-A-App.5 Model for Thermal Stress Analysis

Table (II)-A-App.1 Shielding Plug Lid Bolt and Hole Portion (1)

Parts	Schematic drawing	Modeled value
Bolt and portions other than the bolt hole		E_b : Modulus of longitudinal elasticity $1.92 \times 10^7 \text{ N/cm}^2$ ν : Poisson's ratio 0.3 ρ : Density $7.78 \times 10^{-2} \times \text{N/cm}^3$ ρ' : Density considering the acceleration $= 7.78 \times 10^{-2} \times 135$ $= 10.5 \text{ N/cm}^3$ $\approx 1.07 \text{ kg/cm}^3$ E_B : Modulus of the longitudinal elasticity (bolt) $= 2.14 \times 10^7 \text{ N/cm}^2$ $\approx 2.18 \times 10^6 \text{ kg/cm}^2$
Rear lid Fastening bolt part		<p>(2)</p> A_t : Cross-sectional area of the bolt hole portion $A_t = (10.5^2 - 8.5^2)\pi$ A_b : Cross-sectional area of the bolt head $A_b = \frac{\pi}{4}(1.8)^2$ A_{bt} : Cross-sectional area of the bolt head $A_{bt} = \frac{\pi}{4}(1.8)^2 \times 12$ $E' = \frac{A_t - A_{bt}}{A_t} \cdot E_b$ $= \frac{10.5^2 - 8.5^2 - \frac{1}{4} \cdot 1.8^2 \times 12}{10.5^2 - 8.5^2} \times 1.92 \times 10^7$ $= 1.43 \times 10^7 \text{ N/cm}^2$ $\approx 1.46 \times 10^6 \text{ kg/cm}^2$ V_t : Volume of the bolt hole portion $V_t = 1.3(10.5^2 - 8.5^2)\pi$ V_{bt} : Total volume of the bolt head $V_{bt} = \frac{\pi}{4}(1.8)^2 \times 1.2 \times 12$

Table (II)-A-App.1 Shielding Plug Lid Bolt and Hole Portion (2)

Parts	Schematic drawing	Modeled value
		$\rho' = \frac{V_i - V_k}{V_i} \rho \times 135$ $= \frac{13(10.5^2 - 8.5^2) - \frac{1}{4}1.8^2 \times 1.2 \times 12}{1.3(10.5^2 - 8.5^2)} \times 10.5$ $= 8.02 \text{ N/cm}^3$ $\approx 0.818 \text{ kg/cm}^3$ <p>(3)</p> $E' = \frac{A_k}{A_i} E_B$ $= \frac{\frac{1}{4}1.82 \times 12}{10.5^2 - 8.5^2} \times 2.14 \times 10^7$ $= 5.4 \times 10^6 \text{ N/cm}^2$ $\approx 5.58 \times 10^5 \text{ kg/cm}^2$ $\rho' = \frac{V_k}{V_i} \rho \times 135$ $= \frac{\frac{1}{4}1.8^2 \times 1.2 \times 12}{1.3(10.5^2 - 8.5^2)} \times 10.5$ $= 2.48 \text{ N/cm}^3$ $\approx 0.253 \text{ kg/cm}^3$ <p>The same as above,</p> <p>(4)</p> $E' = 1.59 \times 10^7 \text{ N/cm}^2 \quad \rho' = 8.66 \text{ N/cm}^3$ $\approx 1.62 \times 10^6 \text{ kg/cm}^2 \quad \approx 0.883 \text{ kg/cm}^3$ <p>(5)</p> $E' = 3.74 \times 10^6 \text{ N/cm}^2 \quad \rho' = 1.83 \text{ N/cm}^3$ $\approx 3.81 \times 10^5 \text{ kg/cm}^2 \quad \approx 0.187 \text{ kg/cm}^3$ <p>(6)</p> $E' = 1.56 \times 10^7 \text{ N/cm}^2 \quad \rho' = 8.51 \text{ N/cm}^3$ $\approx 1.59 \times 10^6 \text{ kg/cm}^2 \quad \approx 0.868 \text{ kg/cm}^3$ <p>(7)</p> $E' = 4.10 \times 10^6 \text{ N/cm}^2 \quad \rho' = 1.99 \text{ N/cm}^3$ $\approx 4.18 \times 10^5 \text{ kg/cm}^2 \quad \approx 0.203 \text{ kg/cm}^3$

Table (II)-A-App.1 Shielding Plug Lid Bolt and Hole Portion (3)

Parts	Schematic drawing	Modeled value
Shielding plug lid fastening bolt part		<p>(8)</p> $A_t = (17.6^2 - 14.4^2) \pi$ $A_b = \frac{\pi 3^2}{4}$ $A_k = \frac{\pi 3^2}{4} \times 16$ $E' = \frac{A_t - A_k E_b}{A_t}$ $= \frac{17.6^2 - 14.4^2 - \frac{1}{4} 3^2 \times 16}{17.6^2 - 14.4^2} \times 1.92 \times 10^7$ $= 1.25 \times 10^7 \text{ N/cm}^2$ $\approx 1.27 \times 10^6 \text{ kg/cm}^2$ $\rho' = \frac{V_t - V_k}{V_t} \rho \times 135$ $= \frac{2.2(17.6^2 - 14.4^2) - \frac{1}{4} 3^2 \times 16 \times 2}{2.2(17.6^2 - 14.4^2)} \times 10.5$ $= 7.14 \text{ N/cm}^3$ $\approx 0.728 \text{ kg/cm}^3$
		<p>(9)</p> $E' = \frac{A_k E_b}{A_t}$ $= \frac{\frac{1}{4} 3^2 \times 16}{17.6^2 - 14.4^2} \times 2.14 \times 10^7$ $= 7.52 \times 10^6 \text{ N/cm}^2$ $\approx 7.66 \times 10^5 \text{ kg/cm}^2$ $\rho' = \frac{V_k}{V_t} \rho \times 135$ $= \frac{\frac{1}{4} 3^2 \times 16 \times 2}{2.2(17.6^2 - 14.4^2)} \times 10.5$ $= 3.36 \text{ N/cm}^3$ $\approx 0.342 \text{ kg/cm}^3$
	The same as above,	<p>(10)</p> $E' = 1.48 \times 10^7 \text{ N/cm}^2 \quad \rho' = 8.11 \text{ N/cm}^3$ $\approx 1.51 \times 10^6 \text{ kg/cm}^2 \quad \approx 0.827 \text{ kg/cm}^3$
	<p>(11)</p> $E' = 4.85 \times 10^6 \text{ N/cm}^2 \quad \rho' = 2.38 \text{ N/cm}^3$ $\approx 4.95 \times 10^5 \text{ kg/cm}^2 \quad \approx 0.243 \text{ kg/cm}^3$	
	<p>(12)</p> $E' = 1.44 \times 10^7 \text{ N/cm}^2 \quad \rho' = 7.88 \text{ N/cm}^3$ $\approx 1.47 \times 10^6 \text{ kg/cm}^2 \quad \approx 0.803 \text{ kg/cm}^3$	
	<p>(13)</p> $E' = 5.34 \times 10^6 \text{ N/cm}^2 \quad \rho' = 2.63 \text{ N/cm}^3$ $\approx 5.45 \times 10^5 \text{ kg/cm}^2 \quad \approx 0.268 \text{ kg/cm}^3$	

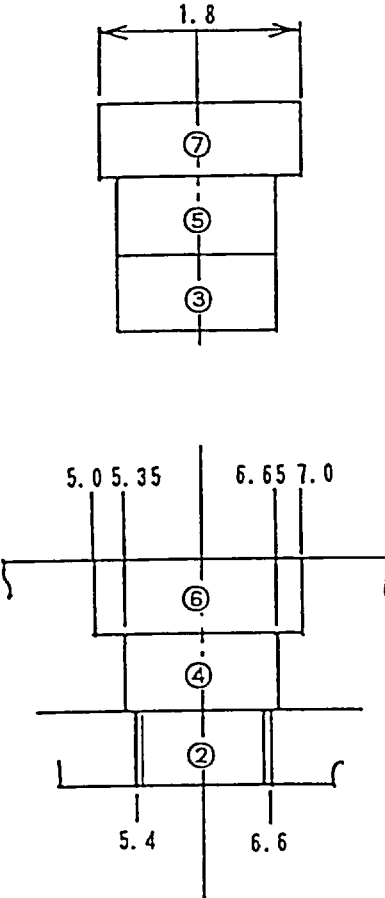
Table (II)-A-App.2 Rotating Plug Lid Bolt and Hole Portion (1)

Parts	Schematic drawing	Modeled value
Front lid fastening bolt part		<p>(2)</p> $A_t = (13.0^2 - 11.0^2)\pi$ $A_b = \frac{\pi}{4}1.8^2$ $A_b = \frac{\pi}{4}1.8^2 \times 12$ $E' = \frac{A_t - A_b E_b}{A_t}$ $= \frac{13.0^2 - 11.0^2 - \frac{1}{4}1.8^2 \times 12}{13.0^2 - 11.0^2} \times 1.72 \times 10^7$ $= 1.53 \times 10^7 \text{ N/cm}^2$ $\approx 1.56 \times 10^6 \text{ kg/cm}^2$ $\rho' = \frac{V_t - V_b}{V_t} \rho \times 135$ $= \frac{1.3(13.0^2 - 11.0^2) - \frac{1}{4}1.8^2 \times 1.2 \times 12}{1.3(13.0^2 - 11.0^2)} \times 10.5$ $= 8.53 \text{ N/cm}^3$ $\approx 0.870 \text{ kg/cm}^3$ <p>(3)</p> $E' = \frac{A_b E_b}{A_t}$ $= \frac{\frac{1}{4}1.8^2 \times 12}{13.0^2 - 11.0^2} \times 2.14 \times 10^7$ $= 4.33 \times 10^6 \text{ N/cm}^2$ $\approx 4.11 \times 10^5 \text{ kg/cm}^2$ $\rho' = \frac{V_b}{V_t} \rho \times 135$ $= \frac{\frac{1}{4}1.8^2 \times 1.2 \times 12}{1.3(13.0^2 - 11.0^2)} \times 10.5$ $= 1.96 \text{ N/cm}^3$ $\approx 0.200 \text{ kg/cm}^3$ <p>The same as above,</p> <p>(4)</p> $E' = 1.66 \times 10^7 \text{ N/cm}^2 \quad \rho' = 9.04 \text{ N/cm}^3$ $\approx 1.69 \times 10^6 \text{ kg/cm}^2 \quad \approx 0.922 \text{ kg/cm}^3$ <p>(5)</p> $E' = 2.96 \times 10^6 \text{ N/cm}^2 \quad \rho' = 1.45 \text{ N/cm}^3$ $\approx 3.02 \times 10^5 \text{ kg/cm}^2 \quad \approx 0.148 \text{ kg/cm}^3$ <p>(6)</p> $E' = 1.64 \times 10^7 \text{ N/cm}^2 \quad \rho' = 8.92 \text{ N/cm}^3$ $\approx 1.67 \times 10^6 \text{ kg/cm}^2 \quad \approx 0.910 \text{ kg/cm}^3$ <p>(7)</p> $E' = 3.21 \times 10^6 \text{ N/cm}^2 \quad \rho' = 1.58 \text{ N/cm}^3$ $\approx 3.27 \times 10^5 \text{ kg/cm}^2 \quad \approx 0.161 \text{ kg/cm}^3$

Table (II)-A-App.2 Rotating Plug Lid Bolt and Hole Portion (2)

Parts	Schematic drawing	Modeled value
Rotating plug lid fastening bolt part		<p>(8)</p> $A_t = (25.6^2 - 22.4^2)\pi$ $A_b = \frac{\pi}{4} 3.0^2$ $A_k = \frac{\pi}{4} 3.0^2 \times 20$ $E' = \frac{A_t - A_k E_b}{A_t}$ $= \frac{25.6^2 - 22.4^2 - \frac{1}{4} 3.0^2 \times 20}{25.6^2 - 22.4^2} \times 1.92 \times 10^7$ $= 1.36 \times 10^7 \text{ N/cm}^2$ $\approx 1.39 \times 10^6 \text{ kg/cm}^2$ $\rho' = \frac{V_t - V_k}{V_t} \rho \times 135$ $= \frac{2.2(25.6^2 - 22.4^2) - \frac{1}{4} 3.0^2 \times 2 \times 20}{2.2(25.6^2 - 22.4^2)} \times 10.5$ $= 7.7 \text{ N/cm}^3$ $\approx 0.785 \text{ kg/cm}^3$
		<p>(9)</p> $E' = \frac{A_k E_b}{A_t}$ $= \frac{\frac{1}{4} 3.0^2 \times 20}{25.6^2 - 22.4^2} \times 2.14 \times 10^7$ $= 627 \times 10^6 \text{ N/cm}^2$ $\approx 639 \times 10^5 \text{ kg/cm}^2$ $\rho' = \frac{V_k}{V_t} \rho \times 135$ $= \frac{\frac{1}{4} 3^2 \times 2.0 \times 20}{2.2(25.6^2 - 22.4^2)} \times 10.5$ $= 2.79 \text{ N/cm}^3$ $\approx 0.285 \text{ kg/cm}^3$
	<p>The same as above,</p>	<p>(10)</p> $E' = 1.56 \times 10^7 \text{ N/cm}^2 \quad \rho' = 8.51 \text{ N/cm}^3$ $\approx 1.59 \times 10^6 \text{ kg/cm}^2 \quad \approx 0.868 \text{ kg/cm}^3$
	<p>(11)</p> $E' = 4.05 \times 10^6 \text{ N/cm}^2 \quad \rho' = 1.99 \text{ N/cm}^3$ $\approx 4.13 \times 10^5 \text{ kg/cm}^2 \quad \approx 0.203 \text{ kg/cm}^3$	
	<p>(12)</p> $E' = 1.52 \times 10^7 \text{ N/cm}^2 \quad \rho' = 8.32 \text{ N/cm}^3$ $\approx 1.55 \times 10^6 \text{ kg/cm}^2 \quad \approx 0.848 \text{ kg/cm}^3$	
	<p>(13)</p> $E' = 4.44 \times 10^6 \text{ N/cm}^2 \quad \rho' = 2.19 \text{ N/cm}^3$ $\approx 4.54 \times 10^5 \text{ kg/cm}^2 \quad \approx 0.223 \text{ kg/cm}^3$	

Table (II)-A-App.3 Penetration Hole Lid Bolt and Hole Portion (1)

Parts	Schematic drawing	Modeled value
Bolt and portions other than the bolt hole		E_b : Modulus of longitudinal elasticity $1.83 \times 10^7 \text{ N/cm}^2$ $\approx 1.87 \times 10^6 \text{ kg/cm}^2$ ν : Poisson's ratio 0.3 E_b : Modulus of the longitudinal elasticity (bolt) $2.07 \times 10^7 \text{ N/cm}^2$ $\approx 2.11 \times 10^6 \text{ kg/cm}^2$
Rotating hole lid fastening bolt part		<p>(2)</p> A_t : Cross-sectional area of the bolt hole portion $A_t = (6.6^2 - 5.4^2)\pi$ A_b : Cross-sectional area of the bolt head $A_b = \frac{\pi}{4}(1.2)^2 \times 4$ $E' = \frac{A_t - A_b}{A_t} \cdot E_b$ $= \frac{6.6^2 - 5.4^2 - \frac{1}{4}1.2^2 \times 4}{6.6^2 - 5.4^2} \times 1.83 \times 10^7$ $= 1.65 \times 10^7 \text{ N/cm}^2$ $\approx 1.68 \times 10^6 \text{ kg/cm}^2$ <p>(3)</p> $E' = \frac{A_b}{A_t} E_b$ $= \frac{\frac{1}{4}1.2^2 \times 4}{6.6^2 - 5.4^2} \times 2.07 \times 10^7$ $= 2.07 \times 10^6 \text{ N/cm}^2$ $\approx 2.11 \times 10^5 \text{ kg/cm}^2$ <p>The same as above,</p> <p>(4)</p> $E' = 1.66 \times 10^7 \text{ N/cm}^2$ $\approx 1.70 \times 10^6 \text{ kg/cm}^2$ <p>(5)</p> $E' = 1.91 \times 10^6 \text{ N/cm}^2$ $\approx 1.95 \times 10^5 \text{ kg/cm}^2$ <p>(6)</p> $E' = 1.59 \times 10^7 \text{ N/cm}^2$ $\approx 1.62 \times 10^6 \text{ kg/cm}^2$ <p>(7)</p> $E' = 2.79 \times 10^6 \text{ N/cm}^2$ $\approx 2.85 \times 10^5 \text{ kg/cm}^2$

3. Model Test and Analysis

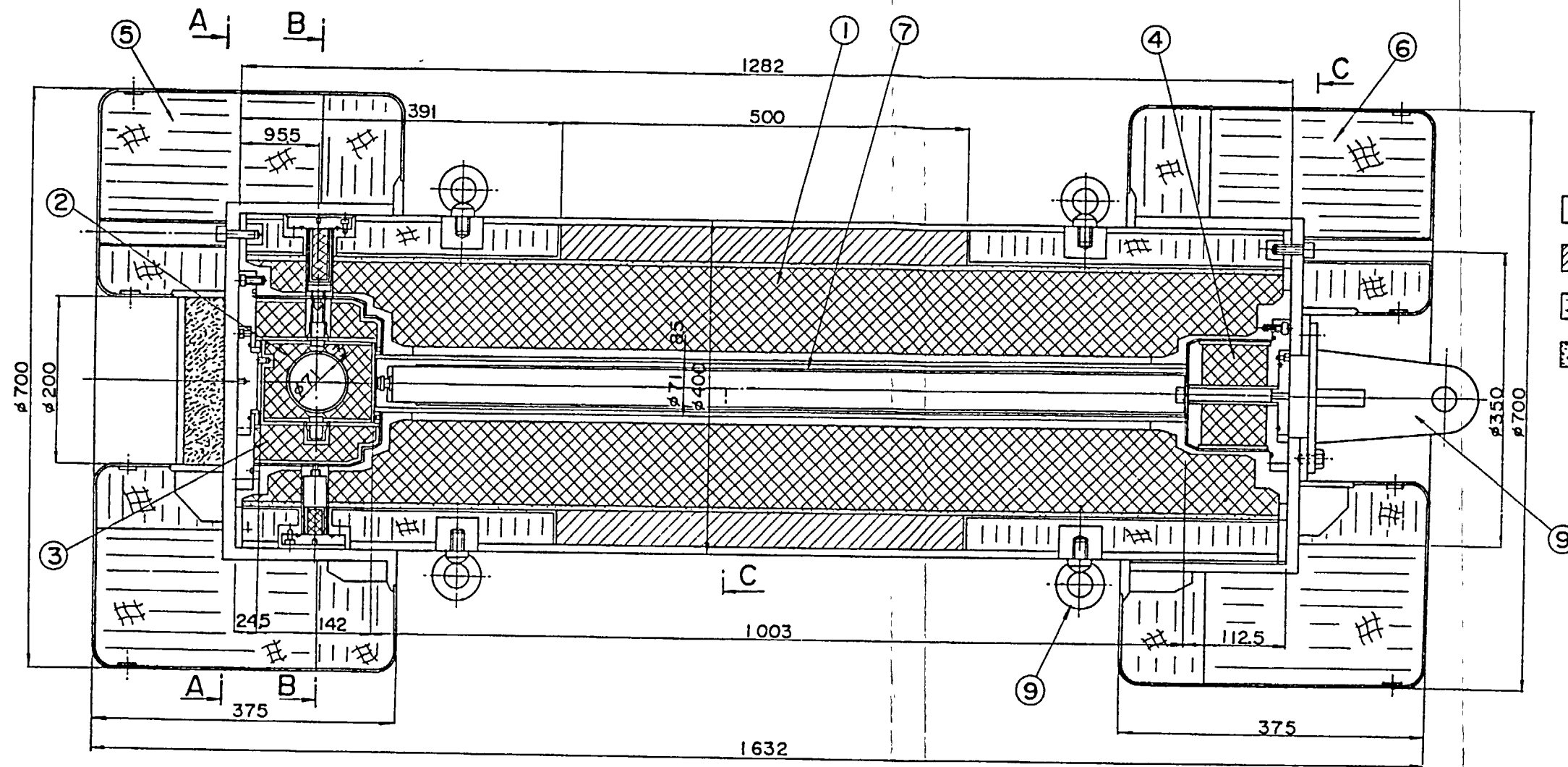
3.1 Objective of the model test

Using a 1/2-scale model packaging (not simulating the shielding plug mechanism block) that faithfully simulates the rotating plug mechanism block of the TN6-4 packaging, accident tests (drop test I: horizontal drop, vertical drop, corner drop, and oblique drop, and drop test II: horizontal drop, vertical drop, corner drop, and oblique drop) were conducted to measure the deceleration, deformation value, strain value, and leakage rate.

By comparing the results obtained above and the results obtained by using an analysis model, it was confirmed that the results based on the analysis were on the safe side, thereby verifying that the analysis method used in the actual packaging was valid.

3.2 Actual packaging and 1/2-scale model

Fig. (II)-A-App.6 shows the 1/2-Scale model. The dimensional ratio is one half that of the actual package. The weight is approximately 1/9 (1.25 t) that of the actual package. Table (II)-A-App.4 lists the portions that have not been modeled.

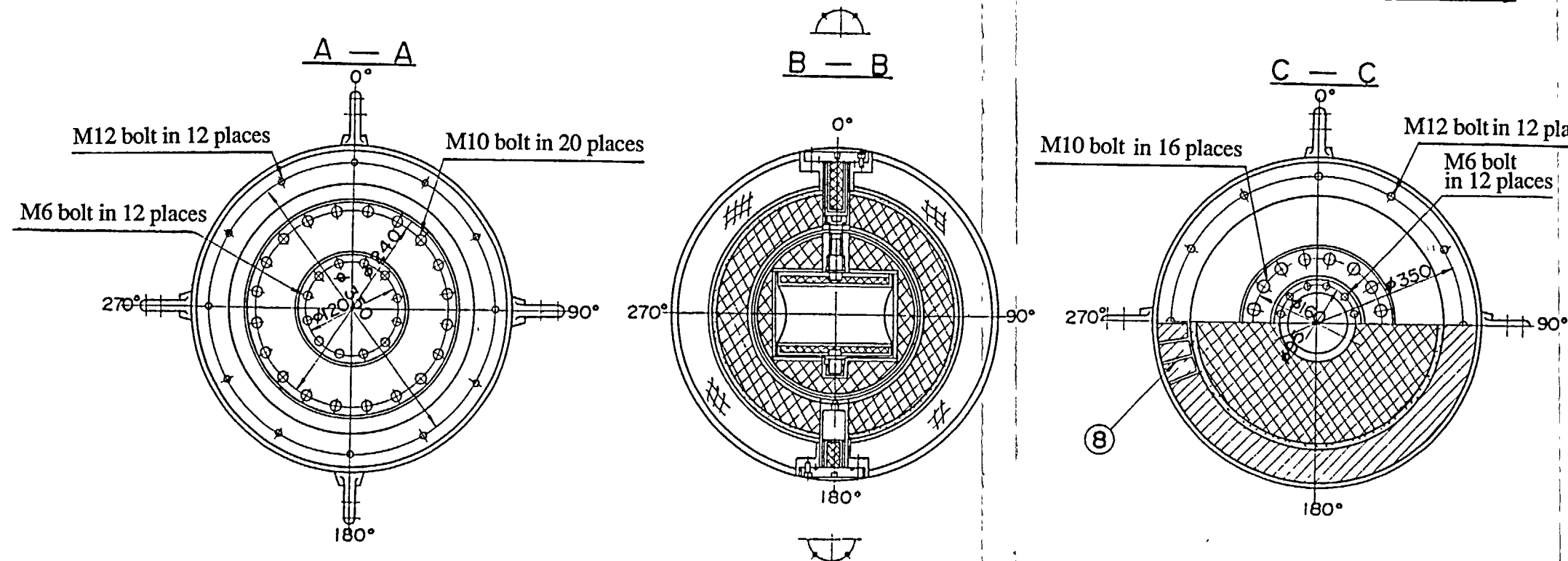


Material

SUS 304	Lead
Resin	Cement
Balsa wood	
Fir-plywood	

**ANSTEC
APERTURE
CARD**

Also Available on
Aperture Card



- ① Body
- ② Rotating plug
- ③ Rotating plug lid
- ④ Shielding plug lid
- ⑤ Front shock absorber
- ⑥ Rear shock absorber
- ⑦ Dummy fuel supporting can
- ⑧ Heat dispersion fin
- ⑨ Hook for test

Fig. (II)-A-App.6 1/2 Scale Model Container

9601260203 - 33/02
(II)-A.App-17

Table (II)-A-App.4 Portions Omitted from the 1/2-Scale Model

Parts	Actual packaging	1/2-scale model	Remarks
Shock absorber * Fastening bolt hole * Cement layer * Shock absorber lifting lug * Fusible plug	12 ○ ○ ○	6 × × ×	The number of fastening bolt holes was reduced to half of the actual package by using pipes that had the same thickness as those used in the actual package.
Packaging body * Lifting lug * Trunnion * Base plate * Fusible plug * Heat dispersion fin	○ ○ ○ ○ 6° -clearance	Eyebolt × × × 12° -clearance	The number of fins was adjusted by using fins that had the same thickness as those used in the actual package.
O-ring packing * Front lid * Penetration hole lid * Front sampling valve lid	2 2 2	1 1 1	In the 1/2 scale model, the O-ring for the leakage test was simulated using a single-O-ring system rather than the double-O-ring system, which is used in the actual package.
Rear lid Shielding plug Shielding plug lid		Simulated only the external form.	The shielding plug has greater strength than the rotating plug. Therefore, it has been omitted.
Rear sampling valve	○	×	The front sampling valve lid has been simulated in the model, therefore the rear sampling valve has been omitted.

○ : provided with

× : not provided with

3.3 Model drop test

3.3.1 Test procedure

For a mechanical test, drop tests I and II under accident test conditions are conducted. Horizontal, vertical, corner, and oblique drop attitudes are used. One packaging body, which includes five shock absorbers, is provided as the drop test specimen. The packaging body is used for all tests, and the shock absorbers are replaced by new ones (whose form is unchanged) for each drop attitude.

If the tests are conducted in the order of drop test II and drop test I, the partial deformation generated during drop test II is assumed to disappear without being accumulated in the uniform deformation during drop test I. If the tests are conducted in the order of drop test I and drop test II, the partial deformation appears in the uniform deformation as a cumulative form. As a result, maximum damage occurs in the shock absorbers. Therefore, in this case, drop test II was conducted after drop test I. Moreover, a leakage test with a Halogen leak detector was performed before and after each test. Fig. (II)-A-App.7 shows the contents of each test, while Table (II)-A-App.5 lists the sequence of each test.

3.3.2 Test equipment

The test equipment consists of a drop test tower and a drop test target. A crane is used for the drop test tower. This crane has a maximum lift of 24 m and a capacity of 25 t. A compact electromagnetic lifter (lifting capacity of 1.9 t) is provided as the separation unit of a specimen after lifting.

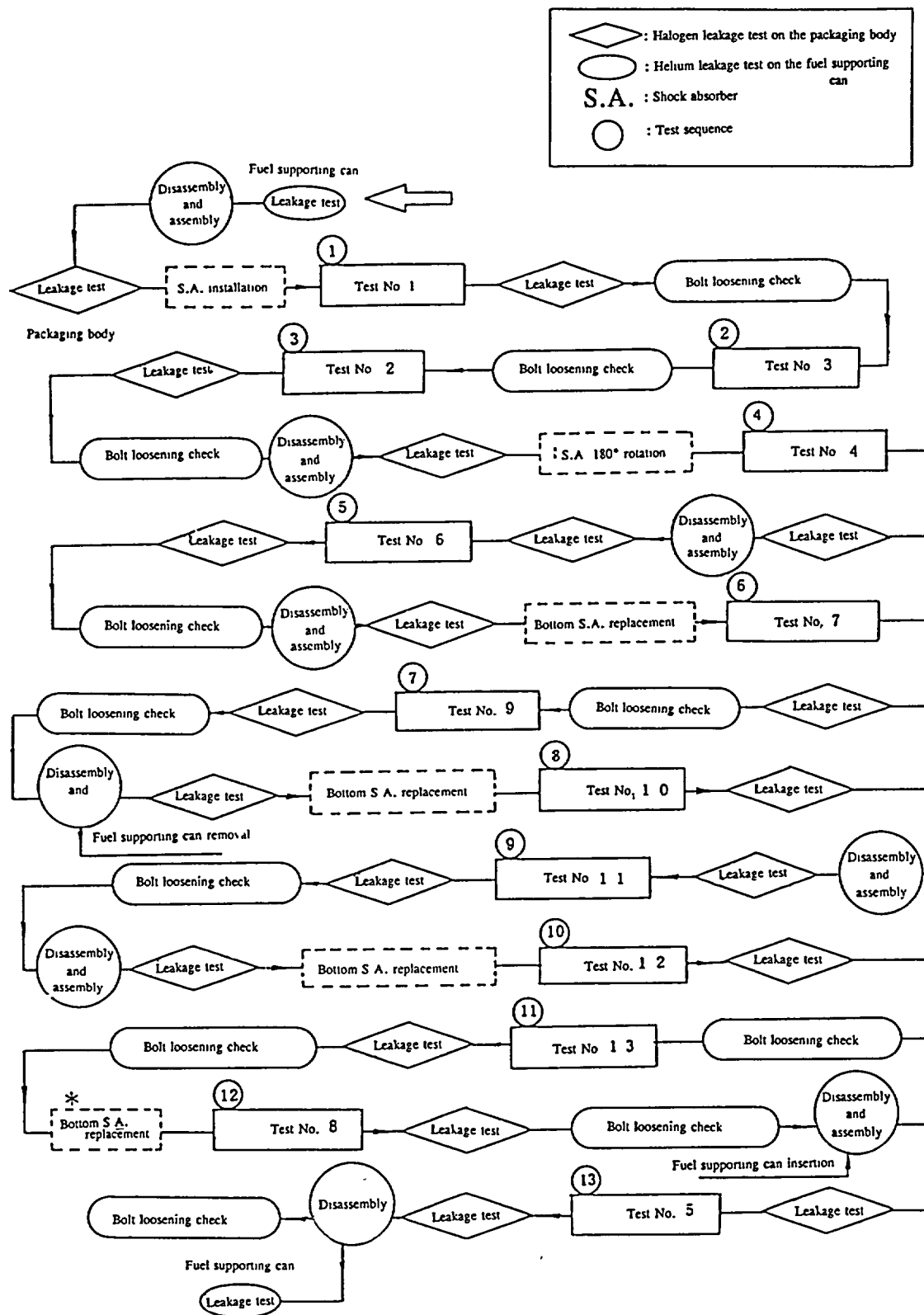
The drop target stand is a concrete rectangular-solid stand that is 5-m high, 3-m wide, 1-m thick, and weighs 36 t. This target consists of a test target for drop test I and a test target for drop test II. For the test target for drop test I, a steel plate that is 4.0-m long, 3.2-m wide, 12-mm thick, and weighs 1.2 t is placed on this concrete target. For the test target for drop test II, a cylindrical bar, 75 mm in diameter and 250 mm in length (made of mild steel with its upper end finished so that it is flat and horizontal with its edges rounded off to a radius of not more than 6 mm), which is welded to a circular plate 350 mm in diameter and 14 mm in thickness, is bolted to the test target for drop test I. Fig. (II)-A-App.8 outlines the test equipment mentioned above.

3.3.3 Test method

According to this test method, a specimen is lifted to the specified height using a crane via an electromagnetic lifter and is dropped onto the test target by turning off the power of electromagnetic lifter. The dropping height is adjusted by measuring the prescribed height from the lowest point on the specimen to the upper surface of the target before the test. To prevent the specimen and instruments from being damaged by collision with the attraction plate of electromagnetic lifter, which drops together with the specimen because the power of the lifter is cut off, special measurements are taken to keep the attraction plate from a dropping with the specimen. A wire and shackle are also prevented from colliding with the specimen from behind by a rope. It is designed so that there is no obstruction to the free dropping of the specimen in this case. The specimen is dropped horizontally from two directions by changing the direction of the rotating plug. The specimen is also dropped vertically and on a corner with the rotating plug facing downward. During the corner drop, the specimen is arranged so that the line tying the corner and the center of gravity of the specimen is perpendicular to the ground.

During an oblique drop, the specimen is arranged so that the angle formed by its center line and horizontal line equals 30 degrees, and the rotating plug faces upward. The drop attitude of the specimen is adjusted by the length of the lifting wire rope and the turnbuckle. The swing of the specimen after lifting is limited by tightening the two ropes attaching in the specimen.

Table (II)-A-App.5 Test Sequence



* The shock absorber (S.A.) at the bottom is used in test No. 1.
 The shock absorber (S.A.) shown at the top is used in test No. 12 shown at the bottom of test No. 12.

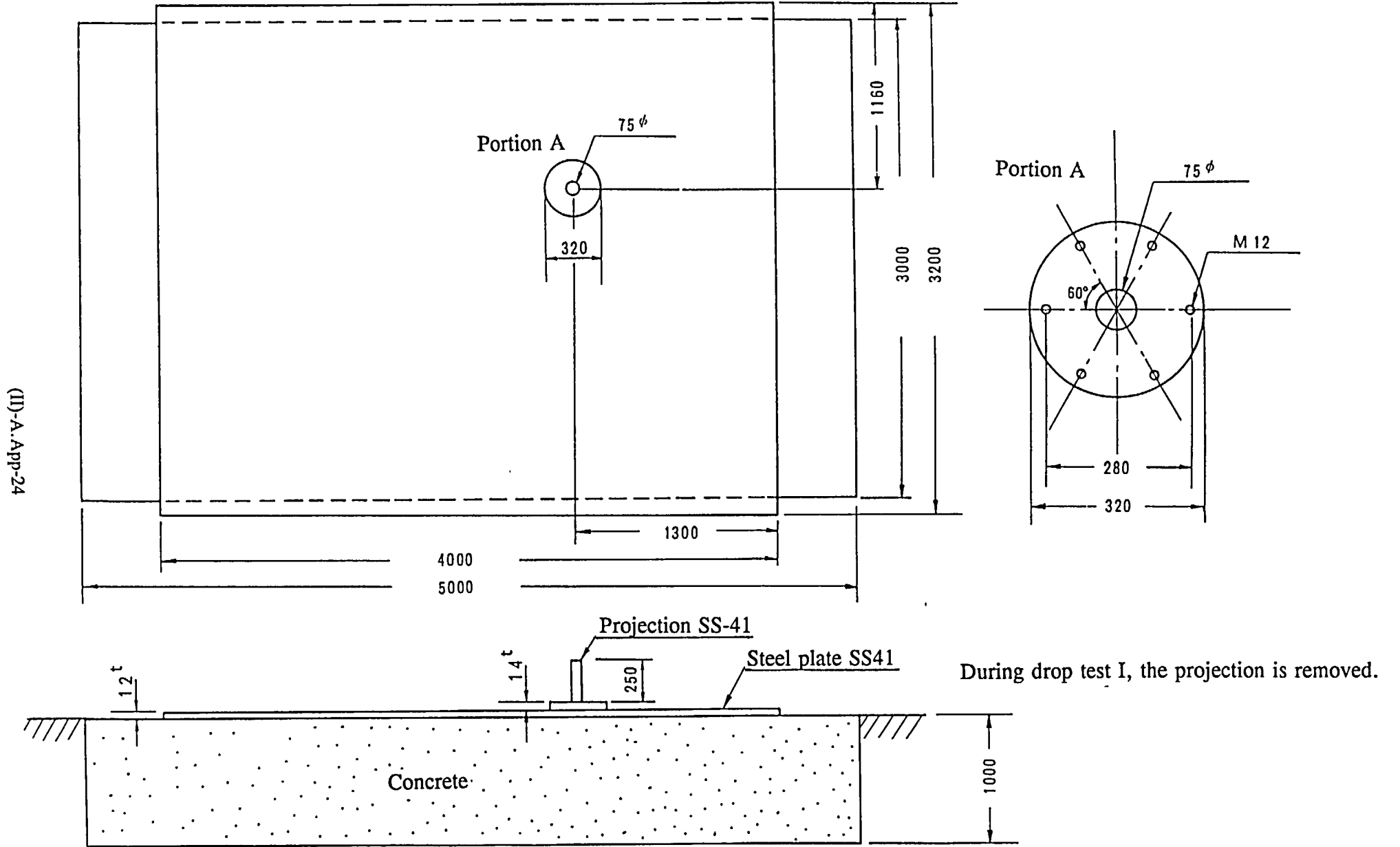
Fig. (II)-A-App.7 Contents of the Test

Drop test I (Drop test under accident conditions)		Drop test II (Penetration test under accident conditions)	
Horizontal drop 1	<p>①</p>	Center	<p>②</p>
		Eccentricity	<p>③</p>
Horizontal drop 2	<p>④</p>	Center	<p>⑤</p>
		Eccentricity	<p>⑥</p>
Vertical drop	<p>⑦</p>	Center	<p>⑧</p>
		Eccentricity	<p>⑨</p>

	Drop test I (Drop test under accident conditions)	Drop test II (Penetration test under accident conditions)
Corner drop	<p>⑩</p>	<p>⑪</p>
Oblique drop	<p>⑫</p>	<p>⑬</p>

Notes:

- 1) The figure in the circle indicates the test number.
- 2) To apply the maximum shock to the rotating plug part, the dropping attitude of the package is arranged so that its lower part faces downward during vertical and corner drops. During an oblique drop, the rotating plug part is arranged so that it faces upward since the secondary impact is expected to be stronger than the primary impact.



(II)-A-App-24

Fig. (II)-A-App.8 Drop Test Stand